

# Measurement and Optimization of LTE Performance



**Stefania Zinno**

Supervisor: Prof. Giorgio Ventre

Department of Electrical Engineering and Information Technology  
Università degli Studi di Napoli Federico II

This dissertation is submitted for the degree of  
*Doctor of Philosophy*



**A Sasà**





## Acknowledgements

First and foremost I want to thank my advisor Professor Giorgio Ventre for the continuous support of my studies and related research, for his patience, motivation, and immense knowledge.

This PhD thesis is the result of a long path journey, planned and thrived together. We started back with my bachelor thesis in “Definizione della Qualità del servizio in Reti Wireless Beyond 3G” and then kept on going with “Un Algoritmo di Load Balancing Per Reti LTE contro gli Attacchi Denial of Service” to finally reach this milestone. He is THE guide and THE light in my professional carrier and has always forecasted my professional growth. He gave me the opportunity to learn and to learn how to teach others keeping always in mind that curiosity is the key that leads to a good work. I’ve spent the last years being a student between fellow students from all around the world. This experience has given me the opportunity to teach but most of all to learn from each and every of them. To this day I could not be more grateful for an opportunity that still blows my mind every day. I am also thankful for the excellent example he has provided as a successful Head of the Department and Professor.

Besides my advisor, I would like to thank Prof. Stefano Avallone and Prof. Nicola Pasquino for their insightful comments and encouragement, but also for the hard demand that kept me incented to widen my research from various perspectives. I really appreciate Stefano’s caring patient and faithful support during all and the final stages of this Ph.D. I would also like to express my special appreciation and thanks to Nicola. I very much appreciated his enthusiasm, intensity, willingness to do frequent experiments and amazing ability to cleave and challenge me.

Another amazing thank you goes to Giovanni who has been there from ground zero and still has my back.

I thank my fellow ARCLAB and all my PhD mates in for the stimulating discussions, for the lunch breaks and for all the fun we have had in the last four years.

And eventually I am forever indebted to my Academy Colleagues for their enthusiasm, guidance, and unrelenting support throughout this process. They have routinely gone beyond

their duties to soothe my worries, concerns, and anxieties, and have worked to instil great confidence in both myself and my work.

Lastly, I would like to thank my family for all their love and encouragement.

## **Abstract**

4G Long Term Evolution (LTE) mobile system is the fourth generation communication system adopted worldwide to provide high-speed data connections and high-quality voice calls. Given the recent deployment by mobile service providers, unlike GSM and UMTS, LTE can be still considered to be in its early stages and therefore many topics still raise great interest among the international scientific research community: network performance assessment, network optimization, selective scheduling, interference management and coexistence with other communication systems in the unlicensed band, methods to evaluate human exposure to electromagnetic radiation are, as a matter of fact, still open issues.

In this work techniques adopted to increase LTE radio performances are investigated. One of the most wide-spread solutions proposed by the standard is to implement MIMO techniques and within a few years, to overcome the scarcity of spectrum, LTE network operators will offload data traffic by accessing the unlicensed 5 GHz frequency. Our Research deals with an evaluation of 3GPP standard in a real test best scenario to evaluate network behavior and performance.



# Table of contents

<b>List of figures</b>	<b>xiii</b>
<b>List of tables</b>	<b>xv</b>
<b>List of Symbols</b>	<b>xvii</b>
<b>Introduction</b>	<b>xxi</b>
<b>1 LTE Architecture and Radio Procedures</b>	<b>1</b>
1.1 Overview of LTE Architecture . . . . .	1
1.1.1 The User Equipment UE . . . . .	1
1.1.2 Evolved UMTS Terrestrial Radio Access Network E-UTRAN . . . .	2
1.1.3 Evolved Packet Core EPC . . . . .	2
1.2 LTE Radio Procedures . . . . .	3
1.2.1 LTE Radio Resource . . . . .	5
1.2.2 LTE Carrier Aggregation . . . . .	8
1.2.3 Adaptive Modulation and Coding (AMC) . . . . .	10
1.3 Feedback mechanism in LTE . . . . .	12
1.3.1 Reference Signal Received Power (RSRP) . . . . .	13
1.3.2 Received Signal Strength Indicator (RSSI) . . . . .	13
1.3.3 Reference Signal Received Quality (RSRQ) . . . . .	13
1.3.4 Signal to Interference plus Noise Ratio (SINR) . . . . .	14
1.4 Throughput Estimation . . . . .	14
<b>2 LTE MIMO Techniques</b>	<b>19</b>
2.1 Improving Efficiency and Throughput with MIMO . . . . .	19
2.1.1 MIMO in LTE . . . . .	19
2.1.2 Mode Support in LTE . . . . .	23
2.2 SU-MIMO . . . . .	24

2.3	Open, Closed Loop - Spatial Multiplexing . . . . .	25
2.3.1	Open Loop . . . . .	26
2.3.2	Closed Loop . . . . .	26
2.3.3	Transmit Diversity and Closed-Loop Rank-1 - Spatial Multiplexing . . . . .	26
2.4	MU-MIMO . . . . .	27
2.5	MIMO Reporting . . . . .	27
<b>3</b>	<b>LTE in Unlicensed Bandwidth</b>	<b>31</b>
3.1	Brief Overview of LTE and Wi-Fi Access Techniques . . . . .	31
3.1.1	Wi-Fi . . . . .	31
3.2	Problem Statement . . . . .	35
3.3	Basic techniques for a fair coexistence of Wi-Fi and LTE . . . . .	36
3.3.1	Listen-Before-Talk . . . . .	36
3.3.2	Almost Blank Subframe . . . . .	37
3.3.3	Minor techniques . . . . .	39
3.4	Standardization Efforts . . . . .	40
3.4.1	LTE-U . . . . .	40
3.4.2	Licensed Assisted Access . . . . .	42
3.4.3	MuLTEfire . . . . .	44
3.5	LTE First Steps in the Unlicensed Spectrum . . . . .	45
3.6	Performance analysis of Wi-Fi in presence of LTE cells . . . . .	47
3.7	Research proposals for a fair coexistence of LTE and Wi-Fi . . . . .	51
3.7.1	Approaches based on Listen-Before-Talk . . . . .	51
3.7.2	Almost Blank Subframe . . . . .	64
3.7.3	Minor techniques . . . . .	66
<b>4</b>	<b>A Smartphone-Based Assessment of LTE Measurement Procedures</b>	<b>69</b>
4.1	Aim of the Research . . . . .	69
4.2	Smartphone-based Assessment and Methodology Overview . . . . .	69
4.3	Experimental Setup . . . . .	72
4.3.1	Smartphone-Based Measurement Methodology . . . . .	72
4.3.2	Test Methodology . . . . .	75
4.3.3	Aim of the Research . . . . .	76
4.4	Experimental Results and Discussion . . . . .	77
4.4.1	SINR . . . . .	77
4.4.2	CQI, SINR and RSRP Analysis . . . . .	79
4.4.3	Modulation and CQI Analysis . . . . .	82

---

4.4.4	Modulation and Throughput . . . . .	84
4.4.5	Downlink throughput . . . . .	86
4.4.6	Comparing SINR and Throughput . . . . .	89
4.5	Conclusions . . . . .	90
<b>5</b>	<b>LTE MIMO: Experimental Assessment</b>	<b>93</b>
5.1	Aim of the Research . . . . .	93
5.2	MIMO Overview in LTE . . . . .	93
5.3	Experimental Setup . . . . .	96
5.3.1	NEMO Handy Assessment . . . . .	96
5.4	Preliminary Results . . . . .	99
5.4.1	Reference Signal Received Power (RSRP) . . . . .	99
5.4.2	Reference Signal Strength Indicator (RSSI) . . . . .	101
5.4.3	Reference Signal Received Quantity (RSRQ) . . . . .	103
5.4.4	Signal to Interference Noise Ratio (SINR) . . . . .	103
5.5	MIMO Analysis . . . . .	106
5.5.1	Physical Layer Quantities Statistical Analysis . . . . .	108
5.5.2	Channel State Information (CSI) Reporting Analysis . . . . .	111
5.6	Conclusions . . . . .	113
<b>6</b>	<b>Conclusions</b>	<b>115</b>
	<b>References</b>	<b>117</b>





# List of figures

1.1	3GPP LTE Architecture . . . . .	2
1.2	eNodeB Functional Structure . . . . .	4
1.3	Downlink OFDM Frame - TS 36 213 . . . . .	6
1.4	Mapping of downlink reference signals Normal CP - TS 36 211 . . . . .	7
1.5	3GPP Carrier Aggregation (FDD) . . . . .	9
1.6	3GPP Inter and Intra Band Carrier Aggregation . . . . .	9
1.7	Scheduling Architecture . . . . .	12
2.1	MIMO Implementation . . . . .	21
2.2	SU-MIMO . . . . .	24
2.3	MU-MIMO . . . . .	28
2.4	Rank Reporting for mapping MIMO layers . . . . .	30
3.1	Distributed Control Function - RTS/CTS . . . . .	34
3.2	Almost Blank Subframe Structure . . . . .	38
3.3	LTE Duty Cycle . . . . .	39
3.4	Channel Assessment Procedure . . . . .	41
3.5	Listen Before Talk based on LBE - TR 36.889 . . . . .	43
4.1	eNodeBs Crowd Sensing . . . . .	73
4.2	eNodeB's Map along the Route and Handover Occurrence . . . . .	73
4.3	SINR Evolution . . . . .	78
4.4	SINR empirical distribution. . . . .	78
4.5	CQI vs. SINR . . . . .	80
4.6	Regression of SINR as a function of CQI . . . . .	82
4.7	CQI CDF per Modulation . . . . .	83
4.8	SINR vs Throughput . . . . .	85
4.9	Downlink throughput . . . . .	86
4.10	Downlink throughput over time. . . . .	87

4.11	Throughput empirical CDF. . . . .	88
4.12	SINR vs. Throughput for PCC. . . . .	90
4.13	Handover Map . . . . .	91
5.1	Typical test drive configuration . . . . .	95
5.2	MIMO Configuration . . . . .	97
5.3	Reference Signal Received Power - RSRP . . . . .	100
5.4	Reference Signal Strength Indicator - RSSI . . . . .	102
5.5	Reference Signal Received Quality - RSRQ . . . . .	104
5.6	RS Signal Reported - SINR . . . . .	105
5.7	TM Implementation with respect of frequencies . . . . .	106
5.8	RS-related quantities density for each Transmission Mode and CodeWord for Freq. 800 MHz . . . . .	107
5.9	RS-related quantities density for each Transmission Mode and CodeWord for Freq. 2100 MHz . . . . .	107
5.10	RS related quantities for Freq. 800 MHz . . . . .	109
5.11	RS related quantities for Freq. 2100 MHz . . . . .	109
5.12	CQI Reporting for each Transmission Mode and CodeWord for Freq. 800 MHz	110
5.13	CQI Reporting for each Transmission Mode and CodeWord for Freq. 2100 MHz	110
5.14	Rank Reporting for each Transmission Mode . . . . .	112
5.15	PMI Reporting for each Transmission Mode . . . . .	112

# List of tables

1.1	CQI per Coding Rate and Modulation . . . . .	15
1.2	UE Category and Maximum number of TB bits . . . . .	16
1.3	Modulation and TBS Index Table . . . . .	17
2.1	Different Antenna Schemes and Benefits . . . . .	20
2.2	Transmission Mode Table 7.2.3-0 - TS 36213 . . . . .	22
2.3	TM 1,2,3,4 vs CSI . . . . .	28
3.1	Wi-Fi Physical Layers . . . . .	33
3.2	Mean e.i.r.p. limit in dBm - ETSI EN 301 893 . . . . .	39
3.3	Taxonomy of research works . . . . .	53
4.1	Measurement device and software versions . . . . .	74
4.2	Peak Throughput . . . . .	76
4.3	SINR Statistics . . . . .	79
4.4	CQI as a function of RSRP and SINR . . . . .	81
4.5	CQI Statistics per Modulation . . . . .	84
4.6	Throughput Statistics per Modulation . . . . .	85
4.7	Downlink throughput statistics . . . . .	88
4.8	SINR statistics per throughput classes . . . . .	89
5.1	Measurement Tools . . . . .	96
5.2	Nemo Handy Documentation CELLMEAS . . . . .	97
5.3	Nemo Handy Documentation CQI . . . . .	98
5.4	Nemo Handy Documentation CI . . . . .	98
5.5	Nemo Handy Documentation CHI . . . . .	98
5.6	RSRP Mapping - TS 36133 . . . . .	99
5.7	RSSI Mapping - TS 25133 . . . . .	101
5.8	RSRQ Mapping - TS 36133 . . . . .	103

5.9	Port Mapping . . . . .	108
-----	------------------------	-----

# List of Symbols

**SISO** Single Transmission Antenna and Single Receiver Antenna

**SU-MIMO** Single User MIMO

**MU-MIMO** Multi User MIMO

**RS** Reference Signal

**RRM** Radio Resource Management

**QoS** Quality of Service

**TB** Transport Block

**CP** Cyclic Prefix

**AMC** Adaptive Modulation and Coding

**ARO** Application Resource Optimizer

**BLER** Block Error Rate

**CA** Carrier Aggregation

**CQI** Channel Quality Indicator

**CSI** Channel State Information

**FDD** Frequency Division Duplexing

**FIA** Fast and Independent Adjustment

**KPI** Key Performance Indicator

**LTE** Long Term Evolution

<b>MCS</b>	Modulation Coding Scheme
<b>MIMO</b>	Multiple Input Multiple Output
<b>OFDM</b>	Orthogonal Frequency Division Multiplexing
<b>OFDMA</b>	Orthogonal Frequency Division Multiple Access
<b>PCC</b>	Primary Component Carrier
<b>RB</b>	Resource Blocks
<b>RE</b>	Resource Elements
<b>SCA</b>	Slow and Centralized Adjustment
<b>SCC</b>	Secondary Component Carrier
<b>SINR</b>	Signal-to-interference-and noise Ratio
<b>TDD</b>	Time Division Duplexing
<b>TTI</b>	Transmission Time Interval
<b>UE</b>	User Equipment
<b>PRB</b>	Physical Resource Block
<b>RI</b>	Rank Indicator
<b>PMI</b>	Pre-coding Matrix Indicator
<b>CP</b>	Cyclic Prefix
<b>RSRP</b>	Reference Signal Received Power
<b>RSRQ</b>	Reference Signal Received Quality
<b>RSSI</b>	Reference Signal Strength Indicator
<b>3GPP</b>	3rd Generation Partnership Project
<b>HO</b>	Handover
<b>TBS</b>	Transport Block Size
<b>SFBC</b>	space-frequency block code

**FSTD** frequency switched transmit diversity

**SNR** Signal to Noise Ratio

**E-UTRAN** Evolved UMTS Terrestrial Radio Access Network

**EPC** Evolved Packet Core

**SAE** System Architecture Evolution

**EPS** Evolved Packet System

**ME** Mobile Equipment

**P-GW** The Packet Data Network Gateway

**PDN** The Packet Data Network

**APN** Access Point Name

**GGSN** GPRS Support Node

**SGSN** Serving GPRS Support Node

**HSS** Home Subscriber Server

**S-GW** Serving Gateway

**MME** Mobility Management Entity

**PCRF** Policy Control and Charging Rules Function

**UICC** Universal Integrated Circuit Card

**USIM** Universal Subscriber Identity Module

**MT** Mobile Termination

**TE** Terminal Equipment

**LTE-LAA** Licensed Assisted Access-Long Term Evolution

**epdf** experimental probability density function

**TM** Transmission Mode

**CSI** Channel Status Information

**FDPS** Frequency domain packet scheduling

**SM-MIMO** Spatial multiplexing Multiple Input Multiple Output

**MLD-IS** maximum-likelihood detection interference suppression

**ICI** Inter Carrier Interference



# Introduction

The aim of this work is to investigate on the LTE network operating in both licensed and unlicensed spectrum, in order to propose ways to improve performance and efficiency.

LTE MAC layer uses Carrier Aggregation (CA) mechanism exploiting both licensed and unlicensed spectrum to achieve higher performances, throughput and efficiency. LTE mobile system also adopts Adaptive Modulation and Coding (AMC) [1] as a link adaption mechanism and can schedule frequencies both in the licensed and unlicensed bandwidths. In fact, MAC is based on the User Equipment (UE) periodically reporting channel condition summarized through Channel Quality Indicator (CQI) which, in turn, is based on Signal-to-Interference-plus-Noise Ratio (SINR) and Reference Signal Received Power (RSRP).

Since Release 8, 3rd Generation Partnership Project (3GPP) adopted MIMO techniques in LTE standard [2]. The use of MIMO allows the network to improve performance due to the main features of the Multiple Input Multiple Output transmission modes. With MIMO, rather than considering multi-path propagation signals, present in all terrestrial communications, as thermal noise, LTE physical transmissions can consider as a constructive redundancy signals propagating along different paths.

Adopting MIMO involves having multiple antennas at both the transmitter and receiver sides. Also the antennas are able to distinguish different paths between the entities, processing power levels available at both end-point of the link, providing improvements in data rate of signal to noise. To investigate these topics, this thesis deals with the efficient evaluation of the relationship between SINR, RSRP and CQI and also with how to assess AMC effects on LTE performance and with the basic procedures related to MIMO implementation and adoption.

As suggested by the present state of the art, to fully investigate how these techniques work, experimental campaign were conducted through software simulations or measurement campaigns performed in controlled environment such as anechoic chambers. Simulations are commonly adopted because it is very hard to access operators statistics and data, and changes in the network configuration are easy to evaluate and to arrange using a software, while in a real test-bed scenario involving a real operator, even minor variations in the

network configuration can affect end-users QoS perception. In our vision campaigns [3–6] lack precious information, not accounting properly actual channel condition and physical phenomena that a user commonly experiences in his/her everyday usage of the network. To fully address real issues and to fully assess network performance it was fundamental to have a real-time interaction with a real network operator. Although in its early stages of development, the methodology here adopted benefit from smartphones as measurement devices. Due to its novelty it arises as the most appropriate and led us the opportunity to test network performance during actual usage and in a common user scenario.

To overcome the lack of spectrum resources and to further improve LTE capacity, the proposal of extending the standard to the readily available unlicensed spectrum is receiving much attention. However, gaining capacity in a band where Wi-Fi is widely used and guaranteeing a fair coexistence between systems is not an easy-to-address issue. Analyzing the impact of operating LTE in the unlicensed band on the performance of Wi-Fi and devising solutions to minimize such an impact have been the goals of a considerable amount of work carried out by the research community, standardization bodies and telecom operators. A solution to overcome the scarcity of spectrum is to extend LTE by introducing the capability to directly exploit the unlicensed spectrum [7]. The targeted band is the 5 GHz U-NII (Unlicensed National Information Infrastructure) band, because of the availability of approximately 600 MHz already released for usage. However, this band is already being used by Wi-Fi networks (IEEE 802.11a/n/ac/ax), weather radar transmissions, medical devices and some other wireless systems. Therefore, it is necessary for LTE to *fairly* coexist with such technologies in the targeted unlicensed spectrum. A study on the state of the art and current measurement methodologies, advocating the fair coexistence of LTE and other systems in the unlicensed spectrum, exploring standards and coexistence mechanism, is provided in chapter three.

# Chapter 1

## LTE Architecture and Radio Procedures

### 1.1 Overview of LTE Architecture

The System Architecture Evolution (SAE) offers a number of key advantages over previous technologies and systems used for cellular networks spanning from higher spectral efficiency, higher peak data rates, shorter round trip time, increase in variety of frequencies to use and wider bandwidths. Nowadays in fact, the focus of mobile broadband systems is to be able to handle much greater numbers of data transmissions and to ensure levels of latency that have been reduced to around 10 ms.

The Long Term Evolution (LTE) Evolved Packet System (EPS) architecture is comprised of following three main components:

- User Equipment (UE)
- Evolved UMTS Terrestrial Radio Access Network (E-UTRAN)
- Evolved Packet Core (EPC).

The evolved packet core represents the link between packet data networks (Internet), private enterprise networks or an IP multimedia system.

#### 1.1.1 The User Equipment UE

As for UMTS and GSM, the architecture of the user equipment for LTE is called Mobile Equipment (ME). The mobile equipment is composed by the following:

- Mobile Termination (MT) taking care of all the communication functions,
- Terminal Equipment (TE) terminating the informations streams,

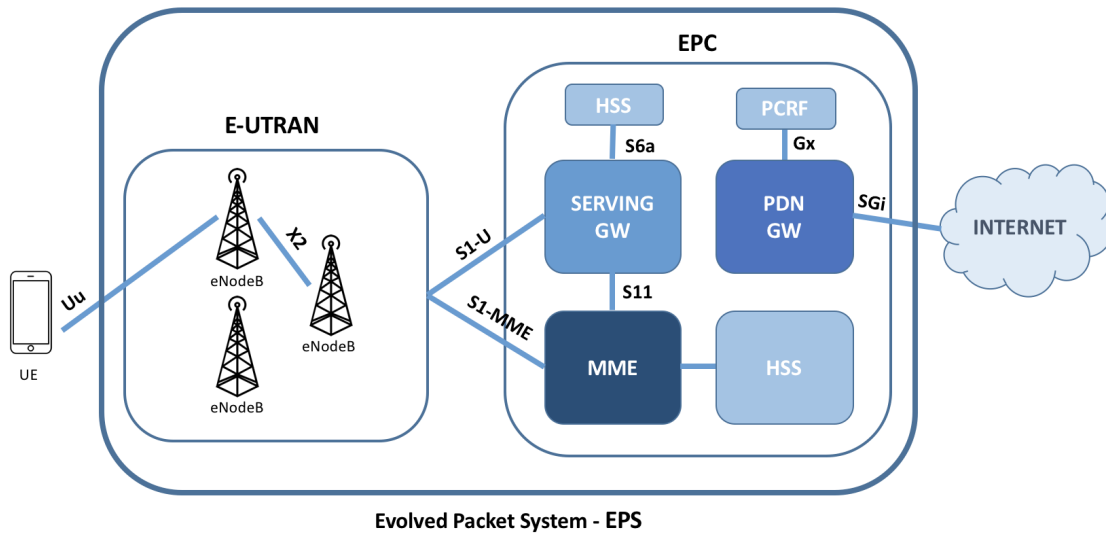


Fig. 1.1 3GPP LTE Architecture

- Universal Integrated Circuit Card (UICC) known as the SIM card for LTE equipments. It comes with the well-known application called USIM.

### 1.1.2 Evolved UMTS Terrestrial Radio Access Network E-UTRAN

E-UTRAN was first introduced in 3GPP Release 8 as the access part of LTE Architecture. E-UTRAN handles the radio communications between the mobile and the EPC and is composed by evolved base stations, called eNodeBs or eNBs. The eNB controls also low-level operation sending signalling messages such as handover commands. Each eNB controls the UEs in one or multiple cells but LTE mobiles communicate with just one base station and one cell at a time. Each eNB then, connects with the EPC by means of the S1 interface and it can also be connected to nearby base stations by the X2 interface as shown in Fig. 1.1.

### 1.1.3 Evolved Packet Core EPC

While with GSM, the architecture relies on circuit-switching, LTE was designed to adopt IP as the key protocol to handle all services. EPC in SAE handles the overall control of the UE.

Here is a brief description of each of the components shown in Fig. 1.1:

- The Packet Data Network Gateway (P-GW) represents the conjunction with a The Packet Data Network (PDN), through SGi interface. Each PDN is labelled by an Access Point Name (APN). A PDN gateway acts as the GPRS Support Node (GGSN) and the Serving GPRS Support Node (SGSN) used in UMTS and GSM networks.

- Serving Gateway (S-GW) behave as a router and forwards informations between an eNodeB and the PDN gateway.
- Home Subscriber Server (HSS) is a centralized database that contains information about all the network operator's subscribers.
- Mobility Management Entity (MME) in charge of all the higher-level operation of the UE interpreting signalling messages and HSS. It is also responsible for tracking area list management, selection of PGW/SGW and also selection of other MME during handovers. MME takes care of bearer management functions including establishment of dedicated bearers for all signaling traffic flow.
- Policy Control and Charging Rules Function (PCRF) is the main responsible for what concerns policy control and decision-making. The serving and PDN gateways are connected through the S5/S8 interface.

## 1.2 LTE Radio Procedures

To improve LTE performances and to share the channel among multiple users, 3GPP introduced Orthogonal Frequency Division Multiple Access (OFDMA). OFDMA uses Orthogonal Frequency Division Multiplexing (OFDM) for downlink physical transmission. All the resources that can be allocated to a user are scheduled by eNodeBs equipped with fully structured packet schedulers.

To even further improve LTE performances the architecture combines a large number of separate LTE carriers to provide a wider spectrum to users, in fact Carrier Aggregation (CA) mechanism was introduced by 3GPP since Release 10. CA allows the user to have a Primary Component Carrier (PCC) as an anchor to the eNodeB and one or multiple Secondary Component Carrier (SCC) as offloading carries. OFDM as a digital multi-carrier modulation method together with CA tries to take network performance at a whole new level [8].

Eventually 3GPP addressed the need to improve transmission reliability and rate, so it adopted Adaptive Modulation and Coding (AMC) to adapt the Modulation Coding Scheme (MCS) used by the user. A UE periodically reports to the eNodeB the measured channel quality trough the Channel Quality Indicator (CQI) to properly set MCS.

OFDMA also facilitates frequency-domain scheduling and is strongly suited to advanced Multiple Input Multiple Output (MIMO) techniques. With MIMO data stream is multiplexed over a large number of narrow-band and orthogonal sub-carriers. The large number of parallel, narrow-band transmission on orthogonal sub-carriers in the frequency domain reduces the

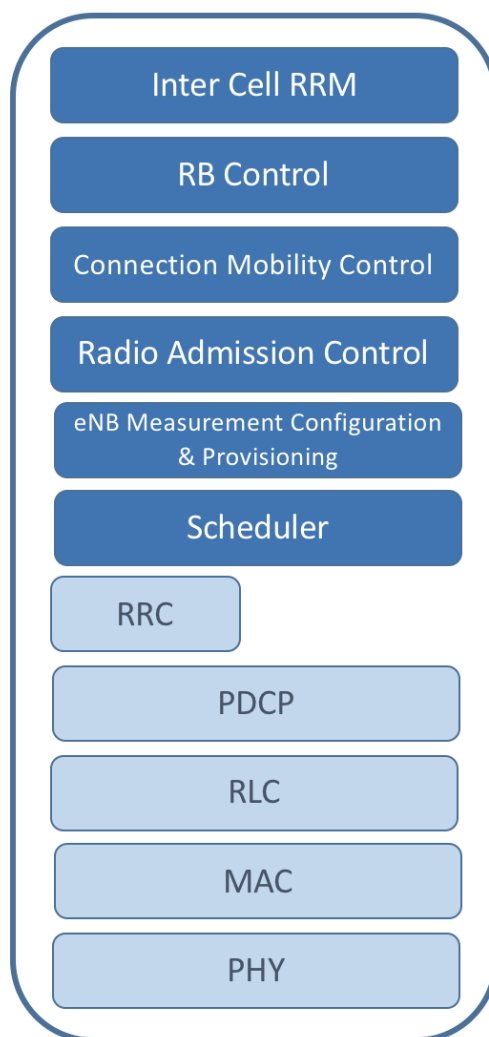


Fig. 1.2 eNodeB Functional Structure

impact of interference and increase performance. The following section are going to describe into more detail some of the basic functionalities of an eNodeB (Fig. 1.2).

### 1.2.1 LTE Radio Resource

OFDM in LTE has two different frame structure: *Type 1*, which is used for the LTE Frequency Division Duplexing (FDD) mode systems and *Type 2* used for the LTE Time Division Duplexing (TDD) systems [9]. Also recently 3GPP Release 13 provided a frame structure of *Type 3* to allow a fair coexistence in unlicensed bandwidths with Wi-Fi systems [9]. Type 1 frame and type 2 frame have an overall length of 10 ms, with a total of 10 subframes in a frame. Every single subframe is composed by 2 time slots.

The standard also defines together with the *frame*, composed of 10 adjacent sub-frames, the *half-frame*, half of the former, which are both used basically to allow for the synchronization between UEs and eNodeBs and to carry all the necessary control information.

The basic unit of resource is the Resource Blocks (RB). Each RB lasts 1 time slot and occupies 180 kHz spanning on a set of sub-carriers. A RB is the smallest entity that can be scheduled to a UE. Different sets of RBs can then be allocated to different users to support the sharing of the channel resources. Such a division in time and frequency domains allows to efficiently allocate several users on the same channel with fine granularity. The number of available RB depends also on the channel bandwidth that in LTE can have different widths up to 20 MHz. A RB is composed by 12 consecutive subcarriers in the domain of frequency and 6 or 7 symbols in the domain of time. The number of symbols in a frame depends on the Cyclic Prefix (CP) in use. A CP, as the name suggests, is an information that is periodically repeated working as a guard band between LTE symbols. When a normal CP is implemented, every RB has 7 symbols. When an extended CP is used, the Resource Elements (RE) contains 6 symbols. With Type 2 the radio frame is composed of two half frames, each of 5ms duration with a total frame duration again of about 10ms. Every radio frame has a total of 10 subframes and for each subframe 2 time slots are occupied. Also in the standard a RE is defined as the smallest unit which consists of one OFDM sub-carrier during one OFDM symbol interval.

Mostly all LTE channels reserve space for carrying special informations, as a sequence of bits. Reference Signal (RS) is in fact, a special signal that exists at physical layer and higher layer channel rely on its transmission. This is not for carrying any specific information but has the purpose of deliver the reference point for the downlink power. Basically in addition to data, each sub-frame carries also signaling and control information in addition to users' traffic. Reference symbols are composed by complex values which are determined accordingly to the symbol position as well as of the cell. RS are computed by a two-dimensional orthogonal

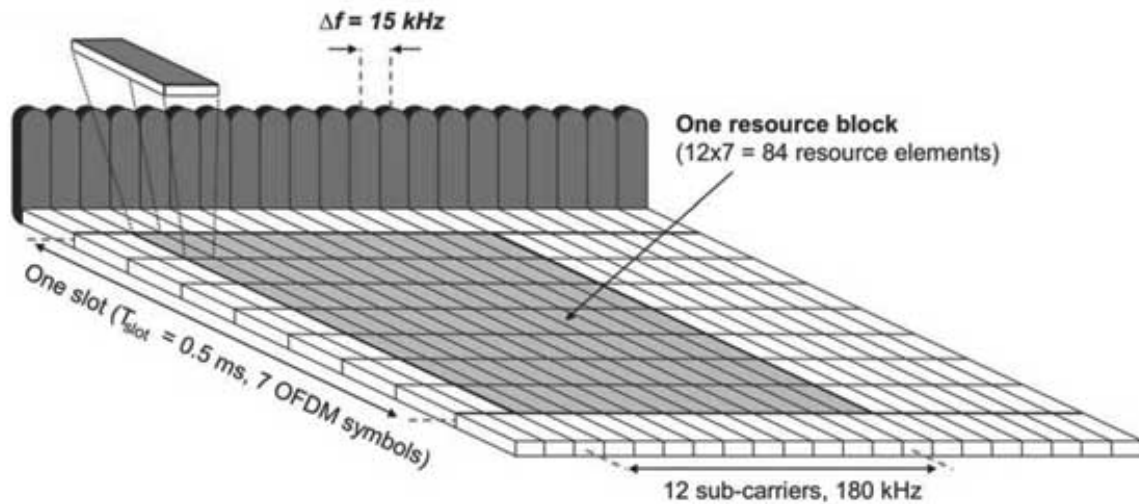


Fig. 1.3 Downlink OFDM Frame - TS 36 213

and a two-dimensional pseudo-random sequence. Downlink data and control informations are multiplexed in time within the same subframe. In each subframe the first 1-3 OFDM symbols are mainly devoted to signaling purpose while the remaining carry out users' data. This pattern design though is quite flexible from a eNodeB point of view is also able to avoid unnecessary overhead. Data transmission is allowed to occupy the remaining 14 symbols, depending on the containing frame format. LTE cells are always occupying the channel since signaling and control data is continuously sent, even when there is no user data to transmit. Such persistent signal is able to prevent other technologies deployed on the same frequency from transmitting. For instance, Wi-Fi users refrain from transmitting when detecting a signal power above a fixed threshold. RS signals are carried by particular RE in every time slot and the location of the resource elements are specifically determined by the eNodeB transmission configuration. Also when MIMO techniques and different antenna schemes are adopted, knowing that LTE standard defines antenna ports as virtual entities distinguished by their own RS it is pretty straightforward that multiple antenna ports signals can be transmitted on a single transmit antenna and on the contrary a single antenna port can be spread on multiple transmit antennas. In case of two transmit antennas, RSs are inserted from each antenna where the reference signals on the second antenna are offset in the frequency domain by three subcarriers.

The eNodeB scheduler based on configurable parameters measurement adopt different channel characteristics for users' transmissions. Since OFDMA ideally provides no inter-channel interference, schedulers work with a granularity of one Transmission Time Interval (TTI) and one RB in the time and frequency domain, respectively. At the eNodeB, a first scheduling algorithm is performed in the time domain, and here users are selected for



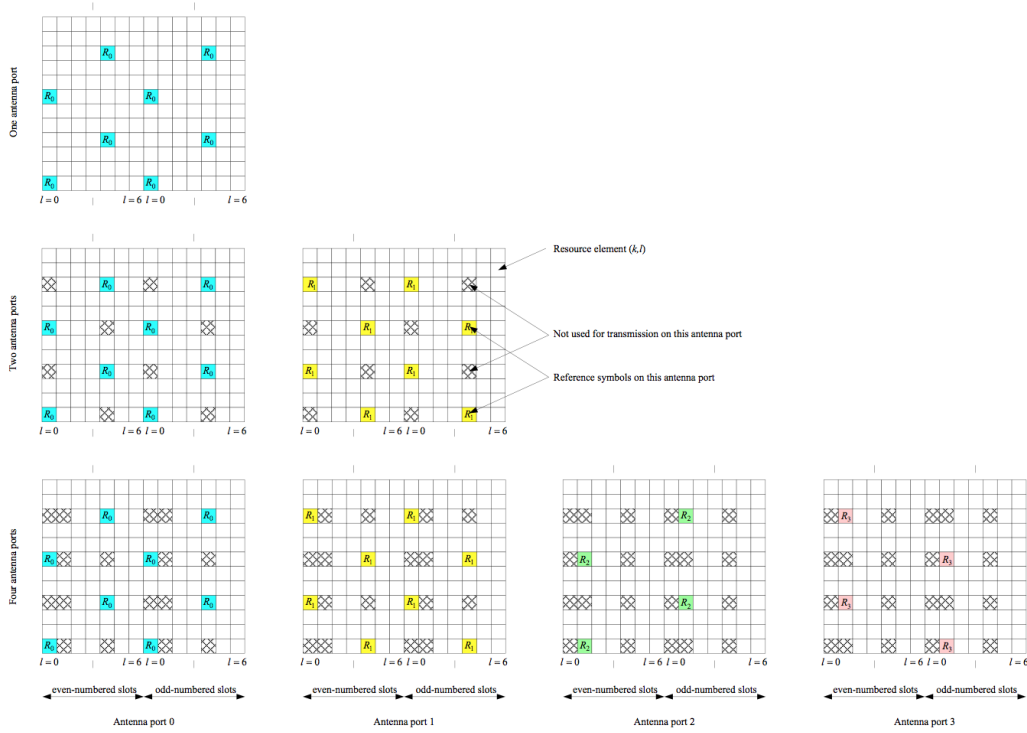


Fig. 1.4 Mapping of downlink reference signals Normal CP - TS 36 211

potential scheduling based on their required QoS. If some user then have pending data for transmission they are re-configured for scheduling in the next TTI. Then the second algorithm in the frequency domain allocates RBs to them.

There are, indeed, several possible methods for scheduling RBs to users, and the LTE standard does not prescribe any particular algorithm to follow. 3GPP LTE Releases left vendors free to adopted their own scheduling algorithm and therefore different networks can employ different scheduling policies, depending on the manufacturer of the devices and the configuration made by the operators. The main goal of an efficient scheduling algorithm has two main purposes, maximize throughput and achieve fairness between users. Today in use there are many algorithms developed for wireless system, such as maximum rate scheduling, Round Robin, best CQI, Proportional Fair, max-min and Resource Fair. Data from the upper layer given to the physical layer in LTE system is basically referred as multiple of Transport Block (TB)s. TBs scheduling process are deployed in the eNodeB which is the one implementing the feedback mechanism to improve channel transmissions based on periodical reports CQIs. Every TTI, all the assessment AMC procedure are performed by the UE, they result into the CQI Report containing all the channel quality information see Fig. 1.7

Based on AMC the eNodeB at first picks the modulation scheme that could be used and then checks for the available physical resources in the RB grid as well as the transmission

parameters including the type of MCS. The FD algorithm uses the channel conditions matrix available from the Channel State Information manager to avoid experiencing deep fading.

### 1.2.2 LTE Carrier Aggregation

In order to achieve a higher channel capacity and thus throughput, carrier aggregation was introduced by 3GPP since Release 10. CA allows mobile network operators to combine a number of separate LTE carriers in frequency to provide a wider spectrum to its end-users. CA technology aggregates multiple small band segments into maximum 100 MHz virtual bandwidth to achieve a higher data rate. Extra channels, called *Component Carriers*, can have different widths and can be allocated and de-allocated on needs. Each station is always connected, though, to a licensed carrier, which is called PCC. While being connected to such PCC, the station can connect to other unlicensed carriers which are called SCC. To each UE several SCC are accessible at the same time. Accordingly to the UE QoS demand and cell capacity, configuration information can be sent via PCC to dynamically remove or add more or less SCCs. All of the SCCs, as mentioned above, can be changed dynamically during the time the user is served by the eNodeB, by means of configuration messages over the PCC. There are two operation modes for LAA: supplemental downlink (SDL) and TDD. SDL mode is the easiest form where the unlicensed bandwidth is mainly used for downlink transmission, as downlink traffic is typically oriented towards user's information traffic offloading. When using a TDD mode, the unlicensed bandwidth is adopted for both downlink and uplink, as the LTE TDD system practically works in licensed bands. TDD mode grants the flexibility to dynamically exchange resource allocation between downlink and uplink. Although on the user side implementation complexity increases with the implementation of mechanisms such as LBT features and radar detection requirements.

LTE channels can vary in widths, spacing up to 20 MHz in frequency in order to further improve width limits and therefore increase throughput. This technique allows the use of extra frequency space, both in the licensed and, hopefully, in the unlicensed spectrum, together with the main channel, to obtain higher capacity. Such extra frequency channels, called *component carriers*, as shown in Fig. 1.5, can have different bandwidths, i.e. 1.4, 3, 5, 10, 15 or 20 MHz, and can be allocated and de-allocated dynamically. Up to five CC can be simultaneously aggregated to the principal carrier allocated to the UE.

All the configured Component carriers are usually not contiguous in the frequency domain. A dynamic allocation of the component carriers allows, for example, telecommunication operators with a higher granularity in fragmenting the spectrum that can provide users a higher data rate by exploiting the overall bandwidth in both unlicensed and licensed spectrum.

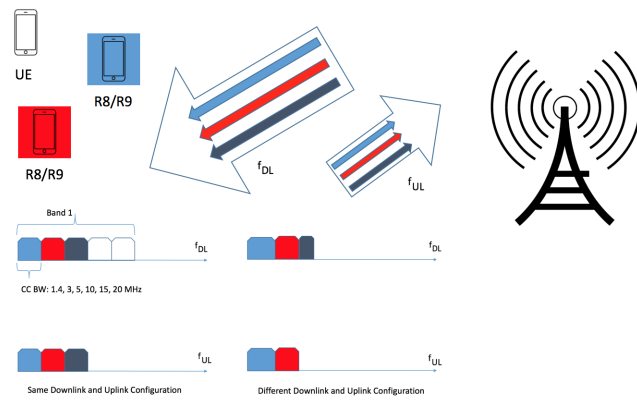


Fig. 1.5 3GPP Carrier Aggregation (FDD)

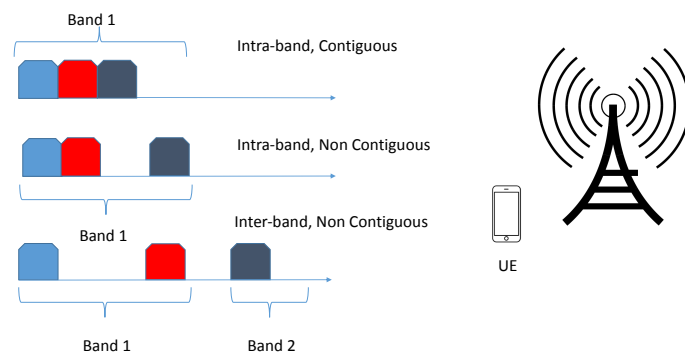


Fig. 1.6 3GPP Inter and Intra Band Carrier Aggregation

With respect to the frequency location of the different component carriers, three different cases are possible (Fig. 1.6):

- *Intra-band aggregation with frequency-contiguous component carriers;*
- *Intra-band aggregation with non-contiguous component carriers;*
- *Inter-band aggregation with non-contiguous component carriers.*

Eventually 3GPP proposed a new concept for LTE radio access network to operate in the unlicensed spectrum as part of a Release 13. It is possible for user to adaptively change from using LTE or Wi-Fi. Obviously a coordination between different Radio Access Technologies is needed and also modification to protocols stacks and interface functionalities need to be improved. Resource allocation becomes an issue to resolve as also user service continuity. In order to meet these requisites, Licensed Assisted Access-Long Term Evolution Licensed Assisted Access-Long Term Evolution (LTE-LAA) is emerging as the candidate technology to be utilized in unlicensed spectrum for wireless data traffic offloading. LAA-LTE uses carrier aggregation combining licensed and unlicensed bands, delivering cellular services to mobile users in the 5-GHz unlicensed band. The deployment of most interest is small cell, which provides access to both licensed and unlicensed spectrum for indoor and outdoor environment.

### 1.2.3 Adaptive Modulation and Coding (AMC)

Radio Resource Management (RRM) is performed by eNodeBs with the goal of maximizing network efficiency and Quality of Service (QoS) over the air interface. RRM functionalities deal with a range of algorithms employed to perform in a whole cell function such as packet scheduling, admission and load control as well as making Handover (HO) decision based on specific algorithms. With packet scheduling function and AMC the eNodeB is in charge of allocating available radio resources among active users.

To improve transmission reliability and rate, in fact, LTE uses AMC [1] that enables the ability of the network to change modulation type and the coding rate dynamically, accordingly to the current radio channel conditions. eNodeBs in fact, have a channel dependent scheduling policy and decisions are made based on channel conditions. Using a feedback mechanism, the UE periodically reports to the eNodeB the measured channel quality through the CQI. The reported CQI is used to satisfy the following purposes:

- selection of the appropriate modulation and coding scheme
- time and frequency efficient scheduling

- interference management
- transmission power control

The overall procedure takes place periodically. The basic principle here adopted is to allocate RBs to the users with relatively better channel conditions, and to avoid RB allocation to those experiencing deep interference or fading. All users involved in AMC need to report the CQI computed by decoding the reference signals to the eNodeB which determines MCS based on instantaneous channel quality. If channel conditions are favorable, higher-order modulation schemes with higher spectral efficiency (hence with higher bit rates) like 64QAM are adopted. On the other hand when poor conditions are detected, AMC can select a lower-order modulation scheme like QPSK, which is more robust against transmission errors at the cost of a lower spectral efficiency. Depending on channel quality for each specific modulation scheme, an appropriate code rate can be eventually chosen. The better the channel quality, the higher the code rate adopted and of course the higher the data rate achieved.

The 3GPP standard defines the Key Performance Indicators (KPIs) at all network levels to correctly evaluate network efficiency. The most relevant parameters are:

- *Throughput*
- *Latency*
- *Packet Loss*
- *Reference Signal Received Power, RSRP*
- *Received Signal Strength Indicator, RSSI*
- *Reference Signal Received Quality, RSRQ*
- *Signal-to-Interference-plus-Noise Ratio, SINR*

The elaboration of the above listed parameters is the basics knowledge required for the CQI computation. It is hard though to correctly estimate these parameters and to efficiently map the quantities to obtain the maximum throughput possible and to improve the network overall performance.

To estimate channel conditions the user equipment will interpolate over multiple RSs. UEs use RS for downlink channel estimation. Based on the signaling and control signals stations evaluate the quality of the received transmissions and send the measures back to the base station in a CQI feedback report.

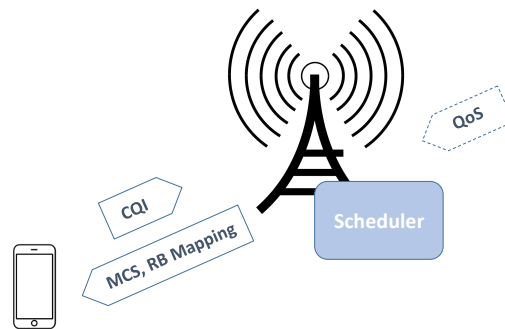


Fig. 1.7 Scheduling Architecture

### 1.3 Feedback mechanism in LTE

In LTE network, UEs usually estimate channel state information and aggregate it into a Channel Status Information (CSI) Report, simply analyzing network data retrieved from physical layer measurement.

CSI comprises:

- Channel Quality Indicator - (CQI)
- Precoding Matrix indicator - (PMI)
- Precoding Type indicator - (PTI)
- Rank Indication - (RI)

Measurements should be conducted to determine the optimal CQIs under different CSI conditions. The reported CQI is a number between 0 (worst case) and 15 (best case), as shown in Table 1.1, indicating the most efficient MCS which would lead to a Block Error Rate (BLER) of 10%. BLER measures the successful transmission rate at MAC and physical layer. Each CQI value in fact, is sharply associated with an MCS index, a spectral efficiency (b/s/Hz) and coding rate. Depending on the CQI a combination of modulation scheme, number of spatial streams and code rate MCS is selected [10]

Also there are two kinds of CQI reporting: *periodic* and *aperiodic*. Usually periodic CQIs are employed but if eNodeB needs channel quality information at a specific time, aperiodic CQIs are triggered. Aperiodic CQIs are mainly due to used loss of synchronization or handover and requested by the eNodeB by setting a CQI request bit on the Physical Downlink Control Channel (PDCCH).

To compute CQI in LTE downlink, channel quality parameters are measured and aggregated periodically. Although CQI is defined by the 3GPP, numerical computation and

measurement represent an issue to address if they rely only on the CQI to perceive network status [11]. It is pretty obvious that Signal-to-interference-and noise Ratio (SINR), Reference Signal Received Power (RSRP), Reference Signal Strength Indicator (RSSI), Reference Signal Received Quality (RSRQ) play important roles to CQI measurement. Channel quality is represented by SINR which is usually computed for link adaptation along with packet scheduling, whereas RSRP and RSRQ are key values for handover making decision when intra E-UTRAN handover occur in LTE.

### 1.3.1 Reference Signal Received Power (RSRP)

For a particular cell, RSRP is defined as the average power (in Watts [W]) of the REs that carry cell-specific RSs within the considered bandwidth. RSRP measurement, normally are expressed in dBm. If a single UE is capable to receive multiple RS over different antenna ports, their combination is quite powerful and constructive to determine RSRP. For the purpose of RSRP determination a cell-specific reference signals R0 according [9] shall be used. Basically RSRP is a power measurement for a single subcarrier, a cell-specific signal strength related metric that is used as an input for cell resection and handover decisions. The value does not change with bandwidth or number of RBs currently assigned for data transmissions. So, this measurement would give you the lowest value comparing to other parameters and an idea of the strength of the signal a UE gets from the network, but it is not clearly stated which the signal quality is. RSRP is used mainly to rank among different candidate cells in accordance with the signal strength they provide.

### 1.3.2 Received Signal Strength Indicator (RSSI)

RSSI is the linear average of the *total received power* observed, including co-channel non-serving and serving cells, adjacent channel interference and thermal noise, within the measurement bandwidth over N RBs. RSSI is defined as the received wide band power, taking into account also thermal noise and noise generated in the receiver, within the bandwidth defined by the receiver demodulator. A reference point for the measurement should be the antenna connector of the single user.

### 1.3.3 Reference Signal Received Quality (RSRQ)

RSRQ measurement is a cell-specific signal quality metric. As RSRP measurement, this parameter is used mainly to provide ranking among different candidate eNodeB accordingly with their signal strenght and quality. This metric can be employed as an input in making

cell re-selection and handover decisions in scenarios, for example, in which the RSRP measurements are not sufficient to make reliable cell-re-selection/handover decisions. Reference Signal Received Quality (RSRQ) can be defined as:

$$RSRQ = N \cdot \frac{RSRP}{RSSI} \quad (1.1)$$

where N is the number of RB's of the E-UTRA carrier of the LTE carrier RSSI measurement bandwidth. The measurements in the numerator and denominator should be assessed over the same set of RBs. If higher-layer signaling indicates that a particular subframes is suitable for performing RSRQ measurements, then RSSI is taken over all OFDM symbols in the preferred subframes. The reference point for the RSRQ should be the antenna connector of the user. RSSI is used as a primary quantity to compute LTE RSRQ measurement. It is also clear that due to the inclusion of RSSI, RSRQ includes also the effect of signal strength and external interferences. It is also possible to observe that mathematically RSRQ is proportional to RSRP.

### 1.3.4 Signal to Interference plus Noise Ratio (SINR)

SINR is measured by UE on RB basis. UE's granularity on SINR computation is per RB. It converts it into CQI and send it to eNodeB where it is adopted to select the most suitable MCS for user informations transmissions within a particular RB. SINR suggests which MCS to use for a particular Resource Block, the quantity of bits per symbol to be sent and the throughput to be obtained for that RB as well as the number of RBs to be allocated by eNodeB to UEs. SINR is defined as the ratio of the signal power to the summation of the average interference power from all the neighbor cells and the thermal noise. RSRP, RSRQ and RSSI measurements are defined by 3GPP, however SINR is not defined in 3GPP specifications, but fully addressed in UE vendors standards.

## 1.4 Throughput Estimation

Most commonly LTE in its physical layer adopts only FDD, to achieve in both uplink and downlink symmetrical bandwidth. To fully understand the potential of the FDD paired spectrum, LTE adopting it, is capable to achieve 20 MHz in throughput both in uplink and downlink. Also different bandwidth are presented: 1.4, 3, 5, 10, 15, 20 MHz [12] and play a key role in affecting throughput value. Each bandwidth is composed by a specific number of RBs which as previously stated represent the smallest unit of resources that can be allocated to a single user. When estimating throughput, it is needed to take into account that RBs



Table 1.1 CQI per Coding Rate and Modulation

CQI	Modulation	Code Rate	MCS	Efficiency
0		Out of Range		
1	QPSK	78	1	0.1523
2	QPSK	120	3	0.2344
3	QPSK	193	5	0.3770
4	QPSK	308	7	0.6016
5	QPSK	449	9	0.8770
6	QPSK	602	11	1.1758
7	16QAM	378	13	1.4766
8	16QAM	490	15	1.9141
9	16QAM	616	17	2.4063
10	64QAM	466	19	2.7305
11	64QAM	567	21	3.3223
12	64QAM	666	23	3.9023
13	64QAM	772	25	4.5234
14	64QAM	873	27	5.1152
15	64QAM	948	29	5.5547

Table 1.2 UE Category and Maximum number of TB bits

<b>Cat.</b>	<b>Max Nr° TB bits</b>
1	10296
2	51024
3	102048
4	150752
5	299552
6	301504
7	301504
8	299856
9	2998560
10	2998560
11	603008
12	603008

have a total size of 180 kHz in the frequency domain and 0.5 ms in the time domain. In time domain a TTI lasts 1 ms and consist of 12 subcarriers in the frequency domain, and since 12 OFDM subcarriers are used in a single RB, the bandwidth of a RB is 180 kHz. An OFDM subcarrier is 15 kHz, so with a bandwidth of 20 MHz the overall system deploys  $18\text{MHz}/15\text{kHz} = 1200$  subcarriers. A 10% of the BW is reserved for guard band but this assumption is not valid with 1.4MHz wide carrier.

As previously stated MAC layer selects the modulation and coding scheme to configure the physical layer transmissions. The data at MAC level, are now in the shape of Transport Block Size (TBS), and the quantity of bits transferred in a 1ms transport block size strictly depends on the MCS and the number of resource blocks assigned to each UE [10].

User Category Information plays also a key role in maximizing throughput. Knowing a UE Category allow the eNB to transmit efficiently with all the UEs connected to it. The UE-Category defines the ability of the device in terms of DL/UL throughputs as specified in [13]. The maximum number transport block bits received within a TTI are shown in Tab. 1.2. For each TBS index specifies the TB dimension with regard to the number of RB assigned to that particular user. Higher modulation order corresponds to higher TBS dimension and MCS as shown in Table 1.3. With higher CQI values AMC uses higher order modulation but also in this case if a user is assigned with a larger number of RBs (NRBs) also uses a

Table 1.3 Modulation and TBS Index Table

<b>MCS</b>	<b>Modulation Order</b>	<b>TBS Index</b>
$I_{MCS}$	$Q_m$	$I_{TBS}$
[0, ..., 9]	2	[0, ..., 9]
[10, ..., 16]	4	[9, ..., 15]
[17, ..., 28]	6	[15, ..., 26]
29	2	Reserved
30	4	Reserved
31	6	Reserved

bigger size of TBs. TB size depends in fact, from the data quantity to send to the user. If the amount of data to send is smaller than the selected TBS a smaller TB would be used. Knowing the size of the TB is straightforward to compute throughput [14]. If the eNodeB selects a MCS 20 and assigns 2 RBs based on the received CQI, from 1.3, it is evident that TBS index is equal to 18. Referring to the standard Table 7.1.7.2.1-1 of [10], to a index 18 with 2 RB corresponds a TB of 776 bit. We will have a single TB in a TTI (1ms):

$$T_{nom} = 776 \text{ bits} \cdot 1000 = 776000 \text{ bits/second} = 0.77 \text{ Mbps}$$



# Chapter 2

## LTE MIMO Techniques

### 2.1 Improving Efficiency and Throughput with MIMO

MIMO has been adopted since many years in Wireless Networks, Wi-Fi standards in fact incorporated this technology since 802.11n. *Multiple-Input Multiple-Output* as the name suggests means that this technology allows to transmit at faster speeds by sending data through multiple receiving and transmitting antennas.

Using MIMO enhances the performance and enriches network connections compared to those adopting single-antenna techniques. Although its development dates back at ten years ago, only recently LTE networks involved MIMO in standard's architecture. 3GPP technology in fact, has lastly evolved from the original Single-User transmission to a Single User MIMO (SU-MIMO) and a Multi User MIMO (MU-MIMO). LTE standard adopts multiple antenna techniques to improve system and radio network performance in a variety of different scenarios.

Multi-antenna technologies for reception and transmission at the eNodeB and in UEs in LTE today play a critical role in achieving the high performance offered to LTE. MIMO in fact, grants radio systems to reach higher performances by using multiple antennas at both their transmitters and receivers. From Release 10, LTE is able to implement up to eight antennas in downlink.

#### 2.1.1 MIMO in LTE

With LTE MIMO can adopt the following configurations 2x2, 4x4 and 8x8, respectively for Transmit and Receiver Antennas. It can also be configured in two modes: Spatial Multiplexing and Transmit Diversity.

Table 2.1 Different Antenna Schemes and Benefits

<b>Tx Data Streams</b>	<b>Multiantenna Scheme</b>	<b>Gain</b>	<b>Benefits</b>
One	Transmit Diversity	Diversity Gain	Link Robustness Coverage
	Classical beam forming	Antenna gain	Coverage Capacity
Multiple	Spatial Multiplexing	Capacity Gain	Spectral Efficiency Data Rates

In detail we have:

- *Spatial multiplexing*: the aim of Spatial Multiplexing is to transmit multiple different data streams over different parallel channels in order to increase data rate. it takes advantage of multi-path propagation to create a number of independent transmission channels between the transmitter and receiver, which enables two or more different signal streams to be transmitted simultaneously. Using the proper coding and signal processing informations can be extracted independently at the receiver side. This technique leads to an increase of the available throughput to an individual user or allows to multiplex data from multiple users. The maximum channels that can be multiplexed together is equal to the smaller of the number of antennas on both the transmitter and receiver side.
- *Transmit Diversity*: if a single user is taking advantage of single information flow Transmit Diversity can reach spatial diversity performances with the use of multiple antennas at the transmitter side. Several versions of the same information stream are sent to the receiver to prevent from fading and improve SINR gain. Transmit diversity techniques are adopted when a UE is experimenting the worst channel conditions.

Both closed Loop and Open Loop are implemented to reach spatial diversity in LTE. With Open loop spatial diversity is in adopted blindly while with the use of closed loop control informations will be collected from UEs to properly weight antennas.

To efficiently maximize throughput using MIMO the network needs [15]:

- Max Rich Scattering Conditions
- Configuring eNodeB to properly match channel conditions
- Efficient assessment campaign carried out from UE

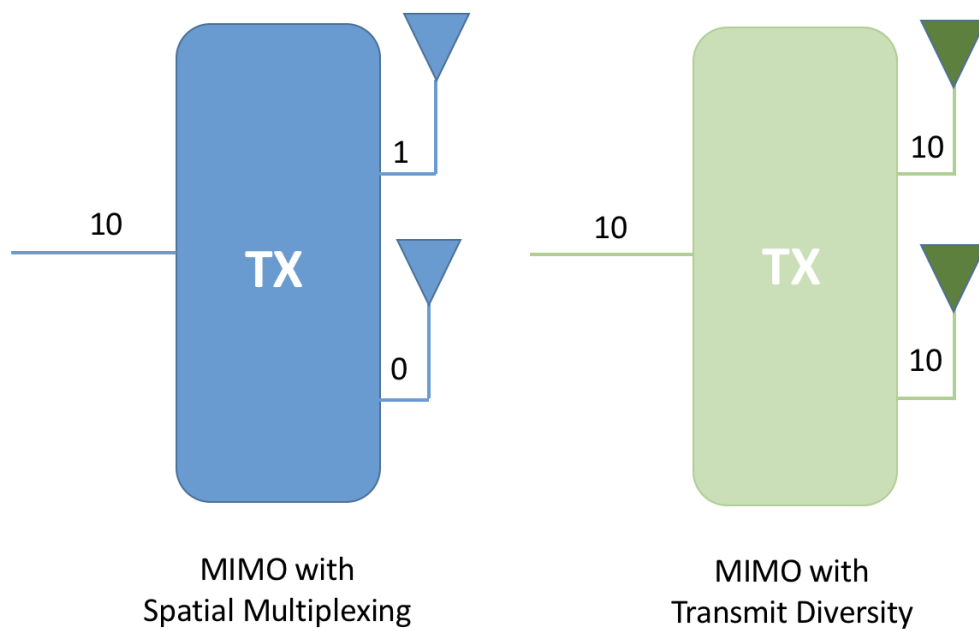


Fig. 2.1 MIMO Implementation

Table 2.2 Transmission Mode Table 7.2.3-0 - TS 36213

<b>TM</b>	<b>Transmission scheme of PDSCH</b>
1	Single-antenna port, port 0
2	Transmit diversity
3	Transmit diversity if rank indicator is 1, or large delay CDD
4	Closed-loop spatial multiplexing
5	Multi-user MIMO
6	Closed-loop spatial multiplexing with a single transmission layer
7	If number of antenna ports is one, Single-antenna port, port 0; or Transmit diversity
8	If UE is configured without PMI/RI reporting: if the number antenna ports is one, single-antenna port 0; or transmit diversity, if the UE is configured with PMI/RI reporting: closed-loop spatial multiplexing
9	If the UE is configured without PMI/RI reporting: if the number of antenna ports is one, single-antenna port 0; otherwise transmit diversity, if the UE is configured with PMI/RI reporting: if the number of CSI-RS ports is one, single-antenna port, port 7; otherwise up to 8 layer transmission, ports 7-14
10	If UE is configured without PMI/RI reporting: if the number of CSI-RS ports is one, single-antenna port 7; or transmit diversity, if UE is configured with PMI/RI reporting: if the number of CSI-RS ports is one, single-antenna port 7; otherwise up to 8 layer transmission, ports 7-14



### 2.1.2 Mode Support in LTE

LTE supports different transmission mode configured for each UE. Mode is computed by both the capability of the user and also the capabilities of the serving eNodeB. All UEs are configured with a particular transmission mode to determine how to work with received data.

In the downlink, LTE uses technologies such as MIMO to achieve high data rates, however, it also offers fall-back technologies such as transmit diversity or Single Transmission Antenna and Single Receiver Antenna (SISO). For example, what it is commonly called SISO is implemented in TM1 (*Transmission Mode 1*). What is usually known as *Diversity* is identified with TM2. Eventually MIMO is introduced in TM4 and TM3.

A good summary of each Transmission Mode is shown in the following Table 2.2 or found in Table 7.2.3-0 of [10].

When Transmission Mode (TM)1 is in use the system transmits one single layer from each antenna port. RS signals combined with data are transmitted adopting the same antenna configuration. In order to demodulate the signal at receiver's side only the RS related to that particular user is required. Although many antennas are simultaneously transmitting, with this technique a single UE is not aware of the actual number of parallel transmission and perceives data as transmitted in a single stream.

To improve SINR and robustness of transmission TM2 implements a classical MIMO. All data are in fact, sent via multiple antennas equipped with different modulation schemes and frequency configurations.

When TM2 is in use only a single layer is mapped with a space-frequency block code (SFBC) that relies on Alamouti code, and transmitted from multiple antennas. When two antennas are adopted, a frequency-based version of SFBC is used, while with a combination of four antennas, a mix of SFBC and frequency switched transmit diversity (FSTD) is used.

In the case scenario of a UE moving at high speed, so when channel information is missing or when the channel rapidly changes, Spatial Multiplexing is implemented with TM3.

When TM4 is implemented each transmission is mapped to one or more layers. TM4 adopts a *Closed Loop* technique which grants channel estimation at the receiver.

Transmission mode 5 implements MU-MIMO enabling single-layer transmission to multiple users sharing the same frequency allocation. TM5 is also based on codebook-based closed loop spatial multiplexing.

TM 6 implements a variation of TM 4 closed loop spatial multiplexing using a single transmission layer. Here UEs estimate the channel and send the index of the most suitable precoding matrix back to the eNodeB. All eNodeBs send the precoded signal via all the antenna ports.

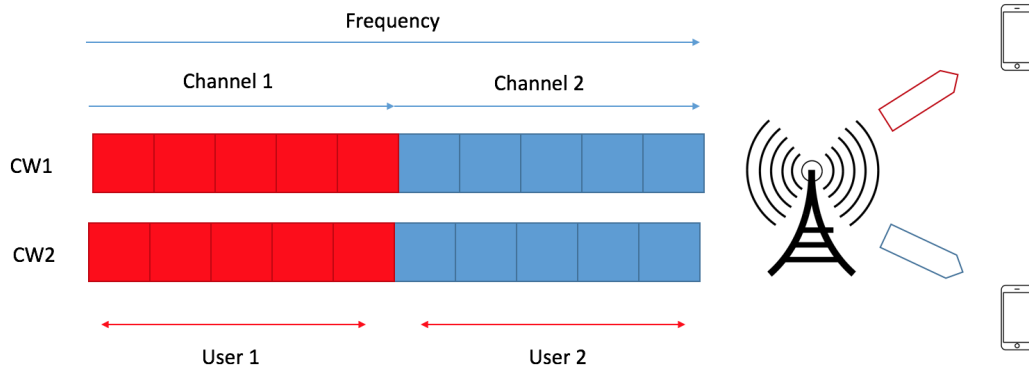


Fig. 2.2 SU-MIMO

With TM 8 Dual layer beamforming is adopted. Release 8 of the LTE standard defines beamforming with one layer. Release 9 specifies dual-layer beamforming. This allows eNodeB to properly configure weight for two different layers individually at the antennas so that beamforming can be used with spatial multiplexing for one or multiple UEs.

Release 10 adds Transmission Mode 9 allow to transmit with Up to 8 layer transmission. With the implementation of this mode up to eight layers can transmit simultaneously, eight physical transmit antennas are obviously needed in this case. The number of used layers can be assigned dynamically. Both single user and multi user MIMO is possible to adopt, dynamically switching between both modes without special signaling by higher layers.

## 2.2 SU-MIMO

The basic idea is to transmit multiple code-word to a single user in the same time-frequency interval so there is only one scheduled user per sub-band or channel. A code-word is defined as a *Coded Transport Block*, but in a wider sense we consider it as a single independently data stream. Spatial Multiplexing schemes can be classified according on if different streams are jointly (multiple code-word) or separately (single code-word) coded. When a single word is in use one coded and modulated TB is spatially multiplexed into several data streams. When multiple code-word are in use different coding and modulation schemas are in use for different transport block that are transmitted simultaneously. The mobile will adjust transmission rate and modulation coding scheme based on measurement report for each code-word adapting transmission for each of the code-words. Network will adapt transmission condition for each code-word independently [15]. From reported channel conditions and the

UE's ability to rapidly send detailed reports on channel conditions, an eNodeB can select among different SU-MIMO modes to implement. Different techniques are then enabled:

- *Spatial Multiplexing Mode*
  - A *Open Loop*
  - B *Closed Loop*
  - C *Closed Loop Rank 1*
- *Transmit Diversity*

## 2.3 Open, Closed Loop - Spatial Multiplexing

Both Open-Loop and Closed-Loop techniques together with Spatial Multiplexing are the main features to SU-MIMO's great achievements in LTE throughput. With the adoption of spatial multiplexing techniques, separate data streams on N multiple antennas are created and its fullest potential is almost close to multiplying the highest throughput from UE by the adopted transmission rank, mainly equal to the number of separate streams transmitted. With spatial multiplexing, the eNodeB can group informations to be transmitted to a particular UE on a given sub-channel into multiple streams, called *Layers*. The number of layers is equal as the rank. Transmission rank is computed accordingly to channel conditions at the user side, as well as many more considerations such as eNodeB's capabilities. Sending different data on each antenna, spatial multiplexing modes require rich scattering of multipath signals and best channel conditions. Under the right configuration, a UE can separate the signals from multiple transmitters, identified by different RS signals, and reconstruct separate information streams within same frequency block.

The simplest implementation for spatial multiplexing, allows a rank-2 transmission on a 2x2 MIMO antenna set-up will transmitting one layer from each Tx. Each layer reaches each UE along a different path. The UE can then reconstructs the layers using multiple information from all antennas.

With this technique, informations arrives encoded from higher level entities in one or more code-words. Each code-word represents one or more layers. In 2x2 MIMO, each code-word corresponds directly to a layer. Each layer is then mapped onto one or more antennas using a pre-coding matrix.

### 2.3.1 Open Loop

Adopting Open-loop technique no knowledge of the channel has to be shared with the transmitter. As a consequence, open loop implementations occur when the radio network layer cannot collect information or feedback from users to do any form of adjustment or when transmission quality is not good enough. This could happen for example when the UE is moving too fast and it is impossible to collect data regarding the channel state. In this case the eNodeB receives only a Rank Indicator (RI) and a CQI Report. A RI is defined as the number of data stream transmitted over the air in the same f and resource corresponding to the number of layers.

### 2.3.2 Closed Loop

Closed loop feedback allows a transmitting entity to retrieve information about channel conditions, provided by the users. If feedback is available, the transmitter can adjust its coding and modulation of the transmitted signals to take into account of the main channel characteristics, just to simplify the signal processing required at the receiver side and enable potentially greater performance gains. Closed-loop systems ask for channel knowledge at the transmitter side. On the other hand, unlike open loop, closed loop is adopted when the radio access network performs dynamic adjustment based on feedback from the user. In this case the eNodeB receives RI, Pre-coding Matrix Indicator (PMI) and CQI.

### 2.3.3 Transmit Diversity and Closed-Loop Rank-1 - Spatial Multiplexing

Transmit Diversity and Closed-Loop Rank-1 Spatial Multiplexing techniques are implemented to boost signal to further improve throughput and capacity. A powerful solution could be experienced the best near the cell edge or in areas where user perceive low SINR or multipath conditions.

When using a *Transmit Diversity Mode*, MIMO the same information are sent from transmitting antennas with the aim to minimize channel interference. The UE receives data streams from both transmitting antennas at both receiving ones and reconstructs a unique stream from all multipath copies of the same signal. Multiple differentiated signals and multiple copies of the same informations decrease the percentage of losing data due to poor channel conditions.

With *Closed-Loop Rank-1 Spatial Multiplexing*, the eNodeB transmits a single set of data for both transmitting antennas. However, Closed-Loop Rank-1 Spatial Multiplexing

uses a linear pre-coding matrix to improve multipath conditions. When decoded at the receiver side, these signals contain the same informations. To combine constructively at the UE multiple signals a pre-coding matrix is adopting. Its role is to shape signals coming from each transmitting antenna. A good performance is achieved by matching a pre-coding matrix to the channel conditions experienced by users. When closed loop is adopted, the eNodeB collects precious information about channel propagation conditions and choose the best among the multiple pre-coding matrices defined for 2x2 MIMO. Taking a look to more conventional Transmit Diversity techniques, Closed-Loop Rank-1 Spatial Multiplexing allows to increase SNR significantly.

## 2.4 MU-MIMO

In MU-MIMO, multiple different data streams are sent to spatially separated users using the same channel configuration. Each user has been equipped with multiple receivers antennas. Adopting MU-MIMO the whole system capacity achieves a strong gain, even though no increase in UE's throughput has been demonstrated. To achieve better results rich scattering conditions are mandatory for all UEs to decode data streams.

LTE adopts a pre-coded configuration for MU-MIMO with several feedback collected from users. Both transmitters and receivers antennas are aware of the set of configured PMIs. Precoding in LTE is implemented mainly for two purposes:

- reduce interference among transmitted signals at the receiver side which is significantly with orthogonal modulations when multiple parallel channels are in use;
- mapping the number of multiplexed streams to the number of transmitting antennas.

Usually, the same pre-coding configurations is used for beam forming and precoded spatial multiplexing in LTE.

## 2.5 MIMO Reporting

Since there are multiple transmission modes in LTE and each one is corresponding to certain multiple antenna techniques CQI reports can be divided into three levels:

- *wide-band,*
- *eNodeB-configured sub-band feedback,*
- *UE-selected sub-band feedback.*

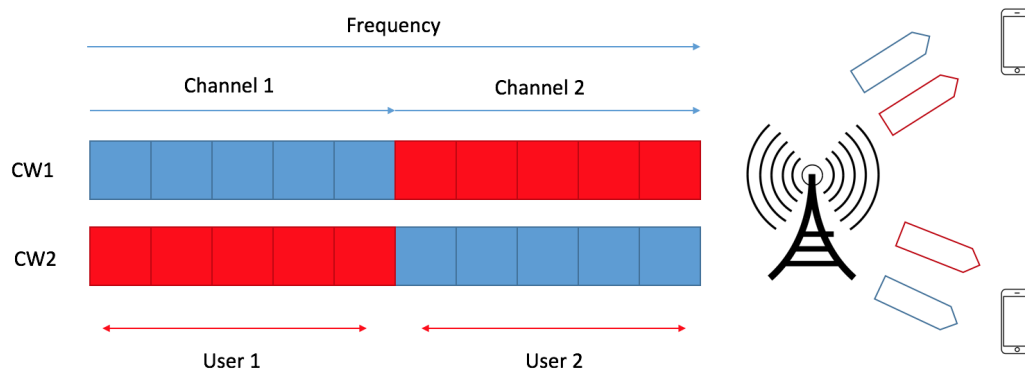


Fig. 2.3 MU-MIMO

Table 2.3 TM 1,2,3,4 vs CSI

Transmission Mode	Payload
1. Single-antenna port; port 0	UE selected sub-band CQI + wide-band CQI or Higher Layer Configured wide-band and sub-band CQI, no PM
2. Transmit diversity	UE selected sub-band CQI + wide-band CQI or Higher Layer Configured wide-band and sub-band CQI, no PMI
3. Open-loop spatial multiplexing	UE selected sub-band CQI + wide-band CQI or Higher Layer Configured wide-band and sub-band CQI, no PMI
4. Closed-loop spatial multiplexing	Wide-band CQI per codeword + PMI for each sub-band or UE selected sub-band and wide-band CQI per codeword + PMI or Higher Layer Configured wide-band and sub-band CQI + PMI

The wide-band report provides an overall CQI value for the downlink bandwidth and with this mode as in the periodic reporting, the UE only reports a single value for the whole bandwidth. In the eNodeB-configured sub-band feedback, two kinds of CQI species are collected, one for the whole system and one for the preferred sub-bands. In the calculation of sub-band CQIs, it is assumed that each transmission occurs only in the preferred bands. In a UE-selected sub-band feedback, as in the eNodeB-configured one, two different species of CQIs are collected, one wide-band CQI value for the whole system bandwidth and one reporting the average measured CQI in  $M$  selected sub-bands, each of a specific size. With a selected sub-bands CQI report, the user divides the system bandwidth into  $N$  multiple sub-bands, selects only a set of preferred  $N$  sub-bands available then reports a single CQI value for the wide-band and one CQI value for the selected set, assuming transmission only over the preferred  $N$  bands. The higher layer configured sub-band report provides the highest granularity [16].

For each transmission mode so, certain combinations of CQI report are defined based on periodic/apperiodic, wide-band/UE selected sub-band/higher layer configured sub-band also depicted in Tab.2.3.

If closed loop MIMO is used, PMI and RI are also collected and reported. PMI suggests the codebook an eNB should use for transmission using multiple antennas computed on the evaluation of received reference signal. RI indicates the number of transmission layers that the UE can receive. In 4G networks, UEs use RI to disclose information about layer mapping. RIs are adopted when open loop transmission are in use as well as in closed loop transmission modes. Spatial multiplexing can be supported only when RI is more than 1. CQI is reported for each codeword when the system works with spatial multiplexing.

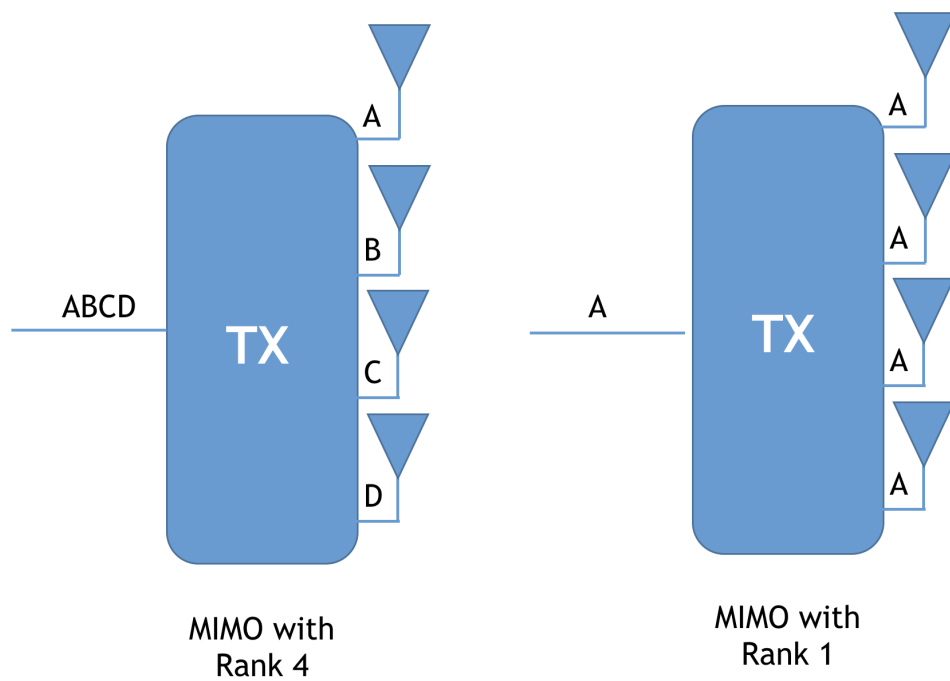


Fig. 2.4 Rank Reporting for mapping MIMO layers



# Chapter 3

## LTE in Unlicensed Bandwidth

### 3.1 Brief Overview of LTE and Wi-Fi Access Techniques

Wireless networks are generally classified in cellular networks and Wi-Fi networks. Each network is characterised by specific elements and allocated spectrum. Cellular networks use mainly licensed bandwidth while Wi-Fi technologies use unlicensed spectrum. Recently the idea of LTE working in the unlicensed spectrum to achieve greater efficiency has been exploited. Since LTE has been designed to operate in licensed bands assuming the absence of any interference its MAC layer is not suitable to work in unlicensed bandwidths. Wi-Fi standard, on the other hand, adopts the LBT approach, along with collision avoidance techniques, that allows to share the spectrum in use with other Wi-Fi other technologies in a fair way. In this chapter, a brief overview of Wi-Fi and LTE MAC layers is given.

#### 3.1.1 Wi-Fi

In 1997 the first version of the IEEE 802.11 standard was published. To widen wireless spectrum, without the need for a government license, in 1985 the Federal Communications Commission (FCC), America's telecoms regulator gave birth to Wi-Fi, the short-range wireless broadband technology.

With 802.11 both ad hoc networks and infrastructure networks can be deployed. Infrastructure topologies consists of one or more independent cells, each of which is managed by a base station called Access Point (AP).

AP usually are interconnected between them and form a Distribution System. The connected access points are usually in an Extended Service Set (ESS). An ESS is a set of connected Basic Service Sets (BSSs). A BSS is a set of all stations that can communicate with each other at physical layer.

Ad hoc networks on the other hands, lets two or more devices communicate with each other directly and each device can access each other's resources directly through a simple point-to-point wireless connection.

Since 1997 also, several new physical layers have been introduced by various amendments Table 3.1 to make higher transmission rates available. 802.11 at first dealt with three different transmission techniques both with 1 or 2 Mbps rate. Since these performances were not sufficient the committee got back to work and in 1999 two new standards were approved: 802.11b and 802.11a. 802.11b was compatible with all the previous standards and added two new main rates 5.5 Mbps e 11 Mbps. 802.11a was adopting a 64QAM modulation and could reach also 54 Mbps thus using the 5 GHz bandwidth. So after two years the committee proposed its variation 802.11g that led to achieve 54 Mbps in the 2.4 GHz band.

Since Wi-Fi operates in the unlicensed bandwidth it requires spread spectrum modulation to be in use. These techniques allow to spread the signal on to a much larger bandwidth then required, letting the signal appear as noise noise to other devices. Spread spectrum first was developed for use by the military because it uses wideband signals that are difficult to detect and that resist attempts at jamming. Two different examples of spread spectrum are: Frequency Hopping Spread Spectrum (FHSS) and Direct Sequence Spread Spectrum (DSSS). In the first case the signal is always switching a carrier among different frequency, using a pseudorandom sequence known to both transmitting and receiving device. With the second the signal is divided into smaller pieces, each associated with a frequency channel. Data signals at transmission points are combined with a higher data rate bit sequence, which divides data based on a spreading ratio. The chipping code is a redundant bit pattern associated with each bit transmitted and this helps to increase the signal's resistance to interference. If any bits are damaged during transmission, the original data can be recovered due to the redundancy of transmission. Apart from 802.11b, all the amendments listed in Table 3.1 use OFDM as the underlying modulation scheme.

MAC protocol for Wi-Fi networks has been obviously designed to be independent from any specific physical layer characteristic. It should be also efficient both for periodic and bursty traffic.

All the stations belonging to the same BSS use the same channel (or channels, starting from 802.11n) to transmit and receive frames. Stations can access the wireless channel according to two basic schemes:

- *Point Coordination Function (PCF)*
- *Distributed Coordination Function (DCF)*

Table 3.1 Wi-Fi Physical Layers

Standard	Frequency	Bit/Rate (Mb/s)	Modulation
802.11a	5.2, 5.4, 5.8 GHz	6, 9, 12, 18, 24, 36, 48, 54	BPSK, QPSK, 16-QAM, 64-QAM
802.11b	2.4 GHz	1, 2, 5.5, 11	DBPSK, DQPSK
802.11g	2.4 GHz	1, 2, 5.5, 6, 9, 11, 12, 18, 24, 36, 48, 54	DBPSK, DQPSK, BPSK, QPSK, 16-QAM, 64QAM
802.11n	2.4 GHz, 5.4 GHz	up to 600	BPSK, QPSK, 16-QAM, 64-QAM
802.11ac	5.4 GHz	up to 6933	BPSK, QPSK, 16-QAM, 64-QAM, 256-QAM

### Point Coordination Function (PCF)

When PCF is used, time is split into *contention-free periods* and *contention periods*. During contention-free periods, the Access Point (AP) is in charge of granting stations the permission to transmit a single frame. During contention periods, instead, stations access the channel by following the DCF scheme, as explained in the following section.

### Distributed Coordination Function (DCF)

The DCF is based on the CSMA/CA (Carrier Sense Multiple Access/Collision Avoidance) approach, which can be classified as a listen-before-talk mechanism because stations sense the channel to check if it is free before starting to transmit. Additionally, other mechanisms are provided to reduce the likelihood of a collision, as explained hereinafter.

Before starting to transmit a frame, both AP and non-AP stations wait for an amount of time equal to DIFS (Distributed Inter-Frame Spacing), or AIFS (Arbitration Inter-Frame Spacing) if QoS is enabled. If the channel remains idle during this time, the node picks a uniform random back-off counter in the  $[0, CW]$  interval and decrements it for every idle slot. When the counter reaches zero, the frame is sent immediately. However, if the medium is sensed to be busy while counting down is performed, the back-off counter value is frozen until the medium returns idle for at least a DIFS interval, after which the counter is decremented starting from its previous value.

The contention window (CW) size is initially set to  $CW_{min}$  and increased when a transmission fails. Indeed, after any unsuccessful transmission attempt, the back-off procedure is performed using a new CW value updated as  $CW = [2 \times (CW + 1) - 1]$ , with the upper bound of  $CW_{max}$ . After each successful transmission, the CW value is reset to  $CW_{min}$ .

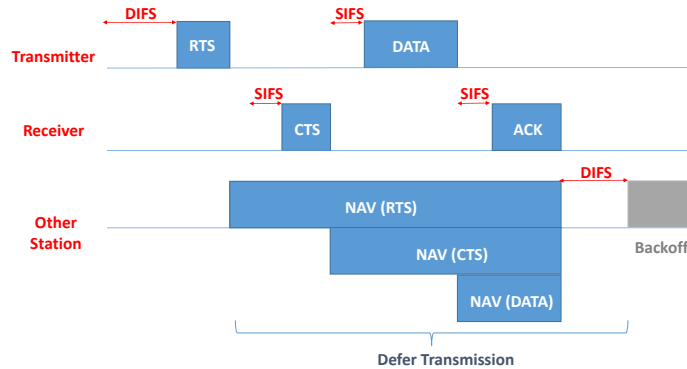


Fig. 3.1 Distributed Control Function - RTS/CTS

The exchange of Request To Send/Clear To Send (RTS/CTS) control frames is an optional mechanism that can be used as a countermeasure for the hidden node problem (Fig. 3.1). Instead of transmitting the data frame, the sender will first transmit a request to send (RTS) frame to the receiver. The receiver will then respond with a clear to send (CTS) frame, if it senses the channel idle. The header of all the 802.11 frames includes a field named *Duration/ID* which is used by the sender to indicate how long other stations should refrain from transmitting to allow the completion of the current frame transmission (including the reception of the acknowledgment frame). Every station receiving a frame uses the value of the *Duration/ID* field to update its Network Allocation Vector (NAV), a timer used to indicate that the channel is *virtually* busy. Thus, if the sender receives the CTS frame, it means that all the stations close to the sender and to the receiver have been informed of the upcoming frame transmission. Hence, the sender can proceed with the transmission of the data frame. The exchange of the RTS/CTS frames is a collision avoidance strategy for data frames. Collision can still take place while transmitting such control frames, but, because their size is just 20 bytes, the retransmission cost is low.

Sensing the channel to assess if it is idle is performed by a procedure called *Clear Channel Assessment* (CCA), which employs two different techniques:

#### - Preamble Detect CCA

Preamble Detect CCA denotes the ability of the receiver to detect and decode a Wi-Fi frame preamble. Once the Wi-Fi preamble has been decoded, the duration of the entire transmission (including the ACK, for instance) can be retrieved from the *Duration/ID* field and the NAV can be set accordingly. Since idle sensing of the channel is one of the main causes of energy consumption for stations, using the NAV reduces the amount of idle sensing required at any node which can overhear a frame and hence enables to save energy. By the Wi-Fi packet header, the time duration for which the medium

will be occupied can be inferred and a CCA flag, indicating the channel occupancy is held busy until the end of data transmission. The sensitivity requirements for Preamble Detect CCA vary according to the transmission bandwidth, but, for the primary 20 MHz operation, a threshold of -82 dBm is typically considered to be required to detect the start of a valid Wi-Fi signal.

#### - CCA Energy Detect

If the station is not able to decode the preamble of a frame, or if the ongoing transmission is done by a node employing a technology other than Wi-Fi, CCA Energy Detect (CCA-ED) is employed. Such procedure consists in detecting the energy level of the operating channel and backing off data transmission if such level is above a certain threshold.

This kind of detection is useful to identify transmissions of non-Wi-Fi stations or transmissions of Wi-Fi stations whose received signal is too low to decode the content of the packet. Energy detection applies due to the physical layer discrepancy in fact the LTE signals are not decodable by WLAN nodes. Default thresholds for CCA-ED are defined by the standard and depend on the channel width. For instance, IEEE 802.11n defines a threshold of -62 dBm for 20 MHz channels. Since these thresholds can be changed by software tools, some works propose to adapt these thresholds to allow a Wi-Fi network to suffer less from the interference of LTE stations operating in the same channel.

## 3.2 Problem Statement

Presenting a basic overview of Wi-Fi and LTE serves the purpose of illustrating why the fair coexistence of the two technologies in the unlicensed band is an issue. Basically, since LTE has been designed to operate in licensed bands, the centralized scheduling performed by LTE eNodeBs saturates all the channel resources, while Wi-Fi stations refrain from transmitting if the channel is sensed busy.

Most Wi-Fi nodes use bandwidth of 20MHz, possible bandwidths of LAA LTE, as seen, can be 1.4/3/5/10/15/20MHz. The bandwidth change can affect the crosstalk interference. It is interesting to understand how LAA-LTE interference with different bandwidth affects Wi-Fi transmissions. In Wi-Fi networks, nodes perform clear channel assessment (CCA) before transmissions. If CCA indicates channel busy, nodes do not transmit. LTE is characterised by a centralised MAC and the use of OFDMA. Operating in unlicensed bands would incur continuous interference to WiFi systems since WiFi adopts a contention-based MAC and will

keep backing off when it detects LTE transmissions. It is possible for LAALTE interference to trigger channel busy indication during Wi-Fi CCA and make Wi-Fi nodes not transmit, which causes throughput degradation. LTE devices are required then, to detect before transmission whether the target channel is occupied by other systems. This procedure is referred to as listen-before-talk (LBT). It is quite necessary to investigate a mechanism of fair coexistence between the two RATs. Then, we illustrate the main approaches proposed to ensure a fair coexistence between Wi-Fi and LTE in the unlicensed band, namely Listen Before Talk (LBT) and Almost Blank Subframe (ABS), along with some other minor techniques. We describe the main solutions that are currently being developed by standardization bodies and telecom industry: LTE-U, Licensed Assisted Access (LAA) and MuLTEfire. Finally, we present an overview of the work appeared in the literature analyzing the impact of LTE on the performance of Wi-Fi and proposing solutions to mitigate such an impact.

### 3.3 Basic techniques for a fair coexistence of Wi-Fi and LTE

In this section, the most important basic techniques for the fair coexistence of LTE and Wi-Fi are illustrated. As LTE was not originally designed to encompass any mechanism for sharing a channel (as it assumes to operate alone on the licensed bands), solutions are being devised for allowing it to share the unlicensed spectrum with other wireless technologies. Several proposals have been made, both by the research community and the industry. Most of such proposals, though, are based on one of the two techniques, *Listen-Before-Talk* (LBT) and *Almost Blank Subframe* (ABS), that will be discussed in detail in the following subsections. In addition to those, other techniques will be presented that can be used in conjunction with the first two to further improve the way LTE can coexist as a good neighbor to Wi-Fi.

#### 3.3.1 Listen-Before-Talk

Listen-Before-Talk (LBT) is a mechanism that consists in the assessment of the channel state before transmitting, mainly by means of detecting the electromagnetic energy. Such a detection reduces the probability of colliding with the transmissions of other devices operating in the same frequencies. It is important to note that a form of LBT, loosely specified, is required both by the European and Japanese legislations in order to operate in the ISM (Industrial, Scientific and Medical) band. For that reason, an LTE solution operating in such a band in such areas is bound to the adoption of the LBT approach.

With respect to the LBT approach, proposals have been classified by 3GPP in four categories [7]:

- 1 **Category 1:** No LBT. No LBT procedure is performed by the transmitting entity (this category is included to classify solutions that do not adopt the LBT approach).
- 2 **Category 2:** LBT without a random back-off procedure. The duration of the time interval during which the channel must be sensed idle before the transmission begins is deterministic.
- 3 **Category 3:** LBT with random back-off having a fixed contention window (CW). If the channel is sensed idle for a fixed amount of time, the transmitter draws a random number from the interval  $[0, CW)$ . Such random number is used in the LBT procedure to determine the additional amount of time slots during which the channel needs to be sensed idle before the transmitter can start to transmit.
- 4 **Category 4:** LBT with random back-off having a contention window of variable size. As for Category 3, but with the size of the CW that varies depending on the outcome of the previous transmission attempts. There can be different criteria for choosing the CW size. One of the possibilities is to tie the CW size to the number of previously failed transmission attempts, similar to what is done by Wi-Fi and Ethernet.

### 3.3.2 Almost Blank Subframe

While the European and Japanese regulations mandate to adopt an LBT approach, in countries such as the United States, China and South Korea, there are instead limits on the maximum duration of a transmission burst in the unlicensed spectrum (and no regulatory requirement for a Listen Before Talk scheme). Such regulations have fostered the development of different techniques according to which LTE cells voluntarily interrupt the transmissions in order to limit the occupation of the channel and to allow other devices, e.g. Wi-Fi stations, to transmit. Such voluntary interruptions are generally performed periodically and their duration is typically determined based on measurements of the channel occupancy by other networks.

As a matter of fact, a specific technique called ABS (Almost Blank Subframe) has been already defined in LTE Release 10 in the context of the LTE *HetNets* (Fig. 3.2). LTE HetNets are heterogeneous networks comprised of LTE cells of different sizes, referred to as macro, micro, pico and femto cells. ABS has been introduced to limit the interference among transmissions of different cells. In the following, we describe the base operation of ABS. In the time domain, data transmissions of the macro cell, e.g., an eNodeB, are restricted to

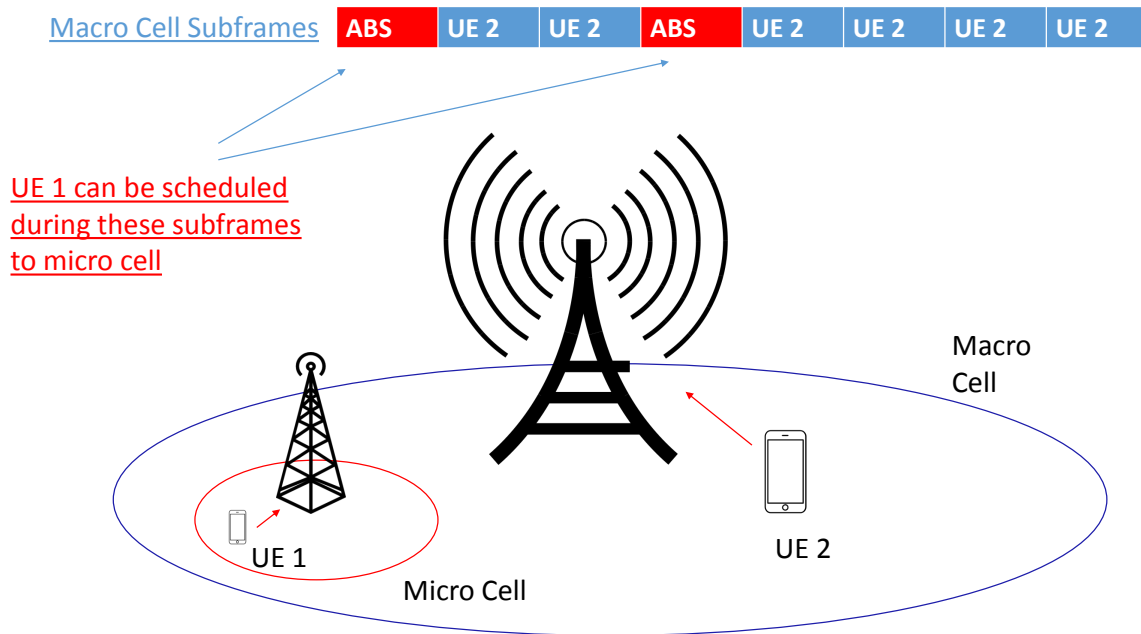


Fig. 3.2 Almost Blank Subframe Structure

happen only in certain sub-frames. Small cells, e.g. pico cells or femto cells, can therefore transmit in the remaining sub-frames (which are called Almost Blank Subframes, ABSs) and experience very little interference (see Fig. 3.3). Interference is not null in such ABS because the main cell is still allowed to transmit for control and signaling purposes.

Basically, LTE transmissions are almost “blanked out” in certain periods of time, leading to a duty cycle-based approach. Other technologies, such as Wi-Fi, can exploit the time intervals corresponding to blank frames to transmit. It is important to note that the basic ABS mechanism, as defined in LTE Release 10, does not perform any sensing of the channel whatsoever, therefore a solution merely employing ABS is not compatible with some regulations, such as the European and Japanese ones.

Involved cells need to exchange messages to coordinate the scheduling of ABSs in a certain area. Such signaling messages are exchanged through the *X2 interface*, which is a mandatory interface provided by LTE cells for control and signaling purposes. The described ABS technique was not designed to work in the unlicensed spectrum, therefore research efforts are ongoing to adapt it for such a scenario.



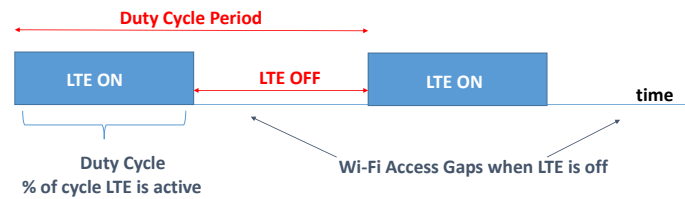


Fig. 3.3 LTE Duty Cycle

Table 3.2 Mean e.i.r.p. limit in dBm - ETSI EN 301 893

Frequency range [MHz]	Mean e.i.r.p limit [dBm]		Mean e.i.r.p density limit [dBm/MHz]	
	with TCP	without TCP	with TCP	without TCP
5.150 to 5.350	23	20/23 (see Note 1)	10	7/10 (see Note 2)
5.450 to 5.725	30 (see Note 3)	27 (see Note 3)	17 (see Note 3)	14 (see Note 3)
Note 1: The applicable limit is 20 dBm, except for transmissions whose nominal bandwidth falls completely within the band 5.150 MHz to 5.250 MHz, in which case the applicable limit is 23 dBm.				
Note 2: The applicable limit is 7 dBm/MHz, except for transmissions whose nominal bandwidth falls completely within the band 5.150 MHz to 5.250 MHz, in which case the applicable limit is 10 dBm/MHz.				
Note 3: Slave devices without a Radar Interference Detection function shall comply with the limits for the band 5.250 MHz to 5.350 MHz.				

### 3.3.3 Minor techniques

In addition to the LBT and ABS techniques, other proposals have had considerable attention in the literature. Most of them can in fact be used in conjunction with LBT or ABS to further enhance the capability of LTE to behave as a good neighbors to Wi-Fi.

- **Transmit Power Control (TPC):** Some regions mandate transmitting devices to reduce the transmit power when other transmissions on the same channel are detected. TPC is a mechanism capable to ensure a mitigation factor of at least 3 dB on the aggregate power from a large number of devices. For devices with TPC, the RF output power and the power density, when configured to operate at the highest stated power level of the TPC range, shall not exceed the levels given in Table 3.2. Devices are allowed to operate without TPC, but the technique is nonetheless useful to reduce the interference generated by LTE cells operating in the unlicensed spectrum.
- **Carrier selection (CS):** As there is a large availability of bandwidth in the unlicensed spectrum, carrier selection is a possible strategy to reduce interference. Indeed, such technique consists in measuring the amount of activity in the different potential transmission channels and then use the one with the least amount of such activity, in order to reduce interference.

- **Automatic Gain Control (AGC):** It is very useful in any receiver, especially in the handset or mobile side. As the signal transmitted from the base station reaches the mobile or the handset through different paths or terrains, it can be very variable in time. In this situation, it is useful to control the level of gain of the signal before it is passed on to the baseband processing chain for data decoding. Such a technique, known as Automatic Gain Control, can be used to reduce the interference in the unlicensed spectrum due to other LTE or Wi-Fi cells operating nearby.
- **Minimum channel occupancy:** European and Japanese regulations mandate that 20 MHz channels must be occupied for at least 80% of the bandwidth for most of the time, while it is allowed to occupy as low as 4 MHz only for short amounts of time. Such a requirement is put in place to make sure that the channel bandwidth is not wasted with low throughput communications.

## 3.4 Standardization Efforts

In this section we describe the standardization efforts being carried out to fairly deploy LTE in the 5 GHz unlicensed band. Currently, three main solutions are being developed to allow LTE to operate in the unlicensed spectrum [17]:

- *LTE-Unlicensed* (LTE-U)
- *Licensed Assisted Access* (LAA)
- *MuLTEfire*

We describe each of such solutions in the following. Further information can be found in [18].

### 3.4.1 LTE-U

As previously mentioned, Qualcomm firstly presented a functional prototype for an LTE cell working in the 5 GHz band based on 3GPP Release 11. Such a prototype required very small changes to standard LTE equipment and the adopted technology was called LTE-U. The product implementation was based on mainly three mechanisms:

- **Channel Selection:** the opportunity to choose a proper channel to transmit ensures to avoid interference between the LTE cell and its neighboring Wi-Fi devices. LTE cells will perform, at both the initial power-up stage and later periodically, a measurement

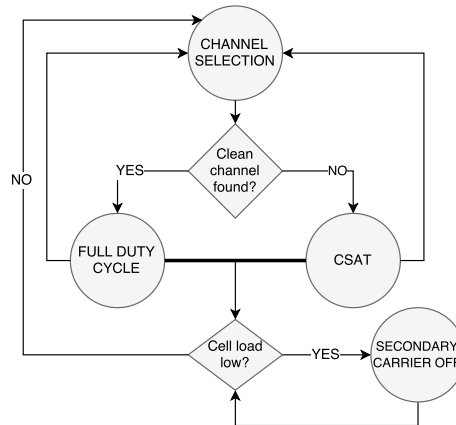


Fig. 3.4 Channel Assessment Procedure

procedure to identify the most suitable channel. The selection algorithm will then monitor the status of the operating channel and, if needed, select a more appropriate one to switch to.

- **Carrier Sense Adaptive Transmission (CSAT):** LTE cells sense the medium for a longer duration with respect to LBT and CSMA. When CSAT is in use, LTE transmissions are backed off depending on the observed medium activity. CSAT defines a time cycle where a small cell transmits for a fraction of the cycle and backs off in the remaining period. During the off period, the channel can be used by neighboring cells, which can resume normal transmissions. Meanwhile, small cells measure medium utilization and adaptively adjust On/Off duty cycle accordingly.
- **Opportunistic Supplemental Downlink (SDL):** SDL in unlicensed band can be seen as an opportunistic resource when component carriers in the licensed bands are highly overloaded. With active users exceeding a certain threshold, in fact, SDL carriers can be turned on for traffic offloading. SDL transmissions can be scheduled opportunistically, based on the traffic demand. Also, the secondary component carrier in the unlicensed band can be dynamically turned off, if, for instance, the small cell is found to be lightly loaded again. The adopted algorithm is shown in Fig. 3.4.

In 2014, the *LTE-U Forum* was created by Verizon in collaboration with Alcatel-Lucent, Ericsson, Samsung and Qualcomm. The LTE-U forum produced several standards with the aim of developing an LTE solution for the unlicensed band. LTE-U is designed to work with 3GPP Releases 10, 11, and 12, and is intended for deployments in USA, Korea, India and China. LTE-U is targeted primarily at regulatory regimes where LBT is not required to

access the unlicensed bands. As previously stated, LTE-U leverages the Carrier Aggregation technique to aggregate carriers in the unlicensed band as a Supplemental Down Link (SDL) with a primary carrier in licensed bands. The SDL mode is the simplest form where the unlicensed spectrum is only used for downlink transmission, as downlink traffic is typically much heavier than uplink traffic. These features thus make it possible for LTE to operate in the unlicensed bands.

The envisioned scenario takes advantage of the heterogeneous network concept introduced by LTE Release 10. In such a scenario, small cells share the same licensed spectrum with macrocells and the unlicensed spectrum with Wi-Fi nodes. An unplanned and unmanaged deployment of LTE-U Secondary Cells (SC) (femtocells, picocells) may result in excessive Radio Frequency interference to the existing Wi-Fi devices operating on the same channel and to the LTE-U nodes deployed by other operators in the vicinity. It is therefore critical for LTE-U SCs to choose the best operating channel while minimizing the interference caused to nearby Wi-Fi and LTE-U networks. Also, mechanisms such as CSAT and ABS frequency selection are properly used to ensure a fair co-existence with Wi-Fi.

### 3.4.2 Licensed Assisted Access

LAA has been recently introduced by the 3rd Generation Partnership Project (3GPP) LTE Release 13. Preliminary investigations started in June 2014 during a workshop, followed by a formal study in September 2014. 3GPP exploited the necessary mechanisms for fair coexistence when operating in the 5 GHz band and envisioned a *single global solution framework allowing compliance with any regional regulatory requirements* [7]. Additionally, this study aimed to guarantee a fair behavior with respect to existing Wi-Fi networks, so as not to affect Wi-Fi devices more than an additional Wi-Fi network on the same channel. 3GPP LTE Release 13 introduced the support for LTE operations in the unlicensed band by exploiting, like LTE-U, the Carrier Aggregation feature to aggregate secondary carriers from the unlicensed spectrum. Also, two operation modes are provided: SDL (Supplemental Downlink), as for LTE-U, and Time-Division Duplex (TDD). In TDD mode, the unlicensed spectrum is used for both downlink and uplink, just like the LTE TDD mode in licensed bands. TDD mode offers the flexibility to adjust the resource allocation between downlink and uplink, at the cost of extra implementation complexity on the user side.

LAA requires the Clear Channel Assessment (CCA) and Listen Before Talk (LBT) mechanisms. The LBT procedure is defined as a mechanism by which a device performs a CCA check before accessing the channel. CCA utilizes at least energy detection to determine the presence or absence of other signals on a channel in order to determine if a channel is occupied or clear, respectively. European and Japanese regulations mandate the usage of

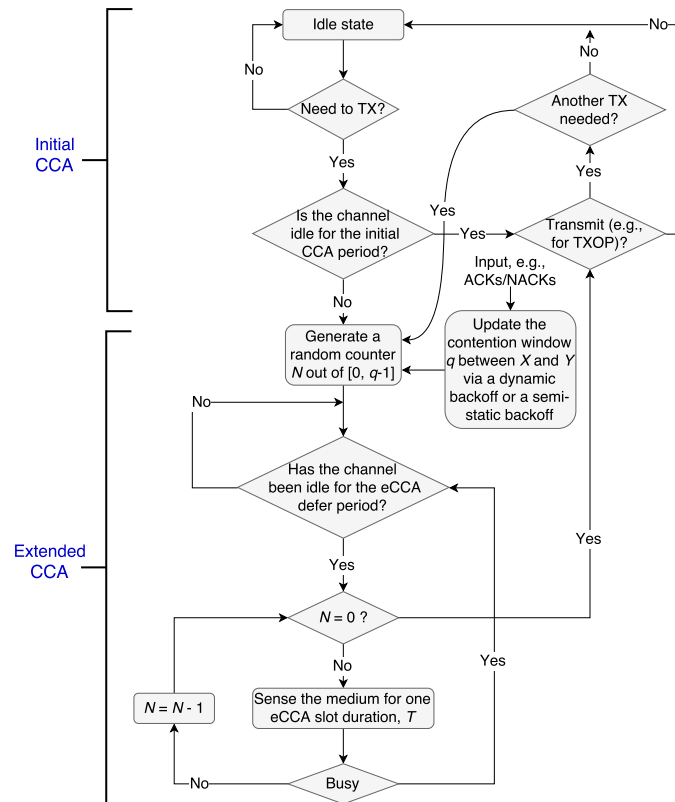


Fig. 3.5 Listen Before Talk based on LBE - TR 36.889

LBT in the unlicensed bands. Apart from regulatory requirements, carrier sensing via LBT is a way to fairly share the unlicensed spectrum and hence it is considered to be a crucial feature to ensure fair operation in the unlicensed spectrum.

Two candidate LBT solutions are then presented:

- **Frame Based Equipment (FBE):** FBE uses a Fixed Frame Period consisting of a *Channel Occupancy Time (COT)* and an *Idle Period*. Before starting transmissions over the medium, the transmitter shall perform a CCA check (lasting at least  $20\ \mu s$ ) towards the end of the Idle Period. If the channel is idle, the device transmits during the Channel Occupancy Time (which should not last longer than  $10\ ms$ ) and then it should have an idle period which is more than 5% of COT. Otherwise, the device shall not transmit on the channel during the next fixed frame period. The major advantage of FBE is the convenient User Equipment (UE) detection. CCA is performed always at the end of the Fixed Frame Period so that the detection complexity of UEs can be greatly decreased since only the first OFDM symbol of each subframe has to be blindly detected to confirm the potential start of a downlink burst.
- **Load Based Equipment (LBE):** LBE provides that the transmitter shall perform a CCA check before every burst of transmissions. The transmitter can immediately occupy the channel if the medium is considered to be idle during the CCA slot ( $\geq 20\ \mu s$ ); otherwise, an extended CCA (ECCA) check shall be performed based on a back-off strategy similar to that adopted by CSMA-CA. The value of the back-off counter is randomly generated in the range of 1 to  $q$  for each ECCA check, where  $q$  is defined by the manufacturer in the range of  $[4, 32]$ . The counter is decremented by 1 every time the medium is considered to be idle during an ECCA slot ( $\geq 20\ \mu s$ ). When the counter reaches zero, the transmitter can occupy the channel for a maximum amount of time of  $q \times (13/32)ms$  (Fig. 3.5). In contrast to FBE, the channel may be sensed in the middle of a subframe, resulting in a higher complexity and power consumption for UEs to blindly detect the start of a transmission. However, LBE may allow for more channel access opportunities, especially in high load scenarios, because the transmitter can continuously detect the channel if one CCA/ECCA check fails to acquire the channel instead of waiting for a long Fixed Frame Period.

### 3.4.3 MuLTEfire

Another approach to enabling the coexistence of Wi-Fi and LTE networks in the unlicensed spectrum is MuLTEfire, a technology developed by Qualcomm. MuLTEfire is the only solution able to work without any simultaneous channel operating as a primary cell in the

licensed spectrum. In other words, muLTefire is designed to operate exclusively in the unlicensed spectrum and adopts spectrum sharing mechanisms similar to the one employed by Wi-Fi to share the channel with other networks.

While MuLTefire will lack the benefits of an anchor channel in licensed spectrum, it would still be able to provide improved performance when compared to other currently available technologies that use the unlicensed spectrum, thanks to the advanced physical and MAC layer techniques it uses.

### 3.5 LTE First Steps in the Unlicensed Spectrum

The exponential growth in mobile data traffic we are currently experiencing has dramatically increased the demand for radio spectrum over the last years. Nonetheless, the amount of data traffic carried over cellular networks is expected to keep increasing for many years to come. Therefore, telecom industry and standardization bodies, primarily 3GPP (Third Generation Partnership Project), have made many attempts at increasing the capacity of LTE networks to cope with the ever growing traffic demands. Mobile data offloading techniques represent an attempt at coping with such an increase of traffic demand and consist in offloading data traffic originally destined to cellular networks to WLANs [19]. Basically, such techniques are implemented by exploiting the multi-homed capabilities of current mobile devices, which are usually equipped with both a Wi-Fi interface and an LTE interface. However, such techniques do not work seamlessly in all the scenarios and, moreover, the leveraged Wi-Fi technology is not considered as efficient as LTE in terms of spectrum usage.

One of the first proposals to make LTE directly access the unlicensed bands was made by Qualcomm [20], which proposed to exploit the already available Carrier Aggregation (CA) feature, consisting in the aggregation of multiple (non-contiguous) channels (called *component carriers*), to allow for the use of (downlink-only) secondary channels in the unlicensed bands. The proposed technique required very slight modifications to LTE as per 3GPP LTE Release 11 standard and was targeting early mobile operators deployments in USA, Korea and India, where the legislation does not require to employ a carrier sense mechanism to control the access to the wireless medium. Such proposal eventually led to a technology called *LTE-U* (LTE Unlicensed), which is being developed by the LTE-U Forum [21].

Meanwhile, 3GPP started working on a feature named Licensed Assisted Access (LAA), aiming at allowing deployments in countries, such as Europe and Japan, where the regulatory environment requires the LBT (Listen Before Talk) approach for accessing unlicensed bands. LAA is being defined as part of 3GPP Release 13. Like LTE-U, LAA exploits the

aggregation of a primary cell, operating in licensed spectrum to deliver critical information and guaranteed Quality of Service, with a secondary cell, operating in unlicensed spectrum to opportunistically boost data rate. Removing the need of using a channel in the licensed bands is instead the goal of MuLTEfire [22], a proprietary technology developed by Qualcomm.

Once such technologies were introduced, studies were made to assess their impact on the performance of Wi-Fi networks using the same unlicensed band. Some initial experiments, mainly carried out by telecom operators, showed that such an impact is rather low [23, 24]. Other experiments, carried out by the research community, showed instead that the performance of Wi-Fi can be seriously affected, while, on the other hand, the performance of LTE is only slightly degraded when a Wi-Fi network operates simultaneously on the same channel [25–27]. Such an outcome is due to the different techniques adopted by LTE and Wi-Fi to access the medium. Indeed, the Wi-Fi MAC protocol is based on a carrier sense and collision avoidance approach and its transmissions are limited in time; LTE, even in some of its unlicensed flavours, performs little sensing and tends to keep the channel constantly occupied.

For this reason, studies are ongoing to improve the original proposals for LTE in the unlicensed spectrum (LTE-U, LTE-LAA) to make them suitable for working in the unlicensed spectrum. The objective of such improvements is to make LTE a “good neighbor” to Wi-Fi, where “good neighbor” is defined <sup>1</sup> as a network that causes the same degradation of performance to other networks that a Wi-Fi network operating on the same channel would cause.

In the rest of this work, we aim at describing the current state of the art related to the LTE technology as being enhanced to work in the 5 GHz unlicensed band as a good neighbor for Wi-Fi. In particular, the chapter is organized providing at first a brief description of the MAC layers of LTE and Wi-Fi, while after summarizing the basic mechanisms proposed so far for a fair coexistence between LTE and Wi-Fi. Eventually we describe the current status of the standardization efforts related to the definition of LTE enhancements for the unlicensed spectrum, such as LAA, LTE-U and MulteFire. We report preliminary results on the performance of LTE and Wi-Fi when they operate in the same channel under different settings and configurations. We then explore the latest proposals from the research community to further improve the behaviour of LTE in the unlicensed spectrum, grouped according to the main technique they use.

---

<sup>1</sup>By 3GPP and other stakeholders of the LTE unlicensed efforts.



### 3.6 Performance analysis of Wi-Fi in presence of LTE cells

Several research works highlighted how LTE, operating in the unlicensed spectrum without the introduction of appropriate countermeasures, can cause a severe degradation of the performance of nearby Wi-Fi networks.

As easily predictable, Wi-Fi performance is shown in [26] to be significantly degraded by a single nearby LTE network when no coexistence mechanism is in use, while LTE, instead, is only minimally affected by the presence of a Wi-Fi system. In fact, when both transmitting on the same channel, Wi-Fi suffers from a throughput loss ranging from 20% up to 97% while LTE experiences a throughput loss of at most 10%.

In [28], a simulation study shows that Wi-Fi performance is affected the most by LTE transmissions, when several AP stations try to operate concurrently. In [29], a performance analysis based on a statistical model, partly validated through experimental evaluation on the ORBIT testbed [30], is performed. Through such a model, authors were also able to confirm previous studies assessing the performance degradation of Wi-Fi networks when co-located with early prototypes of LTE unlicensed cells. In [31], a simulation study is performed in a scenario where an operator replaces one of its Wi-Fi deployments with an LTE unlicensed cell. Results showed that, notwithstanding the co-located Wi-Fi networks, LTE was able to deliver high capacity to stations compared to the previous Wi-Fi deployment.

In [32] it is shown that, when coexisting with LTE, both the median and 5% tail of Wi-Fi user throughput are, at least, maintained with CSAT, and in fact the median throughput of Wi-Fi users is slightly better by 10-40% in the case of LTE being a neighbor compared to when Wi-Fi is a neighbor. If the LTE system adopts coexistence mechanisms, the overall user experience can be further enhanced. Through first-order analysis, simulation study, and over-the-air indoor test, it is shown that, if properly designed, LTE with coexistence mechanisms can be a good neighbor to Wi-Fi, equally or better than existing Wi-Fi neighbors. Mobile users are going to be able to enjoy significantly better experience, and the spectral efficiency of the entire unlicensed band can be improved by deploying LTE in the unlicensed band. The evaluation framework is based on the assumption that Wi-Fi APs are entirely compliant with 802.11ac specification and adopt *minstrel* [33] as the rate control algorithm.

LTE provides several channel widths (1.4, 3, 5, 10, 15, 20 MHz), which can differently impact Wi-Fi performances. When Wi-Fi is used with 20MHz channels, its performance is highly degraded by LTE transmissions on 15/20 MHz channels due to the heavy cross talk interference and the impossibility in most cases of Wi-Fi to recognize the ongoing transmissions [27]. Even transmissions of 1.4/3/5 MHz can severely impair Wi-Fi throughput, due either to interference or to the triggering of Wi-Fi Carrier Sense/Clear Channel Assessment

which prevents Wi-Fi devices from transmitting. Small impact, though, on Wi-Fi throughput is obtained by using an LTE 1.4 MHz channel with center frequency located on the guard bands or the center frequencies of Wi-Fi channels. Thus, LTE cells may produce different effects depending on which portion of the Wi-Fi channel overlaps with the channel used by LTE.

Regarding the use of MIMO (Multiple Input Multiple Output), the performance of Wi-Fi can be better without using MIMO, when the LTE interference is strong. In the open space, the interference effect decreases as distance increases. However, this property does not always hold in indoor environments due to heavy multipath fading. Presence of obstacles can also change the signal propagation and interference condition. In the case of LAA coexisting with Wi-Fi, increasing the distance between devices does not necessarily decrease the impact of interference in indoor environment. On the other hand, blocking Line Of Sight between LAA-LTE and Wi-Fi links can effectively help decrease the impact of interference.

A system analysis to assess the network performance in an office scenario is performed in [34]. The 900 MHz band was chosen in order to evaluate the coexistence nearby the TV white space, though it is stated that all the conclusions can be extended to other bands. The mean throughput in this scenario shows that LTE is slightly affected by the coexistence, its performance is almost the same as the LTE-only scenario. On the other hand, coexistence causes a reduction in the Wi-Fi performance of almost 70% in the best case and of 100% in the worst case. Due to the interference caused by LTE transmissions, Wi-Fi nodes stay on listen mode for a large amount of time and the interference caused by LTE prevents them from transmitting. Results show in general that LTE outperforms Wi-Fi in similar scenarios including stand alone LTE and Wi-Fi.

Despite the previous work, a minority of studies stated that the performance of Wi-Fi is not affected by LTE, even in its first forms. One of the most important is the one made by Qualcomm that reported the results of several tests in a letter to the Federal Communication Commission of the United States [35]. The letter reports several scenarios where by properly tweaking the parameters of the LTE cell it is possible to reduce at minimum the interference between LTE and Wi-Fi networks.

A novel inter system interference analysis technique is developed based on the continuum field approximation and spiral representation [36]. Such a new approach allows to quantify the effect of interference when LTE and Wi-Fi operate in the same unlicensed spectrum. The optimal cell radius computed for LTE is the one that maximizes the system throughput. Decreasing the radius size in this case seems to be the optimal solution. Decreasing the cell size causes a reduction of inter system interference by blocking more Wi-Fi nodes and increases the intra system interference. Numerical results suggest that the LTE cell radius

needs to be decreased to minimize the impact of coexistence on the LTE performance. Wi-Fi performance in this case is reduced due to the higher rate of Wi-Fi nodes that are blocked.

Both Wi-Fi and LTE-U benefit from the large number of available channels and isolation provided by building shielding at 5 GHz. In typical indoor coexistence scenarios, interference-aware channel selection is more efficient for both Wi-Fi and LTE-U than listen-before-talk mechanisms [37]. When the indoor building shielding is low, the adopted coexistence mechanisms depend on the intended behavior of LTE-U: if the goal is to protect Wi-Fi, interference-aware channel selection isolates Wi-Fi, and LBT among LTE-U femtocells ensures a reasonable throughput to LTE-U; otherwise, if Wi-Fi suffers from additional interference due to fairly sharing channel with LTE-U, then LBT only is preferable. When multiple outdoor LTE-U networks deployed by different cellular operators coexist, outdoor LTE-U picocells and indoor Wi-Fi deployments are two networks isolated from each other, but a listen-before-talk mechanism can increase the throughput of LTE-U users.

The Wi-Fi DCF and LAA Cat 3 and Cat 4 LBT are analytically modelled by using Markov chains in [38], to the purpose of evaluating the downlink performance of coexisting LAA and WiFi networks. The analysis conducted by means of such models reveals the existence of a trade-off between Wi-Fi protection and LAA-Wi-Fi system performance enhancement. Indeed, Cat 4 LBT scheme allows to protect Wi-Fi throughput and delay, while Cat 3 LBT scheme provides higher LAA-WiFi system throughput.

The interaction between multiple operators and the UEs subscribed to the services of the operators in unlicensed spectrum is analyzed by means of a multi-operator multi-UE Stackelberg game in [39]. To limit interference to the Wi-Fi access point, each operator sets an interference penalty price for each UE that causes interference to the AP, and the UEs can choose their sub-bands of the unlicensed spectrum and determine the optimal transmit power. Operators can predict the possible actions of the UEs and hence set the optimal prices to maximize their revenue earned from UEs. Two possible scenarios are considered: in the non-cooperative scenario, operators cannot coordinate with each other in the unlicensed spectrum; in the cooperative scenario, all operators can coordinate with each other to serve UEs and control the UEs' interference in the unlicensed spectrum.

Another tool based on game theory, named the multi-game framework, is proposed in [40] for modeling resource allocation problems in LTE-U. In such a framework, multiple coexisting and coupled games across heterogeneous channels can be formulated to capture the specific characteristics of LTE-U. Such games can be of different properties and types, but their outcomes are largely interdependent. Simulation are conducted to show how such a multi-game can effectively capture the specific properties of LTE-U and make it a friendly neighbor to Wi-Fi.

A general framework for the comparative analysis of spectrum sharing mechanisms in time and frequency is presented in [41], along with a throughput and interference model for inter-technology coexistence, integrating per-device specifics of different distributed MAC sharing mechanisms. Extensive Monte Carlo simulations are carried out, which show that, when Wi-Fi and LTE share the same channel, performance depends on the interference coupling: for low interference coupling, e.g., residential indoor scenarios, duty cycle mechanisms outperform sensing-based LBT mechanisms; for high interference coupling, e.g., outdoor hotspot scenarios, LBT outperforms duty cycle mechanisms.

The coexistence in the unlicensed band between Wi-Fi, adopting the CSMA/CA access scheme, and LTE-U, adopting an ALOHA-like access scheme, is analyzed in [42] by using stochastic geometry. The coverage probability and spatial throughput of Wi-Fi and LTE-U networks is derived. Also, the asymptotic spatial throughput when the density of Wi-Fi and LTE-U nodes go to infinity is computed. It turns out that, when the density of Wi-Fi nodes goes to infinity, both the spatial throughput of Wi-Fi and LTE-U converge to two distinct constants. In contrast, the increase of LTE-U density causes a linearly increase of LTE-U spatial throughput but a diminishing spatial throughput of Wi-Fi network. Furthermore, the retention probability of LTE-U to achieve weighted max-min fairness between Wi-Fi and LTE-U networks is found to be proportional to the density of Wi-Fi and inversely proportional to the density of LTE-U.

A framework for LTE-U indoor planning and optimization based on a statistical system model is presented in [43]. The proposed framework requires as inputs the characteristics of the radio propagation, the statistical description of the service demand, and the preferences of the network operator. It returns a set of optimized network topologies that can be used to plan or optimize the indoor deployment, under the assumption that the Wi-Fi network is already deployed in the indoor environment.

A statistical framework to evaluate the fairness offered by LAA and LTE-U when coexisting with Wi-Fi in unlicensed band is proposed in [44]. The 3GPP definition of fairness is mapped onto the stochastic dominance concept and the two-sample one-sided Kolmogorov-Smirnov test (KS-test) is used to test the specific hypothesis of fairness defined through throughput and latency performance, as proposed by 3GPP. A simulation study is carried out by using the ns-3 network simulator to evaluate throughput and latency. Both the simulation results and the statistical analysis confirm that there is a need to improve the fairness in the coexistence scenario. Also, they confirm that LAA better performs in terms of fairness in both throughput and latency and LTE-U introduces more collisions.

Other unlicensed frequency bands than 5 GHz could also be considered for LTE-U, like the 2.4 GHz ISM band, which comprises 3 non-overlapping channels of 20 MHz and which

is also used by Wi-Fi. However, results show that the good throughput performance achieved by Wi-Fi and LTE-U when coexisting in the 5 GHz band is largely due to the large number of non-overlapping channels in the 5 GHz band and the higher propagation losses at 5 GHz. Results then suggest that selecting the unlicensed 5 GHz band for LTE-U operation is the optimal solution.

The results of the analyses and simulations carried out by the works surveyed in this section indicate that hardly a technique can be considered better than another. The effectiveness of a technique largely depends on the considered scenario. Indeed, a number of factors heavily influence the performance: indoor/outdoor, density of APs, density of LTE eNodeBs, traffic load, interference coupling, etc. Also, different metrics can be considered to evaluate the performance of a technique. Therefore, it is likely that the dispute around the best coexistence mechanism will remain open for a long time and research proposals, like those presented in the next section, will proliferate.

## **3.7 Research proposals for a fair coexistence of LTE and Wi-Fi**

In this section we present an overview of the research work proposing new approaches for a fair coexistence between LTE and Wi-Fi in the unlicensed spectrum. Such works are categorized depending on the main mechanism employed to achieve coexistence, i.e. Listen-Before-Talk, Almost-Blank-Subframe and other minor approaches.

### **3.7.1 Approaches based on Listen-Before-Talk**

The approaches based on Listen-Before-Talk that have been presented in the literature are described next and classified according to the definition given in Section 3.3.

#### **LBT, category 2**

The usage of a special kind of channel sensing method for LTE in the unlicensed bands is investigated in [45]. In order to realize an harmonious LTE/Wi-Fi coexistence, two channel sensing schemes are proposed: periodic sensing and persistent sensing. The periodic sensing scheme enables LTE nodes to sense the channel with several OFDM symbols at the beginning of each sub-frame and to determine whether to transmit in the remaining part of the subframe. The sensing phase contains from 1 to 4 OFDM symbols. Changes should be applied to the LTE architecture to perform such kind of sensing at the beginning of each subframe.

Wi-Fi transmissions are also protected during the LTE sensing phase, giving Wi-Fi devices additional chances to acquire the channel.

Table 3.3 Taxonomy of research works

Paper	CAT	Threshold	CW	Scenario	Model	PTX	Note
[46]	CAT 4	CCA-ED: -62dBm CCA-PD: -82dBm	CW_min 16, CW_max 1024	Indoor	FTP 2	18 dBm	CAT 4 Comparison
[47]	CAT 3		Fixed	LAA-LAA LAA-Wi-Fi			MARKOV
[48]	CAT 1			Indoor Single and Multi-Floor	Full buffer	23 dBm	
[49]	CAT 3	CCA-ED:-82 dBm Indoor -62 dBm Outdoor	Fixed CW and freeze period of 11 OFDM Symbol	2 x Wi-Fi vs Wi-Fi-LTE DL LAA vs DL Wi-Fi (DL+UL) Wi-Fi vs DL LAA	FTP 0.5 Mbyte Non full buffer		
[50]	CAT 1	CCA-ED: -70 dBm	Fixed 18 micro sec	Office Indoor 3GPP Scenario		15 dBm	Channel Selection with Q-LEARNING
[37]	CAT 2?	CCA-ED: 62 dBm		Indoor LTE-U femto-cell, outdoor LTE-U pico-cell vs Wi-Fi indoor		23 dBm	Channel Selection with MATLAB
[51]	CAT 3	CCA-ED: (-52,-62,-72,-82,-92)dBm	Fixed (32,128)	Outdoor/Mixed standalone coexistence	FTP 1 0.5 Mbyte	enodeB 30 dBm AP 20 dBm STA 17 dBm	

[45]	CAT 2	CCA-ED: Adaptive in [-82 dBm, -58 dBm]		Indoor Office	Full Buffer Data	24 dBm BS- AP 23 dBm Ue-STA	
[52]	CAT 3	CCA-ED: -82dBm	Fixed (32,128)	Outdoor - Mixed indoor outdoor - standalone plain coexistence	FTP 1	enodeB 30 dBm AP 20 dBm STA 17 dBm	No licensed band simulated RTS CTS self CTS
[53]	CAT 1			indoor scenario			Channel se- lection with Q-LEARNING
[54]	CAT 3	CCA-ED: Adaptive in [-30 dBm, -80 dBm]	Fixed 32	2xWi-Fi 2xLAA Wi-Fi vs LAA [indoor, outdoor]	FTP 3 0.5 Mbyte	23 dBm	
[55]	CAT 3,4	CCA-ED: -55dBm	QoS Adap- tive	Outdoor Indoor only co- existence 3GPP 1,2,3	FTP 3 0.5 Mbyte	18 dBm	
[56]	CAT 3,4	CCA-ED: -62dBm CCA- PD: -82dBm	Adaptive	Indoor standalone plain coexistence	FTP 0.5 Mbyte	18 dBm with LBT 23 dBm Without LBT	WaLT simulator CTS to self



[57]	CAT 2	CCA-ED: -62 dBm, -72 dBm		Outdoor - Mixed Indoor Outdoor [LTE vs Wi-Fi compared to 2x LTE or 2x Wi-Fi]		30 dBm	Channel selection STOCHAS- TIC 40MHz Bandwidth
[58]	CAT 2						LBT MARKOV
[59]	CAT 3	CCA-ED: -82 dBm E-CCA: 16 SLOTS	indoor building 2xWi-Fi vs Wi-Fi vs LAA	FTP 3 0.5 Mbyte		23 dBm	COT
[60]							MARKOV
[61]	CAT4	CCA-ED: -62 dBm	Adaptive on Channel Load	3GPP Indoor 2xWi-Fi LAA vs Wi-Fi	FTP 1 0.5 Mbyte	18 dBm	
[62]	CAT 4	CCA-ED: -77 dBm , -82 dBm	Dynamic [0,1] [0,2]	2x Wi-Fi vs Wi-Fi -LTE	Poisson	23 dBm AP and eNodeB	STOCHASTIC
[63]	CAT 2					UE 20 dBm STA 15 dBm	800 Mhz Bandwidth STHOCAS-TIC
[64]	CAT 3	CCA-ED: -62 dBm	32	Outdoor, indoor2xLAA-2xWi-Fi, Wi-Fi vs LAA 3GPP 2,3	FTP 1 0.5 Mbyte	eNB 18dBm	BWSIM

[65]	CAT 4	CCA-ED: -62 dBm,-72 dBm,-82 dBm	[15,63] doubled with 80% of NACK	Indoor scenario Single Floor Building	FTP 3 0.5 Mbyte	18dBm	MCOT
[32]	CAT 1			Standalone, Wi-Fi +LTE-U 21-cell wrap- around dense hotspot		27 dBm	ABS - 40 MHz Bandwidth
[66]	CAT 1						ABS
[67]	CAT 1						ABS
[68]	CAT1				FTP 2 - Non full buffer Traffic Data	23 dBm	ABS
[69]	CAT 1						ABS 40 MHz Bandwidth
[70]	CAT 1						ABS
[71]	CAT 1						ABS Monte carlo MATLAB
[72]	CAT 1						ABS Monte carlo MATLAB

The periodic sensing scheme is performed periodically for a certain amount of LTE sub-frames. The transmission of each of such sub-frames is divided into two phases: a *sensing phase* and an *action phase*. During the sensing phase, i.e. the beginning of the sub-frame, the eNodeB senses the channel and, if the channel is sensed free, the transmission is completed during the action phase by sending the remainder of the sub-frame. The persistent sensing scheme works in a different way. If such a scheme is employed, LTE nodes sense the channel by means of one sub-frame and transmit data in the following consecutive sub-frames. Otherwise, LTE nodes keep sensing the channel instead of transmitting. This type of sensing can provide a more accurate sensing because the channel is sensed for longer than the periodic sensing scheme.

In the periodic sensing scheme, Wi-Fi performance gets better as the sensing time gets longer. This happens because Wi-Fi is able to transmit while LTE is sensing the channel. In the persistent scenario, as the number of transmitting sub-frames increases the LTE throughput increases while the performance of Wi-Fi gets worse. With the presented algorithms, the Wi-Fi throughput has a significant improvement and the LTE throughput decays. By applying the periodic sensing scheme, the throughput of Wi-Fi users is about 2.5 times higher than the no-sensing case in two sparse deployment scenarios. The gain becomes larger in dense deployments. Similar results are observed with the persistent scheme. Simulation results show that both the proposed sensing schemes can provide an appropriate trade-off between LTE and Wi-Fi in coexistence.

Authors in [63] derive an analytical optimum radio access for LAA represented by an harmonization between a scheduling based radio access and a random access scheduling among the pool of resource batches. One resource batch in LAA is referred to as a number of RBs used for one uplink transmission. By deriving the optimum switching condition, the paper introduces essential foundations for urgent LAA design requirements.

In [57], the behavior of LTE-U based on LBT, in combination with medium access priority and sensing threshold as control parameters, is discussed. Authors point out that in a scenario where Wi-Fi is used indoor and LTE-U outdoor, the protection offered by walls reduces the interference experienced by Wi-Fi.

An *orthogonal* airtime coexistence mechanism is defined in [73]. Authors propose that an LBT station performs a CCA only at the beginning of an AIFS period (to this end, LBT stations must be equipped with an 802.11 interface). In this way, given that the minimum duration of an AIFS ( $34 \mu s$ ) is longer than the CCA minimum time ( $20 \mu s$ ), the channel is always sensed idle by the LBT stations. Furthermore, at the start of each transmission, an LBT station sends (using the 802.11 interface) a CTS-to-self frame, to ensure that 802.11 stations do not transmit while the LBT station is transmitting. Then, authors derive the

probability with which an LBT station should attempt to transmit in order to maximize its airtime while satisfying the constraint that it must not degrade the throughput of a Wi-Fi station more than what another 802.11 station would.

### **LBT, category 3**

Category 3 LBT provides a random backoff procedure with a fixed contention window size in order to let LTE fairly coexist with Wi-Fi. In [64], a simple LBT scheme with back-off is presented to demonstrate how such a scheme can facilitate the coexistence between multiple LAA operators, without coordination and no degradation in Wi-Fi performance when an LAA cell is deployed. Simulations are carried out by using LTE-A Broadband Wireless Simulator, BWSIM<sup>2</sup>.

Settings for the Clear Channel Assessment thresholds, together with the size of the contention window, play an important role in the simulation scenario. In particular, raising the threshold implies sensing and protecting a smaller area around the eNodeB; on the other hand, a too high threshold is ineffective as it becomes equivalent to the case without LBT [51]. LTE CCA mechanism should be provided with the ability to detect Wi-Fi signals. An outdoor scenario and a mixed outdoor-indoor scenario are investigated. In the first case, LTE standalone performance is significantly better than the Wi-Fi standalone case. With no LBT mechanism, Wi-Fi performance is badly damaged by LTE transmissions. In the outdoor scenario, the LBT mechanism controlling the CCA threshold and the CW size plays an effective role in balancing the performance between LTE and Wi-Fi systems. The correct CW size and CCA thresholds play a key role in safeguarding Wi-Fi operations in the unlicensed band together with LTE. In particular, with a CCA threshold of -52 dBm and a CW size of 32, LTE and Wi-Fi achieve, respectively, 67% and 19% of their standalone performance with an offered load of 40 Mbps. If the LBT threshold is set instead to -92 dBm and the CW size to 128, LTE achieves 11% and Wi-Fi achieves 91% of their standalone performance. In an indoor scenario, instead, it is shown that Wi-Fi is not much affected even when LTE operates without any coexistence mechanism.

In [52], LTE and Wi-Fi performances are studied in an outdoor scenario and it is shown that, without additional coexistence mechanisms, Wi-Fi performance is highly degraded. When Wi-Fi networks are located indoor, instead, their performance is not much degraded by outdoor eNodeBs, due to high penetration loss due to walls. Indoor devices suffer, though, from the hidden node problem since sensing outdoor eNodeBs is not so accurate. The RTS/CTS, or CTS-to-self, mechanism can however solve this problem and boost the performances of both systems. Firstly, a scheme in which the eNodeB transmits a CTS

<sup>2</sup><http://bwsim.cewit.org.in/>

message before its downlink transmission, i.e., a CTS-to-self scheme, is considered. To this end, eNodeBs are assumed to be equipped with a Wi-Fi transceiver. Since virtual carrier sensing is adopted and the NAV of Wi-Fi nodes is triggered, this mechanism has a good performance compared to LBT only. The use of RTS messages sent through the LTE WLAN transceiver to a group of potentially interfering UEs and eNodeBs through a reliable control channel in the licensed spectrum is also investigated. In addition to the mentioned strategy, a proper configuration of the CW size and the CCA threshold at the eNodeBs to control the aggressiveness/friendliness of the LTE system is carried out. In particular, fixing the eNodeB CCA threshold at  $-82$  dBm and playing with the CW size only shows that in the outdoor deployment scenario each system performance is not much different if the same CW size is used, regardless of the adopted coexistence technique. This is due to a good eNodeB sensing resulting in a not so significant hidden node problem. LTE performance improves by using the RTS/CTS mechanism and it is also observed that the RTS/CTS mechanism can boost both the LTE and WLAN performance when compared to the CTS-to-self mechanism.

In [49], an LAA system-level throughput and buffer occupancy evaluation is performed in a purely downlink scenario. An additional deferral period is inserted so that the earliest time that LAA can transmit after the channel becomes idle is at least as large as the Wi-Fi DIFS (Distributed Inter Frame Space). In addition to that, additional transmission opportunities are provided to Wi-Fi, obtained by restricting the LAA CCA starting points to LTE sub-frame boundaries and enforcing *freeze periods* where the backoff procedure and LTE CCA sensing are completely suspended. Conclusions are that the proposed LAA coexistence solution enables the non-replaced Wi-Fi network to achieve a better performance. Experiments on the mutual interference between LAA cells also showed that, with their improvements, LAA is a good neighbor not just to Wi-Fi, but also to other LAA networks. Coexisting Wi-Fi networks consistently exhibit higher mean buffer occupancy even with four unlicensed carriers being available, which implies that Wi-Fi nodes tend to back off more frequently to each other (compared to scenario where at least one LAA cell is present). This comes from the low sensing threshold used by a Wi-Fi node towards another Wi-Fi signal compared to the one used against LAA. In a coexistence scenario, the proposed LBT procedure provides more opportunities for Wi-Fi to obtain channel access, compared to the case where it competes with an identical MAC protocol of another Wi-Fi network. The mean buffer occupancy is significantly lower when LAA and Wi-Fi are coexisting. LAA, in fact, can serve its traffic and vacate the channel quicker compared to a Wi-Fi network.

To keep LTE efficient and to safeguard Wi-Fi, a dynamic adjustment technique for the CCA threshold is studied in [54]. CCA-ED only is considered, because it is mandatory in several legislative domains. By adjusting the CCA threshold, a trade-off can be achieved

between frequency reuse and interference avoidance. In particular, increasing the CCA threshold reduces the sensing range of the two neighboring eNodeBs performing the CCA check, which may lead to simultaneous transmissions. On the other hand, an aggressive channel reuse is achieved at the expense of potentially introducing increased interference.

The User Perceived Throughput (UPT)<sup>3</sup> performance of the proposed adaptive LBT scheme is evaluated and compared to a fixed CCA threshold of -70 dBm. Adopting a fixed CCA threshold shows that both average UPT and 10% UPT of the victim Wi-Fi network are similarly impacted by the coexistence with LTE. The proposed adaptive scheme achieves remarkable improvement in terms of LAA performance as compared to the fixed scheme. A more aggressive reuse with an acceptable increase of interference by configuring a moderately high CCA threshold can lead to a capacity gain of LAA and a fair coexistence with Wi-Fi systems.

In [56], authors describe the development of a network simulator *WaLT* performing simulations mostly focusing on hidden terminal issues. A new LBT scheme is proposed, based on [74]. A CCA is continuously performed with no restriction to frame boundaries. However, there are differences between LTE and the one Wi-Fi uses. [74] mandates the use of coexistence mechanism only if the medium is found busy, while Wi-Fi always applies this procedure. Also, another scheme with ECCA and growth of contention window is proposed. Results shows that ETSI LBT is not fair in terms of channel occupancy with respect to Wi-Fi. Adding a persistent ECCA LBT results to be less aggressive to Wi-Fi performance but adding an exponential back off is not enough to further improve the LAA kindness with a small cost to the aggressor LAA network's throughput. The proposed scheme appears to be too favourable to Wi-Fi system. LTE throughput results in fact to be lower than the Wi-Fi one. However, results change by varying the sensing thresholds.

#### **LBT, category 4**

Category 4 LBT provides the possibility to adapt the contention window size, which further improves performance. This feature enables LBT to achieve a fair coexistence, while at the same time solving the hidden terminal problem, too.

The basic LBT mechanism is a simple and fixed mechanism for sharing the medium and lacks the ability to guarantee the service fairness among different types of traffic flows. Simulation results show that LAA with an LBT mechanism generally does not impact Wi-Fi services more than an additional Wi-Fi network would do. However, with the fixed CW size

<sup>3</sup>The ratio of the amount (in Mbit/s) of data bits received correctly in UE/STA for each packet to the time between the arrival of packet and successful reception of packet at receiver side.

and the maximum channel occupancy time, different nodes receive the same transmission opportunity, regardless of traffic demands and channel conditions. In [55], in order to achieve not only channel access fairness but also QoS fairness, the LBT approach is enhanced with contention window size adaptation for LAA. If the LBT mechanism is designed without taking care of buffers states, the channel occupancy rate and the channel condition service fairness among multiple nodes is difficult to achieve. An innovative solution based on the collection of QoS metric information from neighboring nodes, via the LTE X2 interface, is then proposed. This way, nodes are able to adjust their CW size in order to achieve service fairness. Compared to the fixed LBT mechanism, the proposed LBT algorithm could achieve around 4% and 6% of LAA performance gain in terms of UPT and transmission latency, respectively. Also, more than 25% of reduction in latency can be achieved for Wi-Fi transmissions. All of the aforementioned translates into a number of advantages when the proposed LBT procedure is used.

In [62], authors leverage stochastic geometry to characterize key performance metrics of LAA networks which coexist with Wi-Fi networks. The analysis is focused on a single unlicensed frequency band, where the locations for coexisting eNodeBs and APs are modeled as two independent homogeneous Poisson point processes. Based on an analytical modeling of the channel access procedure, authors derived the Medium Access Probability (MAP), SINR distribution, Density of Successful Transmissions (DST) and data rate distribution for both LAA and Wi-Fi. By adopting more sensitive CAA thresholds and larger contention window sizes, LAA can improve its fairness and data rate performance of Wi-Fi. LAA is also shown to achieve good data rate performance despite using LBT. Choosing a lower channel access priority and a more sensitive sensing threshold for LAA, Wi-Fi is shown to achieve better DST and rate coverage probability, while LAA still maintains acceptable data rate performance.

In [46], authors evaluate two access schemes for LTE, under various traffic scenarios (denoted as *Method A* and *Method B*). The fairness of these schemes largely depends on the signal/energy detection threshold used by the LAA-LBT mechanism. *Method A* is the one described in [74] and is an open loop mechanism. *Method B* has a variable window similar to Wi-Fi DCF and is a closed loop mechanism. It utilizes the most recent ACK received on the uplink of the primary carrier. ACKs are used to update the contention window. A missing ACK beyond a time-out is considered as no ACK (NACK) and the CW is suitably updated. Until a new ACK or NACK is received, the contention window remains the same. Performance of both methods in diverse load settings and sensing thresholds are evaluated. The results suggest that both mechanisms can allow LTE to co-exist with WLANs in a fair manner, if the sensing threshold is suitably chosen.

Method B performs well in most of the considered cases, thanks to its feedback mechanism. However, Method A performs well only if parameters such as the sensing threshold and minimum contention window are properly chosen. Obviously, a trade-off in sensing threshold selection is shown. In particular, it is shown that a high sensing threshold improves the overall network throughput but degrades the Wi-Fi performance, a low sensing threshold results in improved Wi-Fi performance at the cost of overall network throughput. Hence, the sensing threshold must be carefully selected to achieve the appropriate performance trade-off between the WLAN and the overall network.

The Fair Listen Before Talk (F-LBT) [58] approach considers the total system throughput and the fairness between LTE-U and WLAN and then allocates an appropriate idle period for WLAN. An analytical model derives the system throughput when LTE-U and WLAN coexist introducing a Discrete-Time Markov Chain (DTMC) model and then compare F-LBT with the conventional frame-based LBT schemes with the fixed idle period. F-LBT algorithm tries to allocate the appropriate number of idle subframes by considering the fairness between LTE-U and WLAN and the total system throughput estimating the number of WLAN nodes and then determining the number of idle subframes. Evaluation shows that F-LBT can improve the total system throughput while providing the fairness between LTE-U and WLAN.

A cognitive coexistence scheme known as CU-LTE [60] enables spectrum sharing between U-LTE and Wi-Fi networks. The scheme is designed to jointly manage dynamic channel selection, carrier aggregation and fractional spectrum access for LTE-U networks while guaranteeing fair spectrum access for Wi-Fi. A mathematical model of the spectrum sharing problem for the coexisting networks is derived and an algorithm is designed that solves the resulting fairness constrained mixed integer nonlinear optimization problem. Performance evaluation shows that the coexistence scheme achieves near-optimal spectrum access for LTE networks while guaranteeing fairness to Wi-Fi. CU-LTE does not require the coexisting networks to exchange signalling messages.

An LBT mechanism featuring an adaptive distributed control function protocol for the small base stations (SBSs) is presented in [75]. The backoff window size is adaptively adjusted according to the available licensed spectrum bandwidth and the Wi-Fi traffic load to satisfy the quality-of-service requirements of small cell users and minimize the collision probability of Wi-Fi users. An admission control mechanism is further developed for the SBS to limit collision with Wi-Fi traffic. The proposed schemes are evaluated by means of numerical simulations and are shown to outperform non-adaptive channel access mechanisms in the unlicensed spectrum.

An analytical framework to investigate the downlink coexistence performance between two systems when LTE employs a simple LBT mechanism is shown in [47]. Theoretical



models based on Markov chains are established by using this framework and downlink throughput can be calculated. In the presented scenario, all the eNodeBs are assumed to be aware of the transmissions of other eNodeBs and also of the presence of Wi-Fi access points. Also, quite unrealistically, LTE transmissions are available only with two data rates, i.e. low and high. When a transmission fails at the high data rate, a retransmission occurs at the low data rate and it is always assumed to be successful. The overall results show that LTE has always greater probability to acquire the channel. When the number of APs increases, the total traffic load decreases. This trend is due to the low capability of APs to acquire the channel. APs are not capable of coordinating the transmissions of stations in different networks. Numerical results obtained from the model show that the simple LBT scheme is very effective in LAA-LAA or LAA-Wi-Fi scenarios and can improve Wi-Fi performance substantially, compared with scenarios where LAA works with no coexistence mechanisms in place.

LBT parameters can be dynamically adapted to the traffic load and Wi-Fi contention window sizes [59]. Fixed LBT parameters can heavily affect the performances of LAA and Wi-Fi in coexistence scenarios. A limitation with respect to the coexistence performance is shown regarding the COT setting of LAA systems. LAA may set the COT value to the duration of the Transmission Opportunity (TXOP) of Wi-Fi systems (3.4 ms), to allow for a fair coexistence. However, LAA suffers from unnecessary overhead associated with transmitting the initial signal and it becomes more critical when COT becomes shorter. On the other hand, it becomes less favorable to Wi-Fi systems when COT becomes longer. Two different adaptation mechanisms are shown:

- *Channel Occupancy Time, On/Off Adaptation*
- *Idle Time Short-Long Inference and Adaptation*

With *Channel Occupancy Time, On/Off Adaptation*, COTs are reduced if the traffic load of the Wi-Fi system increases, so that LAA does not occupy the channel for too long (and vice versa). Traffic load of the involved Wi-Fi systems can be estimated indirectly by sensing the channel activity.

With *Idle Time Short-Long Inference and Adaptation*, it is attempted to infer the size of the Wi-Fi contention window by observing the channel activity after adopting different values for the duration of the idle time for LAA eNodeBs. Specifically, a typical strategy is to vary the number of short and long idle time intervals, which allows to infer the relative back-off size of the co-located Wi-Fi systems. Simulation results, under varying traffic loads, demonstrated that the proposed scheme can improve the overall system throughput, while mostly preserving the performance of Wi-Fi systems, also when the traffic load was high.

The overall system throughput can even be improved by up to 30-105%, depending on the traffic load, while at the same satisfying the constraints of a fair coexistence.

### 3.7.2 Almost Blank Subframe

In the following, we describe in detail proposals dealing with new approaches for the fair coexistence of LTE and Wi-Fi that are based on the *Almost Blank Subframes* technique.

LTE performance in an outdoor deployment scenario is improved by asynchronously muting patterns due to interference avoidance among LTE eNodeBs [52]. On the other hand, Wi-Fi performance is better with synchronous muting because all the eNodeBs are muted at the same time. In the indoor/outdoor mixed scenario, instead, it is seen that, regardless of the used muting pattern, Wi-Fi performance is fairly good, since, as noted also in other works, indoor Wi-Fi BSSs are anyway not much affected by the outdoor eNodeBs because of the high penetration loss of walls.

In [71], the performance of the duty cycle method is analyzed. Monte Carlo simulations are carried out to determine the number of collisions at the first transmission and the total number of collisions until one transmission per each device is completed. When Wi-Fi and Duty Cycle (DC) devices co-exist, the total number of collisions of Wi-Fi devices until the transmission completion is higher than twice compared to when only Wi-Fi devices are present. The trend is similar when the DC values vary. The total number of collisions for Wi-Fi decreases and approaches a steady state value as the DC-on time increases. The Monte Carlo method is also used in [72] to demonstrate the fairness of Wi-Fi and LTE-U air time sharing.

In [69], a novel proportional fair allocation scheme is derived. This technique differs from previously considered approaches in that its resource allocation scheme requires only quite limited knowledge of network parameters. Fairness is achieved by assigning equal channel times to every competing entity, including idle periods, successful transmissions and collisions for the Wi-Fi network. It can be implemented without explicit coordination among the different networks and no changes are required for Wi-Fi networks. Learning techniques for decentralized collision-free operation are considered.

In [66], an adaptive coexistence mechanism is presented. The performances of LTE and WLAN when both work in fixed subframe configurations are evaluated and then a dynamic configuration is set up by the proposed algorithm. The proposed algorithm, after computing the WLAN throughput, selects the appropriate subframe allocation by looking up a precomputed table. Adaptation mechanisms are useful to allocate resources according to the WLAN traffic. WLAN load is computed as the ratio of the number of frames sensed by the LTE Energy Detect (ED) mechanism to the number of frames muted in that reallocation

cycle. The adaptive mechanism is made up by 13 subframe configuration modes. As the load increases, LTE will leave more subframes to WLAN in the next reallocation cycle. The performance of the proposed mechanism is shown to outperform the existing ones. In a fixed configuration, WLAN throughput increases while LTE decreases. Instead, with the adaptive co-existence mechanism, a higher overall throughput is achieved, while WLAN loses no more than 15% of throughput on average.

In [68], authors propose a Q-Learning based dynamic duty cycle selection approach in which periodic transmission gaps are configured by LTE eNodeBs. Firstly, Wi-Fi and LTE performances are evaluated with a fixed value of LTE transmission gaps. A Time Division Duplexing configuration is determined based on the asymmetrical distribution between downlink and uplink needs. With larger LAA duty cycles, Wi-Fi capacity decreases while LTE throughput increases, as expected. Dynamically adjusting the duty cycle leads to a gain in the overall capacity, as Wi-Fi gets a proper number of transmission opportunities when needed, as opposed to when a fixed duty cycle is employed.

An ABS technique based on the concept of coexistence without priority is presented in [76]. LTE cells operating in unlicensed bands have the same priority as Wi-Fi access points. To avoid interference from neighboring LTE cells, scheduled times for ABSs are often deterministically decided and exchanged between LTE base stations through the X2 interface (to synchronize them and avoid interference). In this work, ABSs are scheduled randomly, but in such a way to cover a certain percentage of air time (if such a percentage is 30%, then 30% of subframes are ABSs). Such a percentage is computed by estimating the number of nearby LTE base stations and Wi-Fi access points so as to reduce interference.

A simple coexistence method in the 900 MHz space, i.e., the TV white space, is presented in [48]. The network is assumed to work in two operational modes: *normal mode*, when no one else is accessing the shared spectrum, and *coexistence mode*. The coexistence mode is triggered by some events (detection of a beacon frame, increase of interference), or periodically. When another technology is detected, a negotiation phase begins for a fair coexistence. Authors propose a modified version of ABS in order to coordinate Wi-Fi and LTE activities. During an ABS, Wi-Fi nodes detect a channel vacancy and, if the overall channel energy is under a certain threshold, they can start transmitting. Blank allocation is statically set and different configurations are tested. Multiple indoor scenarios are investigated and the performance of each technology is evaluated, while increasing the number of users and/or APs. When the proposed coexistence mechanism is not in use, Wi-Fi devices spend all of their time sensing the channel and the decrease in the LTE throughput is proportional to the duration of the blank subframe, as expected. With the coexistence mechanism, an increase in throughput for Wi-Fi networks is observed, which is not linear with the time ceded by

LTE. When the number of APs decreases and the STAs grow in number, the performance is affected more by the CSMA/CA protocol than by the blank subframe allocation. When the scenario is sparse, both LTE and WLANs achieve higher throughputs. Simulations show that the optimal number of blank subframes varies with the distribution of users in the interference range. For such a reason, an initial (or periodic) phase during which parameters are negotiated is needed.

In [70], a time-domain multiplexing technique for interference mitigation is presented under the name of *Inter Cell Interference Coordination (usICIC)*. This technique takes into account the impact on the overall LTE system performance due to the interference resulting from multi-operator LTE channel sharing in non LBT regions. Only a limited number of channels are available in the 5 GHz bandwidth so the probability of two LTE LAA small cells overlapping is high. Authors propose an unlicensed spectrum Inter Cell Interference Coordination mechanism to allow the multi-operator LTE small cells to negotiate orthogonal, non-overlapping, CSAT gating cycles. Extensive simulations prove that the proposed usICIC mechanism will result in 40% or more improvement in overall system performance.

Ensuring fairness in terms of airtime does not necessarily provide each device in the network with the same average data rate, which is dependent upon a number of factors [67]. The amount of time during which LTE is silenced to let Wi-Fi devices transmit is often too short to allow them to access the channel (due to the mandatory inter-frame spaces), thus leading to the risk that Wi-Fi devices spend a significant amount of time in listening mode when a nearby LTE cell operates on the same channel. A probabilistic and numerical analysis reveals that Wi-Fi transmissions are significantly affected by the presence of LTE systems operating on the same channel.

### 3.7.3 Minor techniques

The Channel Selection (CS) technique is adopted in a number of works, mainly exploiting approaches based on machine learning and stochastic geometry.

A distributed mechanism that exploits prior experience is proposed to enable coexistence with other systems in a smart and efficient way [53]. A fully decentralized approach, where the channel selection decision is performed independently by each small cell in the scenario, is considered to initially assess the potentials of the Q-learning solution. Promising results are obtained revealing that the throughput achieved by the proposed approach can be between 96% and 99% of the optimally achievable throughput.

In [50], the robustness of a distributed Q-learning mechanism is exploited in a non-stationary wireless environment. Simulation results allow assessing quantitatively the capability of the mechanism to re-learn proper solutions when changes in the environment

occur. Furthermore, the analysis evaluates quantitatively how fast the learning process has to be compared to the variations in the environment in order to retain an LTE-U throughput performance very close to the optimal one. The time needed by the learning process is in the order of 10 to 15 times the average time between two consecutive channel selection decisions divided by the learning rate. Also this factor can be reduced from 10-15 to 3-4 if the learning process does not start from scratch but uses previously learnt information to react to a change in the environment.

In an outdoor/indoor scenario the problem of hidden nodes is serious. In [57], authors propose a solution based on channel selection. In the 5 GHz band, 12 channels of 40 MHz are available for use and channel selection algorithms may play an important role in the coexistence scenario. Channel selection is conducted while performing the medium access and possible channel selection schemes include:

- *Random selection;*
- *Least power selection;*
- *UE least power selection.*

A least power selection scheme is simulated and the results show that the performance of LTE-U can be improved significantly when channel selection is based on UE measurements.

In [77], a Fast Automatic Gain Control (AGC) Scheme for LAA TDD systems is proposed. A digital AGC scheme based on feedback structure can not only effectively increase the convergence speed of the AGC gain by using the current signal amplitude ratio adaptively but also maintain the stability of AGC operation. Since the received signal has a large power difference between uplink and downlink, using a conventional AGC scheme cannot be efficient in a wireless network. The AGC gain in fact cannot converge fast enough to properly respond. Therefore, the conventional scheme leads to increased AGC gain variation, and the received signal will be attenuated by large AGC gain variation. To overcome this limitation, an AGC scheme based on the average amplitude ratio is proposed. The mechanism can not only effectively increase convergence speed of the AGC gain but also maintain the stability of AGC operation in LTE TDD system. Evaluating the average convergence time and variation of AGC gain of the proposed AGC scheme and the conventional AGC scheme in a variable channel environment shows that the proposed AGC scheme reflects the signal variations quickly and has stable operation. Results are achieved by applying the average amplitude ratio even in LTE TDD mode which has nearly 100 dB difference of the received signal power between downlink and uplink subframe.

In [78], a survey on the coexistence between radar and LTE-U systems in the 5 GHz band is presented. Each portion of U-NII (Unlicensed National Information Infrastructure) is

populated with different types of radar and has its own regulations imposed by FCC (Federal Communication Commission). Authors presented a survey on RF regulations applied in this scenario.

## **Chapter 4**

# **A Smartphone-Based Assessment of LTE Measurement Procedures**

### **4.1 Aim of the Research**

LTE technology gives access to higher bandwidth and assures efficiency at network level for telecommunication operators, providing a reliable and continuous data traffic flow that allows data transmission at extremely high bit-rates. The aim of this chapter is to evaluate LTE network performance in an actual urban environment, with emphasis on the downlink channel throughput. The use of statistical methods shows how standard expectations are too high with respect to a real scenario. Also, an analysis is carried out with reference to key parameters for radio optimization that are not defined in the standard and are implemented and defined differently by each vendor.

### **4.2 Smartphone-based Assessment and Methodology Overview**

Beside a theoretical approach which resorts to network numerical simulation and emulation tools, or to experiments run in a controlled environment, to efficiently evaluate network performance it is required to adopt an experimental approach under real-case conditions.

In [6] authors used numerous C++-based system-level simulations to prove their relay channel measurement and channel quality reporting scheme. They compared their proposal to other channel measurement and CSI feedback scheme showing that the proposed scheme has a significant performance enhancement over the others. In [79] measurements were conducted to demonstrate the performance of a two-dimensional joint time-frequency estimator proposed for the 3GPP LTE downlink system, while in [80] the interference level generated by the LTE

system in a satellite receiver is investigated. In [3–5] the MIMO channel and synchronization strategy is investigated by means of dedicated instruments and a channel analysis and modeling software. Sometimes, network performance can be assessed and monitored on the service provider's side. In [81] connection setups, handovers and capacity utilization are recorded through the *Performance Statistics* application in the Ericsson Operation and Maintenance system. In [82] authors propose a novel algorithm that can adjust the threshold values of MCS according to the CQI and other dedicated performance measurements, when either a Fast and Independent Adjustment (FIA) and Slow and Centralized Adjustment (SCA) policy is adopted for CQI transmission. Results were collected by a system-level simulator and proved a higher average cell throughput and transmission success ratio if compared to the traditional algorithm.

Over the past few years measurements have also been run using smartphone-based measurement devices. In [83] authors designed and implemented a mobile Application Resource Optimizer (ARO), showing its benefits on several essential categories of popular Android applications to detect radio resource and energy inefficiencies. In [84] authors discuss an iPhone 3GS based deployment of LiveLab (a common measurement software) with 25 users to approach the challenges of privacy protection and power impact using LiveLab in iOS. They not only prove the feasibility and capability of LiveLab but also seek to advocate LiveLab as a network and user measurement methodology, and showed that logging detailed smartphone usage and measuring networks from smartphones is not only feasible, but it also provides unique information regarding both mobile users and networks. In [85] authors attempt to establish an equivalent benchmark for comparing network application performance on smartphones studying it on several mobile devices for three mobile platforms: iPhone, Android and Windows Mobile. Authors developed a systematic methodology for assessing and collecting data from 3G network performance as well as smartphone based application tool performance, consisting of several types of experiments crucial to characterize network performance, including TCP throughput, round trip time, re-transmission rate, and capable of enabling users to carry out local experiments informed by realistic 3G network conditions across different locations and network carriers.

In [86] a model of the characteristics of link layer RTT and bandwidth vs link signal strength is derived to evaluate applications and services. It is based on real measurements since an extensive measurement campaign in Dublin, Ireland was carried out using a custom performance measurement tool.

In [87] authors design a new mobile network measurement tool for Android devices, called 4GTest that also allows users to switch among different network types, i.e. 3G, WiFi



and LTE. They observed that LTE has significantly higher downlink and uplink throughput, compared with 3G and even WiFi.

Long Term Evolution Advanced (LTE-A) mobile telecommunication system also provides a significant increase in data rates, reaching 3 Gbps in DL and 1.5 Gbps in UL. With reduced latency and dynamic management of bandwidth LTE network also allow backwards compatibility with older technologies like GSM and UMTS. LTE-A features include an all-IP flat network architecture, end-to-end QoS, higher spectral efficiency, from a maximum of 16 bps/Hz in R8 to 30 bps/Hz in R10 and an increased number of simultaneously active subscribers. The main new functionalities introduced in LTE-A are Carrier Aggregation (CA), improved performance at cell edges and enhanced use of multi-antenna techniques [88].

It is interesting to investigate whether the theoretical throughput values are really achieved by network operators and which relationship exists between physical layer parameters, identifying channel state and quality, radio management mechanism, scheduling, and predicted or estimated throughput values. The interconnection between several widely accepted throughput performance indicators is explored together with how these indicators are related to signal quality statistics in [89]. Throughput and signal quality statistics are collected from live LTE system cell. Measures are strongly affected by voice applications dominating current LTE networks due to the last transmission time interval transmissions. LTE also adopts a link adaption mechanism based on periodical user's channel condition measurements. Different candidate channel feedback schemes are investigated and network performance is evaluated by means of system-level simulations modeling various radio resource-management algorithms [90]. One out of all mechanism, the so-called *average best-M scheme*, resulted to be the most efficient solution. In [91] an algorithm that can adjust the threshold values for link adaption according to a FIA and a SCA is proposed. FIA optimizes the threshold values, then SCA changes the threshold values by the measurement of average cell throughput and the BLER. System level simulation show that the proposed solution yields higher average cell throughput and transmission success ratio compared to the traditional algorithm.

The introduction of MIMO techniques resulted in a strong throughput gain for LTE networks. Also, MIMO adoption and settings are strictly related to channel parameters. In [3, 4, 92] the MIMO channel and synchronization strategy is explored and analyzed with instruments and a channel simulating software.

Recently network performance evaluation are conducted by means of smartphone-based campaigns. In [85] several types of experiments essential to characterize network performance, including TCP throughput, round trip time, retransmission rate were carried out in a realistic 3G network conditions across different locations and network carriers. Net-

work application performance on smartphones were performed on three different mobile platforms: iPhone, Android and Windows Mobile. In [87] authors design a new mobile network measurement tool for Android devices, called 4GTest that also allows users to switch among different network types, i.e., 3G, Wi-Fi and LTE. LTE showed a significantly higher downlink and uplink throughput, compared with 3G and even WiFi.

Previously, we stated that the envisioned 3 Gbps throughput theoretically achievable by the 3GPP LTE-Advanced standard is way beyond actual network capabilities [93]. CQI and throughput are strictly dependent from SINR and it resulted that the latter alone is not enough to represent the overall channel state, because it is influenced by many factors. In this thesis we present the results of a measurement campaign to evaluate the overall scheduling procedure at LTE MAC layer. A smartphone-based measurement session is carried out in a urban and suburban scenario to collect measurement data at the physical layer and to assess the whole adaptive scheduling process, with the ultimate goal to assess the system's performance from the end-user point of view and compare measured values to those predicted by the 3GPP standard.

In this work we present an extensive smartphone-based measurement session carried out in a urban and suburban scenario to measure the characterizing LTE network indicators like received radio frequency power, SINR and throughput directly on the end-user side making use of the end-user equipment. The objective of the presented research is to compare measured values, which are the one that the end-user actually experiences during normal operation of the mobile device, to the values declared in the standard.

## 4.3 Experimental Setup

A campaign was conducted in order to evaluate the network performance in a real-world user case, using a smartphone-based measurement device in a drive test [94, 95] carried out along a motorway to ensure homogeneous propagation conditions along the route.

Smartphone based measurement campaign represents a common and accurate way to obtain results [96].

Data are analyzed by statistical methods to study how different performance are from those set in the standard, with the goal to characterize and possibly model a real network.

### 4.3.1 Smartphone-Based Measurement Methodology

A measurement campaign was conducted in a real-world scenario adopting a drive test methodology by mean of smartphone-based measurement tool. Sessions were conducted

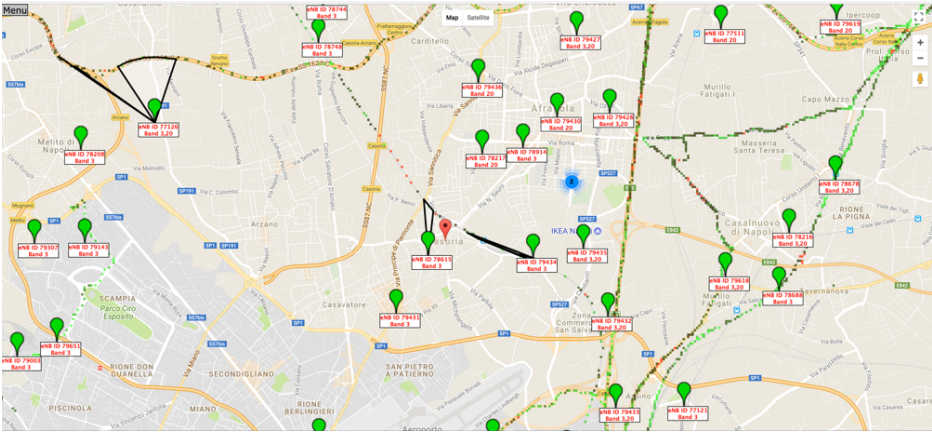


Fig. 4.1 eNodeBs Crowd Sensing

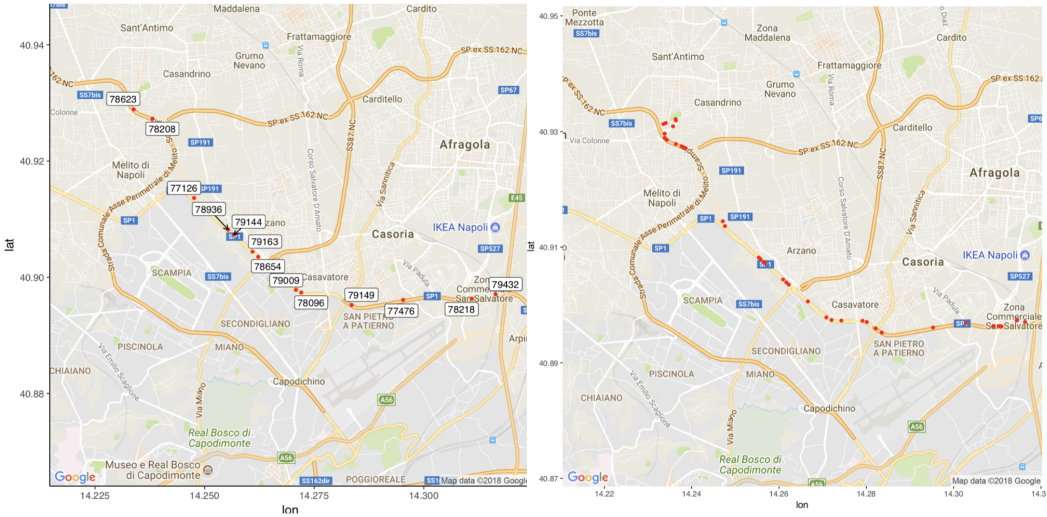


Fig. 4.2 eNodeB's Map along the Route and Handover Occurrence

Table 4.1 Measurement device and software versions

	Version
LG Nexus 5X	Android 6.0 MBD08M
Baseband	Qualcomm M8994F 2.6.28.0.65
Kernel	3.10.73-azq_kernel
AZQ Android Tool	3.0.410(14)

over a 9.75 km extra-city route in the area of Naples, Italy. Measurement device was put in a vehicle moving with an average speed of 49 km/h in a completely *outdoor* scenario. Each measurement result is geo- and time-referenced through the embedded GPS device and handover between different technologies is prevented by forcing the device to connect to LTE network only.

The device used for the measurement session implements LTE-Advanced standard and operates in the 20th band (800 MHz, FDD) with 10 MHz channels. Further characteristics are given in Table 4.1

The 20th bandwidth is always approached by operator as the default anchor component carrier with its highest capacity and high penetration depth factor. Here we are using a category 6 device and are re-proposing the architecture of [93]. To collect real time user data we used the *AZQ Android Driving Test Tool* suite [97] which turns a smartphone into a *full-fledged* measurement device. It makes very easy to collect data about different network parameters of interest and to communicate with all levels of the LTE protocol stack in a real time environment. This work represent our first measurement campaign that was conducted without any agreement with any mobile operator. The AZQ Software then didn't report the eNodeB position, so we are able to retrieve data just from a crowdsensing map shown in Fig.4.1 from [98]. In addition we were able to found out where the UE was able to detect eNodeBs Fig.4.2.

From a metrological point of view, we did not characterize the measurement device in terms of its own uncertainty contribution. Our main objective was indeed to characterize network performance under actual conditions, that is under the influence of the body when the mobile device is being used for a call or when it is in stand-by mode in a pocket and of surrounding objects, and we assumed that such contributions were predominant over the intrinsic uncertainty of the mobile itself.

The suite can be used in two different ways. In the first one, the device is simply a *network monitor* that collects information in a passive way. In the second one, users can define their own script to run and track multiple network parameters. A script is characterized

by a set of high-level instructions (*pseudo-code*) later translated into Java code. Several interesting features are available:

- *Baseband Locking* allows to force the use of one particular technology;
- *LTE PCI/EARFCN Lock* allows to force the connection to a particular eNodeB (PCI), on a specific frequency (EARFCN);
- *LTE Band Lock* allows to force the use of certain frequency ranges supported by the baseband;
- *LTE Radio* allows to display radio interface parameters in *real-time*;
- *LTE Cells* allows to display the list of the eNodeBs that the device can possibly connect to, and information regarding the RSRP and RSRQ received by the eNodeBs;
- *LTE Data* allows to display more low-level information from the baseband such as throughput, MIMO scheme, RB, MCS and TBS.

Measured values are stored in an *SQLite* database for post processing and analysis.

### 4.3.2 Test Methodology

As previously stated, to realistically evaluate network performance, the characterization we present in this work relies on measurements captured in a real world scenario. Different assessments session were run to acquire a significant set of measurement data for the parameters of interest, in different hours of the day under different conditions. Performance is largely affected by the baseband implemented by vendors, beside the specific algorithm adopted to compute the CQI. Furthermore, since a large-bandwidth stress test was run, the device's memory writing speed could affect the throughput perceived by the user.

To avoid an excessive resource device overhead, measurement data are average over 200 ms. This configuration may change with the software version or after a baseband firmware or operating system update. Energy saving mode has been turned off during measurements. To better evaluate KPI indicators each measurement session is characterized by the use of different scripts in order to achieve proper evaluations on network performance. To obtain meaningful results it is necessary to stress out the LTE system during the whole measurement period of time because even a few moments of inactivity could prevent from a correct interpretation of results. Analysis is therefore based on the session which experiment homogeneous boundaries conditions. A *high-bandwidth stress test* was therefore run, which consists in the continuous download of a large files (200 Mb) from a remote server using the

Table 4.2 Peak Throughput

<b>Bandwidth</b>	<b>20 MHz</b>	<b>15 MHz</b>	<b>10 MHz</b>
<i>Peak downlink throughput @ 64 QAM [Mbps]</i>			
MIMO 2x2	150	110	74
MIMO 4x4	300	220	148
<i>Peak downlink throughput @ 16 QAM [Mbps]</i>			
MIMO 2x2	51	38	25
<i>Peak uplink throughput @ 64 QAM [Mbps]</i>			
MIMO 2x2	75	55	37

HTTP protocol and a multi-threaded approach with 10 segments. When a multi-threaded approach is presented with 10 segments, we are stating that 10 parallel TCP connections are opened by the UE. With a single TCP connection, a UE is not capable of saturating LTE Bandwidth. Using multiple parallel TCP connections we are more likely to be in the situation where the band either is completely overloaded or very close to it.

### 4.3.3 Aim of the Research

To efficiently spread all of LTE resources, SINR to CQI mapping is required to determine the proper AMC modulation Scheme to use for users. It is possible to predict from CQI mapping and adopted AMC the maximum throughput value. The CQI report not only indicates the downlink channel quality but also the capabilities of the UE's receiver. A UE with receiver of better quality can report better CQI for the same downlink channel quality and thus can receive downlink data with higher MCS. The category of the UE also, specifies the ability of the device in terms of DL/UL throughput Antenna support and Transport Block Size Modulation Support. Maximum throughput is first calculated as symbol per second and then converted in bits. In a LTE MHz band is made of 100 RB and each having 168 symbol per ms with a normal Cyclic Prefix. If a 64 QAM is used (6 bits per symbol) throughput will be  $16,8 \times 6 \times 100.8$  Mbps. In addition if a 4x4 MIMO system is in use throughput would be 4 times as before.

The tested LTE network operates in the 20th band (800 MHz, FDD) with 10 MHz channels (used as the PCC) and in the third band with 15 MHz channels (used as the SCC whenever possible). Even using a category 6 device, the user is never able to achieve the expected throughput due to a limited availability of bandwidth in the eNodeBs. In particular, when no Carrier Aggregation mechanism is in use, with 10 MHz channels users can experience a

maximum theoretical throughput of 74 Mbps in downlink and 25 Mbps in uplink, whereas with 15 MHz channels, 110 Mbps in downlink and 38 Mbps in uplink are obtainable. Instead, using the Carrier Aggregation with two carriers (B20 and B3), the maximum attainable downlink throughput is 184 Mbps. In table 4.2, the theoretical performance in throughput per user is shown, under ideal conditions.

The system implements LTE FDD TM 2,3 for the overall duration of the measurement assessment. In this first preliminary analysis we didn't take into account how MIMO could affect network performances due to a lack of data and due to the intent of conducting a further measurement campaign on a full data set collected with a partnership with a well known mobile operator.

Since throughput is strictly related to the SINR and the CQI computation it could be interesting to verify the actual throughput achieved by a single user in a real case scenario. Using OFDM modulation, bandwidth is one of the element that mostly affects throughput: an increase in bandwidth (increasing the number of available sub-carriers) leads to a proportional increase in throughput. Also SINR affects clearly throughput and in our case could be interesting to state in a real testbed which is the relationship between SINR and actual throughput.

## 4.4 Experimental Results and Discussion

At first SINR was explored to estimate channel condition since it represents the most significant indicator out of all the available network parameter. Since the performance perceived by the user is strictly related to the quantity of data that can be received within the unit interval, the throughput was the investigated and more specifically, with an empirical approach we are going to evaluate the relationship between SINR and the network actual throughput.

### 4.4.1 SINR

In Fig. 4.3 (made with [99]), the evolution of SINR along the testing route is shown. We can observe a non-homogeneous distribution of values, spanning over 40 dB. The empirical distributions of values for the PCC and SCC carriers are shown in Fig. 4.4. The most relevant statistics are collected in Table 4.3. Although a significant overlap is apparent, they differ in the maximum value, which is 27.58 dB and 25.30 dB for PCC and SCC respectively, and for the median, which is 6.90 dB for the PCC and 8.08 dB for the SCC. Both component carriers present remarkable standard deviation levels, reaching the same order of magnitude as the mean.



Fig. 4.3 SINR Evolution

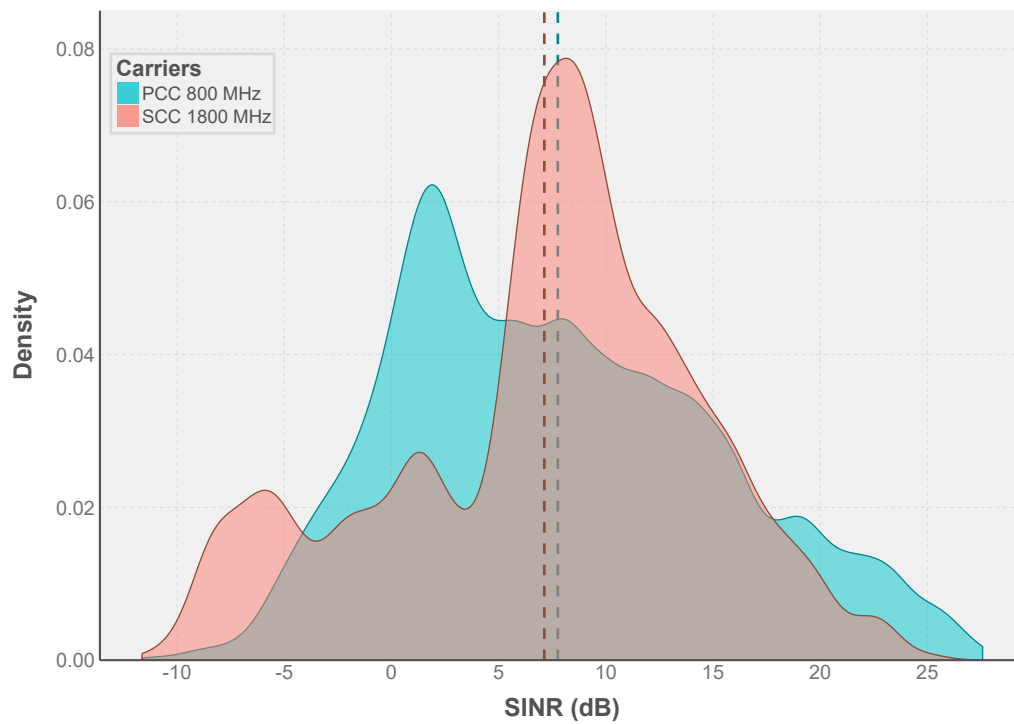


Fig. 4.4 SINR empirical distribution.



Table 4.3 SINR Statistics

SINR [dB]	PCC	SCC
Min	-11.06	-11.64
$\bar{x}$	7.76	7.13
Max	27.58	25.30
Median	6.90	8.08
$s$	7.55	7.30

#### 4.4.2 CQI, SINR and RSRP Analysis

LTE standard do not define how to compute CQI value, even if several times it has been stated that SINR plays a major role into link adaption procedure. But SINR itself does not represent a comprehensive channel state representation. This first analysis we present is able to show the strong relationship between SINR, RSRP and CQI. It is very interesting to characterize which combination of SINR and RSRP values lead to a specific CQI value. In fig. 4.5 CQI evolution is shown based on RSRP and SINR. RSRP values are represented by the different colors in each point in the plane. Generally, a first investigation let us conclude that a certain CQI value leads to a wide range of SINR and RSRP values. Also, it is quite noticeable that a high SINR values correspond high RSRP values.

In Table 4.4 RSRP and SINR statistics calculated with 15225 samples are reported for every possible CQI value. Minimum, Average and Maximum values of SINR and RSRP usually follow the same trend of CQI. If CQI grows also SINR and RSRP grow. Maximum CQI value is 15, with a minimum SINR of 8.28 dB and RSRP of -83.92 dBm, so with not so exciting channel conditions. For a 15 CQI on average it is necessary to have 21.88 dB for SINR and -63.32 dBm for RSRP. The average values shown are the sample means of the measurement data, they have not been returned by the mobile device as measured values. These two values represent really high physical channel parameters and a great channel condition. Taking into account average values, up to a CQI value of 12, SINR and RSRP grow linearly with CQI. From 12 to 15 RSRP is still linearly growing while SINR grows sharply from 13.35 dB with a CQI of 12 to 21.88 dB with CQI of 15. Generally, we can state that we observe a positive correlation between SINR and CQI with a high variability in SINR with a fixed CQI in fig 4.6. Dispersion of data in Fig. 4.6 shows that multiple values of SNR are associated with a common CQI. This is perfectly aligned with technical specifications since CQI is a discrete value that can represent different channel state parameters. The result

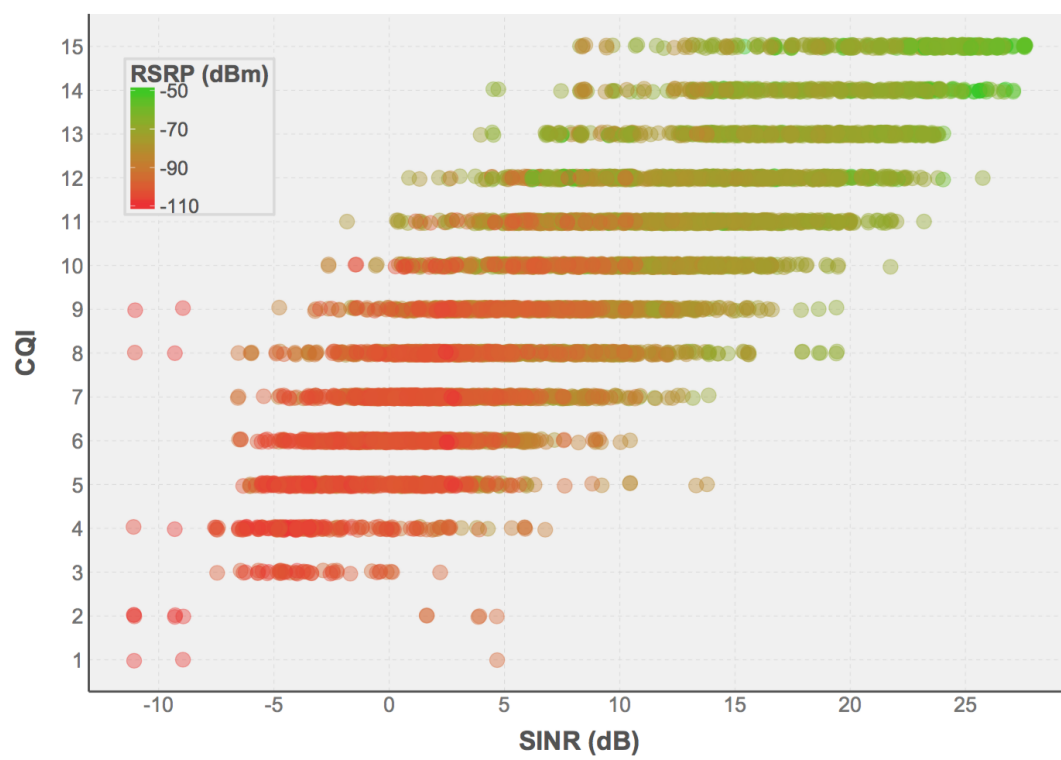


Fig. 4.5 CQI vs. SINR

Table 4.4 CQI as a function of RSRP and SINR

CQI	Minimum		Average		Maximum	
	SINR	RSRP	SINR	RSRP	SINR	RSRP
	dB	dBm	dB	dBm	dB	dBm
1	-11.04	-108.89	-5.11	-105.17	4.65	-98.02
2	-11.06	-108.89	-4.09	-103.16	4.65	-97.26
3	-7.45	-109.72	-3.57	-101.91	2.19	-95.09
4	-11.06	-109.72	-2.90	-100.95	6.81	-80.09
5	-6.35	-109.95	-0.71	-98.16	13.75	-73.38
6	-6.53	-110.20	0.54	-95.97	10.48	-65.74
7	-6.53	-109.95	2.25	-92.86	13.89	-63.90
8	-11.06	-110.20	4.32	-88.43	19.42	-62.78
9	-11.04	-108.89	6.68	-85.31	19.42	-66.36
10	-2.66	-105.50	9.73	-79.56	21.77	-50.80
11	-1.86	-101.19	11.31	-76.02	23.19	-47.27
12	0.82	-100.47	13.35	-72.27	25.77	-47.27
13	3.99	-88.15	17.31	-69.94	24.02	-47.27
14	4.50	-84.17	18.39	-66.98	27.07	-47.27
15	8.28	-83.92	21.88	-63.32	27.58	-48.20

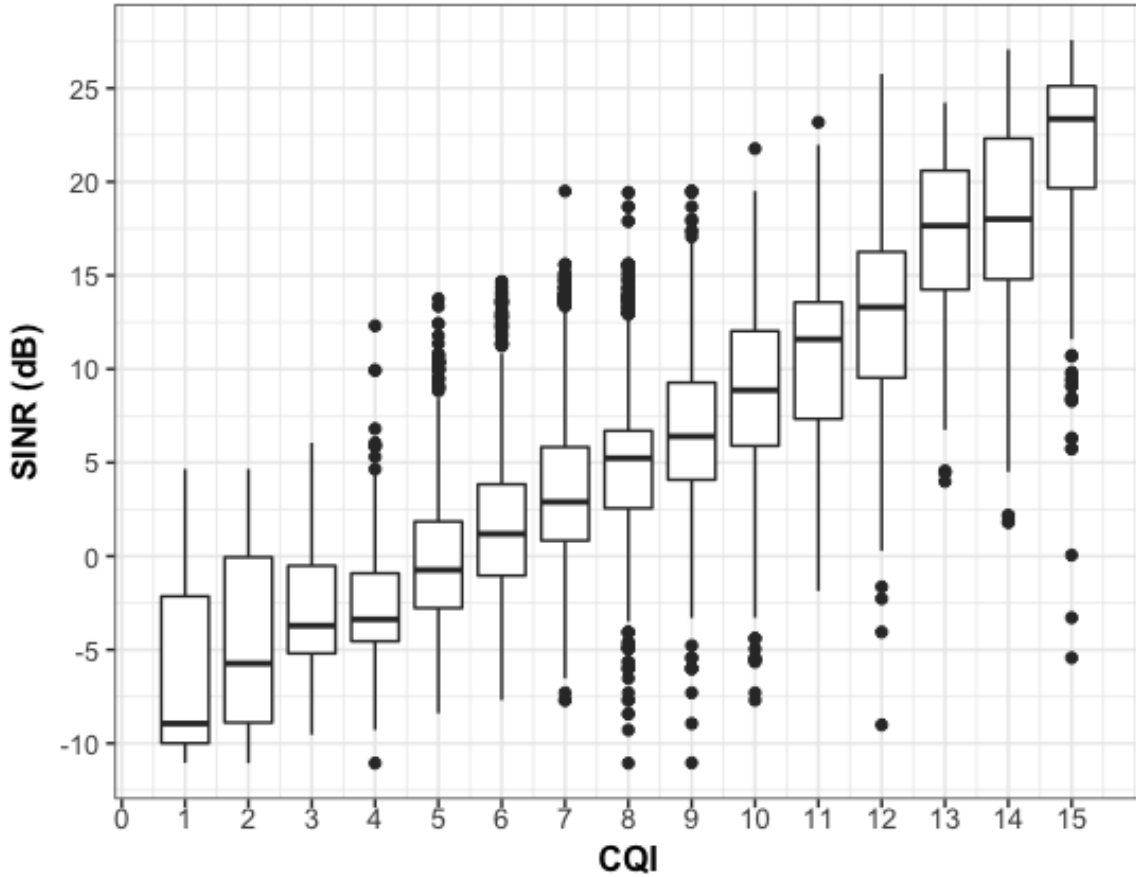


Fig. 4.6 Regression of SINR as a function of CQI

of our measurement campaign suggests to investigate using a multivariate analysis to collect information regarding a wider range of physical layer parameters.

#### 4.4.3 Modulation and CQI Analysis

CQI role is fundamental for Adaptive Modulation and Coding Mechanism. The choice of which modulation to use in fact, is up to the CQI value [10]. In Fig. 4.7 CQI CDF is shown. Measurement are conducted based on the PCC related to primary MIMO stream (codeword 0). Generally different stream could use different modulation code scheme in order to exploit different propagation channel features. In this case, to obtain a meaningful analysis, only values related to MIMO streams using the same modulation scheme were evaluated.

In Table 4.5 statistical data of single modulation schemes are highlighted, here we show some summary statistics obtained from of 20354 samples. QPSK should be in use with a CQI value ranging from 1 to 6. In our measurement campaign we experienced the usage of QPSK even with a CQI value of 13, when 64QAM is supposed to be adopted, the CQI mean

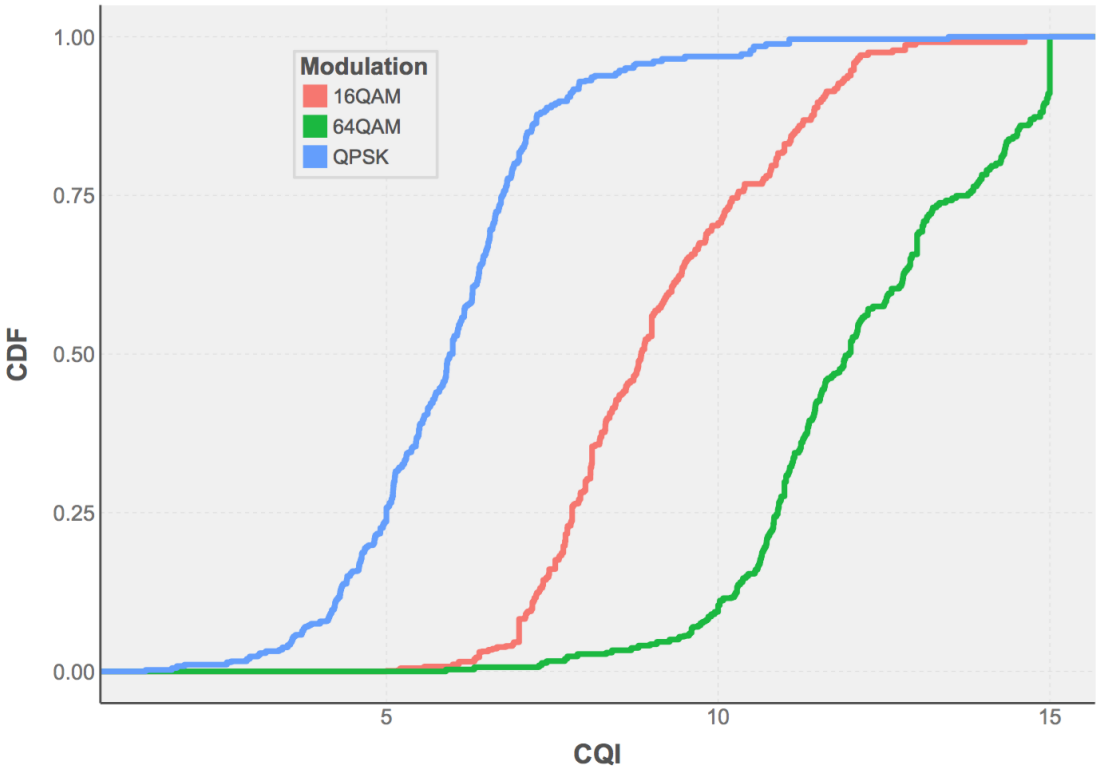


Fig. 4.7 CQI CDF per Modulation

Table 4.5 CQI Statistics per Modulation

CQI	QPSK	16QAM	64QAM
Min	1	5	6
$\bar{x}$	5.97	9.11	12.14
Max	13	15	15
Median	6	9	12
$s$	1.61	1.75	1.89
3GPP Specs.	1-6	7-9	10-15

value for a QPSK is double its predicted ideal value. 16QAM modulation is again supposed to be used with a starting CQI value of 7. Here we find it also with a CQI value of 5 and 15. Higher CQI value should be supported by a 64 QAM, so here LTE system is clearly under performing. On the other hand a 64QAM is adopted also with a 6 CQI value and if we examine the table 4.5 we can clearly stated that LTE system is outperforming. Higher order modulations are in adopted even with poor channel condition. Eventually we can affirm that AMC techniques works accordingly to 3GPP standard looking at CQI mean value. This real case scenarios showed that it would be appropriate to investigate if modulation scheme are efficient in throughout and Block Error Rate terms. Also, to use a 64QAM modulation a CQI mean value of 12.14 is required. In our case the required value is very close to the maximum CQI, meaning that usually this modulation is in use only with very good channel condition. CQI mean value decreases with modulation performance getting from 9.11 for 16QAM to 5.97 for QPSK. The median, underlines further this behavior. 50% measured values for 64QAM modulation are than 12. Low values of standard deviation suggest also that for each modulation there are no evident fluctuation meaning that those value are relatively stable.

#### 4.4.4 Modulation and Throughput

In Fig. 4.8 throughput downlink for PCC is depicted as a function of the modulation in use. All distributions are bimodal and reflect the theoretical performance of each proper modulation coding scheme. In a 10 MHz bandwidth, in the hypothesis of 50 RB and 600 available sub carriers assigned to a unique user and using an encoding rate of 1/1, without redundancy the maximum achievable throughput by QPSK, 16QAM and 64QAM is respectively 16.78 Mbps, 33.56 Mbps and 50.34 Mbps.

In Table 4.6 the main statistics (obtained from 1304 samples) of the distributions of throughput for each modulation are provided. AMC technique influence in this case is

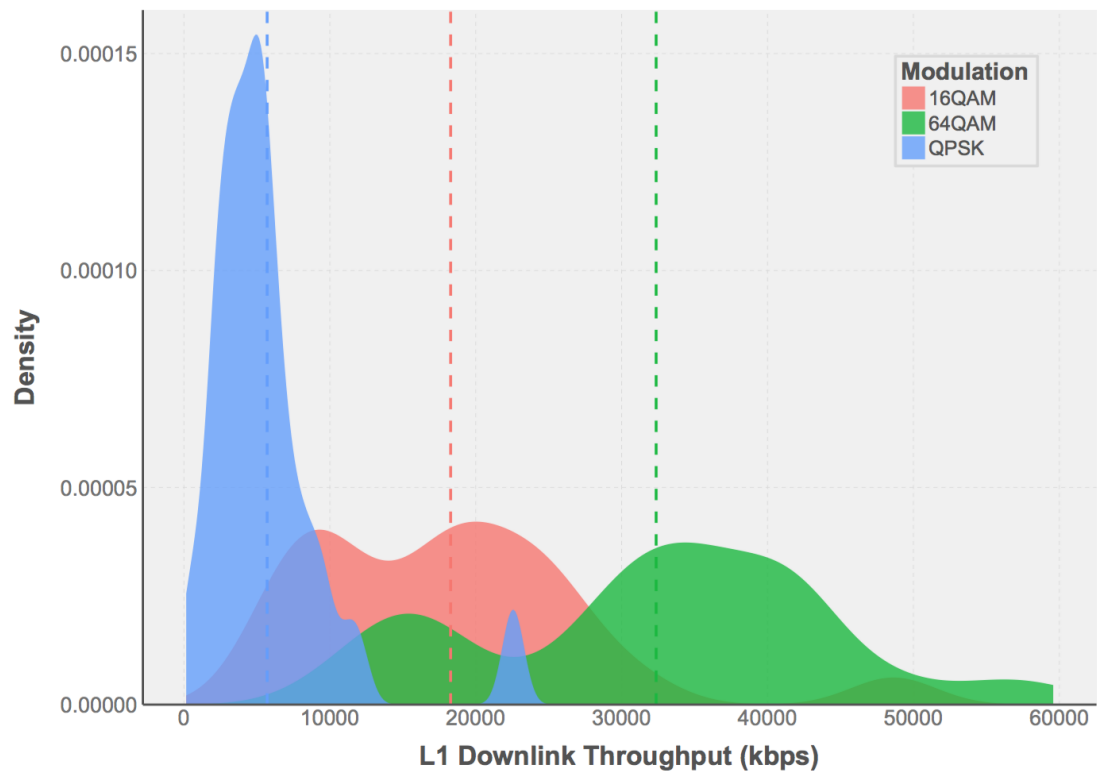


Fig. 4.8 SINR vs Throughput

Table 4.6 Throughput Statistics per Modulation

Throughput [Mbps]	QPSK	16QAM	64QAM
Min	0.153	5.586	10.340
$\bar{x}$	5.701	18.278	32.365
Max	22.568	48.634	59.579
Median	4.863	18.448	33.234
$s$	4.337	9.737	11.894
Predicted	15.981	30.528	73.392



Fig. 4.9 Downlink throughput

pretty obvious. Minimum throughput values lead to a clear classification of modulation techniques. Minimum assured throughput with 64QAM is 10.34 Mbps, with heights if 59.58 Mbps and an average value of 32.36 Mbps. When a 64QAM is in use, as expected PCC reaches the highest performances. Using a 16QAM we can achieve a minimum, average and maximum throughput respectively of 5.59 Mbps, 18.28 Mbps e 48.63 Mbps. Maximum 16QAM throughput is almost equal to 64QAM maximum throughput. It is in fact almost impossible to adopt a 64QAM modulation with a 1/1 encoding rate and reach the theoretical 100 Mbps. Standard deviations are also increasing functions for each modulation showing that QPSK guarantees lower throughputs. A QPSK is in use the 18% of the time, while respectively the 16QAM and the 64QAM ae for 38% and 44%.

#### 4.4.5 Downlink throughput

In Fig. 4.9 the evolution of the downlink throughput along the testing route is shown. LTE aim to improve transmission efficiency is accomplished by a sophisticated mechanism called *Hybrid automatic repeat request* (H-ARQ) through which corrupted packets are not discarded but stored in a 'buffer', and then combined with next retransmission. Downlink throughput is measured at the physical layer (L1), taking into account possible H-ARQ retransmissions. Due to a lack of samples, we were not able to evaluate Radio link control (RLC) layer (L2)



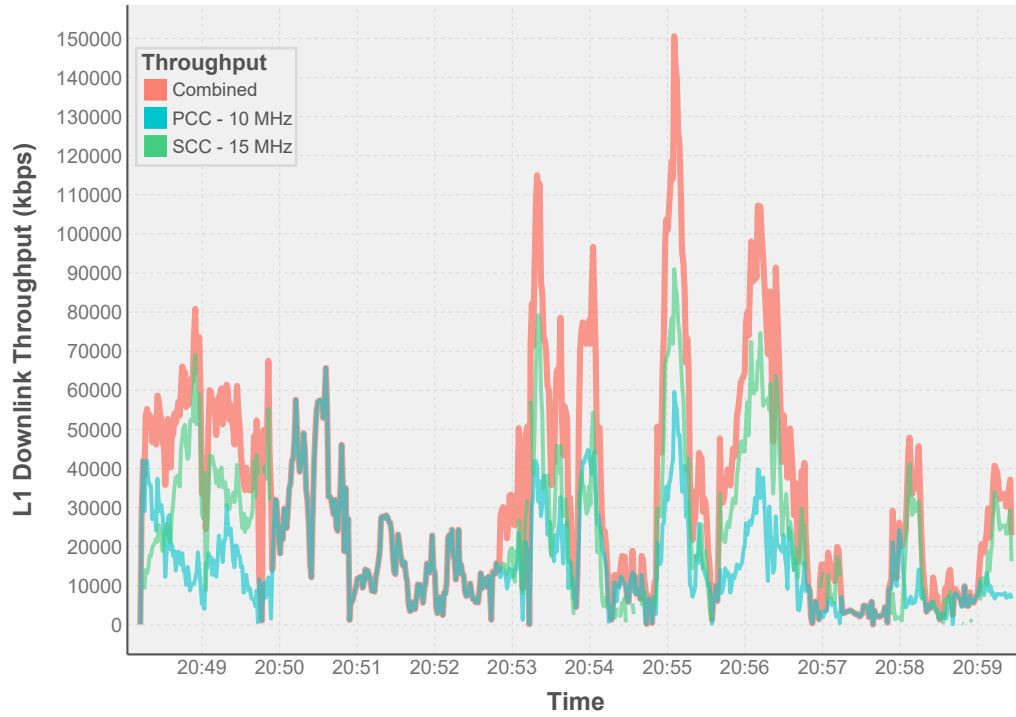


Fig. 4.10 Downlink throughput over time.

or the downlink throughput at the application layer. Generally, however, RLC throughput is lower than the L1 throughput because of H-ARQ re-transmissions.

We can highlight a few points on the route where high values are reached, close to the theoretical limit of 150 Mbps. In Fig. 4.10, the evolution over time of the downlink throughput per component carrier is also shown. A high variability of measured values is immediately noticeable. Peaks are high and well distinguishable and we observe a strong increase in throughput when the Carrier Aggregation mechanism is in use. The combined throughput is the sum of the downlink throughput from both the PCC and SCC channels. Fig. 4.11 shows the empirical cumulative distribution, whose relevant statistics are reported in Table 4.7.

The overall maximum throughput is 150.58 Mbps and, as previously stated, is achieved when Carrier Aggregation mechanism is in use. PCC contribution is 59.58 Mbps and SCC is 91.00 Mbps. SCC throughput is higher than PCC by 50% at any time. The result is well expected thanks to the larger SCC bandwidth and in the smaller number of mobiles that make use of it. Carrier aggregation is widespread and commonly exploited by operators but, as depicted by Fig. 4.10, only in the 58% of time it is available to users. As a matter of fact, at higher frequencies, due to propagation issues, it is hard to cover large areas. As a positive consequence though, the less users share a carrier, the more resources can be granted

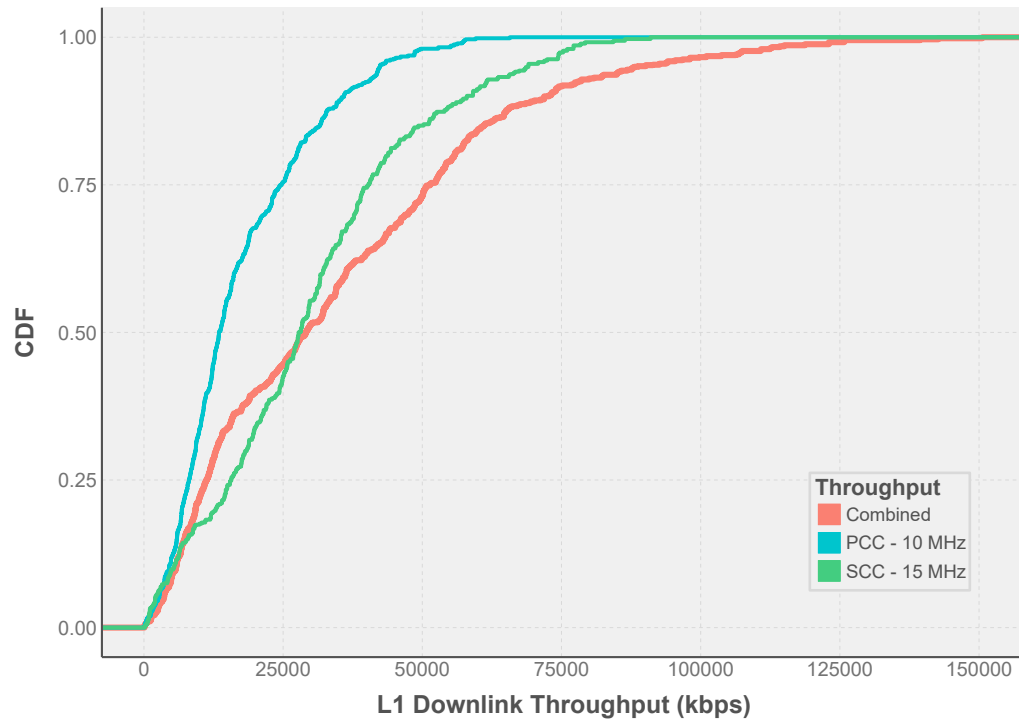


Fig. 4.11 Throughput empirical CDF.

Table 4.7 Downlink throughput statistics

Throughput [kbps]	PCC	SCC	Combined
Min	79.48	193.40	79.48
$\bar{x}$	17344.03	29858.20	34597.05
Max	65730.13	90996.47	150576.1
Median	13481.31	27777.60	29113.37
$s$	12628.90	19400.51	28015.43

Table 4.8 SINR statistics per throughput classes

Throughput [Mbps]	SINR [dB]		
	Min	Avg	Max
5	-11.04	-0.73	14.79
10	-6.53	1.57	9.10
15	-6.00	4.96	20.16
20	0.50	8.25	19.42
25	3.91	10.96	19.42
30	6.45	12.84	19.72
35	7.80	14.96	20.51
40	9.93	16.26	23.53
45	12.57	19.74	27.07
50	20.05	24.11	27.58
60	21.32	24.41	26.65

to each of them which results in a higher overall throughput. Globally PCC is characterized by stabler performance than SCC. The high variability in values on the route is also caused by handover procedures.

#### 4.4.6 Comparing SINR and Throughput

The goal of this analysis is to understand how downlink throughput is related to SINR. In Fig. 4.12 we can observe SINR vs. downlink throughput at the physical layer for the PCC, and state a proportional relationship between the values.

The proportionality explains why, even if vendors and 3GPP standard do not define CQI, throughput is an important factor in estimating channel quality. The Adaptive Modulation and Coding strategy provides the best reachable performance under every possible channel condition. However, it does not allow to forecast the maximum throughput that can be reached under a specific network condition unless CQI is measured, for which standard does not provide any numerical definition.

In Fig. 4.12, the curve interpolating the minimum SINR values required for a specific throughput value is also shown, and in Table 4.8 summary statistics are presented. As an example, 10 Mbps throughput can be reached by a minimum SINR of -6.53 dB. Under good channel conditions, a small increase in SINR can result in a great increase in throughput. It is interesting to notice that, in our experiment, a great increase in SINR is necessary to step

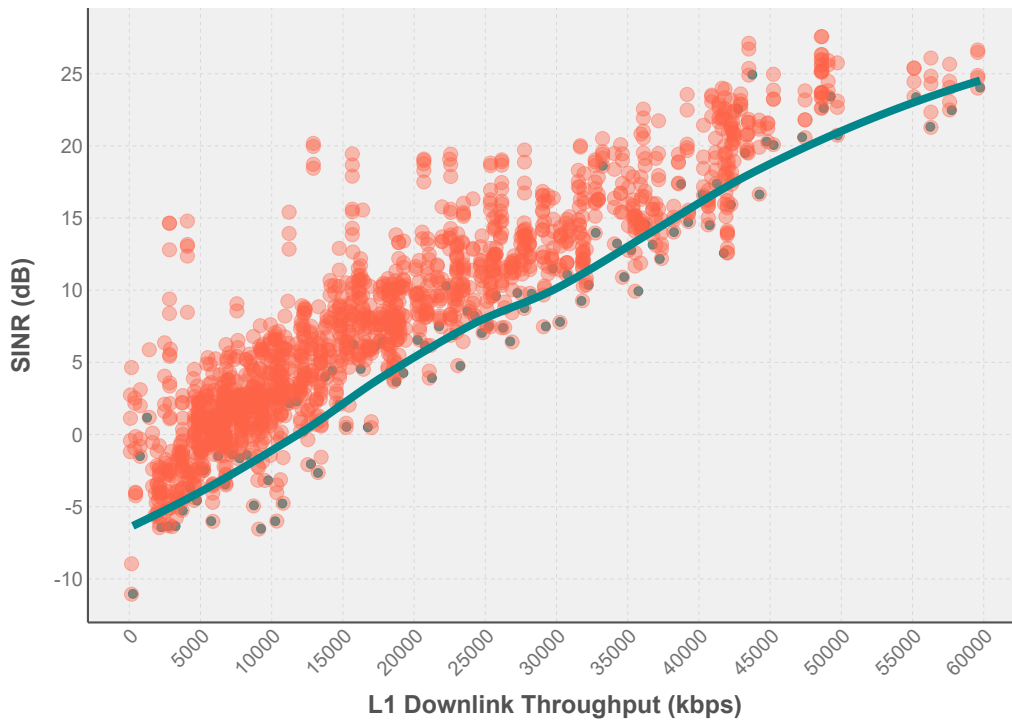


Fig. 4.12 SINR vs. Throughput for PCC.

up from 45 Mbps to 50 Mbps and beyond. This is easily explained by the implementation of higher symbol rate modulations like the 64QAM which adopts high rate encoding strategies that limit redundancy in transmissions. When a 1-to-1 encoding rate is in use, a high SINR is mandatory at the receiver side because a small interference could lead to an error in the received symbol and to a re-transmission which would cause a dramatic drop in the effective throughput. The maximum throughput is 65.73 Mbps and it is achieved with a 22.71 dB SINR. The variability of SINR within each class of throughput shows that SINR as the only evaluation parameter is not enough to predict network performance. Indeed, factors to take into consideration are multiple. For example, if the eNodeB is serving a large number of users, resources may be poor and this could explain why large throughput values can not be reached with large SINR.

## 4.5 Conclusions

The chapter proposes an innovative approach to test performance of the LTE network from an end-user perspective. By using a smartphone-based measurement device, the network is tested under actual working and operational condition without the limitations in terms of variations

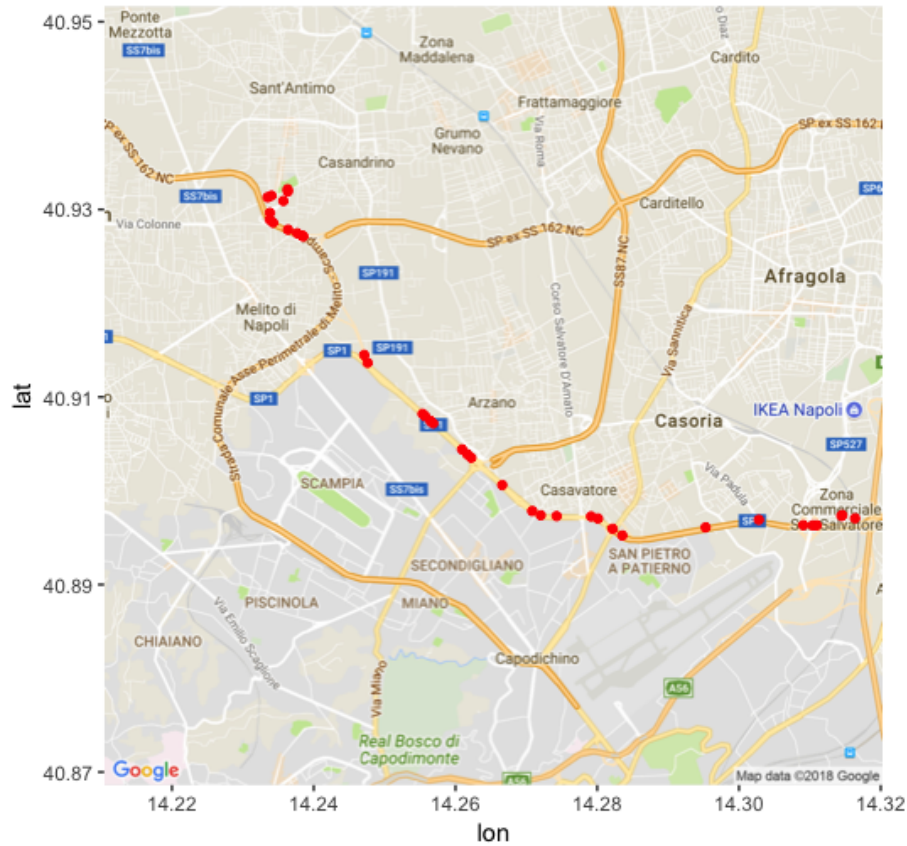


Fig. 4.13 Handover Map

of parameters that a controlled environment would pose. Experimental outcomes are that the 3 Gbps throughput advocated by the standard is far from being achieved. As a matter of fact, performance in a real test-bed scenario are quite under-performing when compared to the 3GPP previsions. We can also state that the adoption of carrier aggregation and higher modulation orders allows LTE network to achieve acceptable end-user performance in terms of throughput although not as good as the expected one. Adaptive modulation and coding adopted by LTE is implemented sharply following the standard as we can determine by the average CQI in use with different modulation order. The ongoing research is now focusing on the relationship between RSRP and SINR and the role played by this factors in the determination of CQI. We observed a positive correlation between SINR and RSRP, but a wider and multivariate analysis is necessary to include possible interactions between factors.



# **Chapter 5**

## **LTE MIMO: Experimental Assessment**

### **5.1 Aim of the Research**

MIMO enables radio systems to achieve significant performance gains by using multiple antennas both at the transmitter and at the receiver side. Dealing with it, our current research is focused on CQI, BLER and, with an even possibly more thorough analysis, on throughput, being it the quantity that the end-user is most interested in, as it characterizes network performance in terms of bit rate in the downlink channel. Correlation of such quantities with physical-layer ones will also be investigated to determine network criticalities and where it is possible to determine how to operate for better performance. At first in this chapter, channel conditions will be investigated to estimate network performance. Therefore, a first study on RSRP, RSRQ, RSSI values is carried out to properly understand how the system works and which resources are efficiently used with respect of 3GPP latest standard. Only then CQI reports are investigated with respect to wide-band and sub-band values and, eventually, also PMI and RI are explored.

### **5.2 MIMO Overview in LTE**

MIMO technology introduce a strong gain in performances for mobile systems. Performances are increased in efficiency and power by the adoption of multiple antennas at both the transmitter and the receiver side [100]. The adoption of multiple antennas introduces a strong improvement to mobile radio systems, thus dealing with reliable procedures to strengthen poor condition signals and gain wider spectral efficiency. However, MIMO is a broader technology, with a number of multiple implementation on its basic technique [101].

LTE standard supports a broad variety of MIMO operating schemes suitable to different radio scenarios and is able to dynamically adjust between schemes to properly address the prevailing circumstances. Spatial Multiplexing is expected to give better robustness over Transmission Diversity and in fact LTE Spatial multiplexing Multiple Input Multiple Output (SM-MIMO) in indoor environment outperforms TD-MIMO and SIMO because a single data stream transmitted by different antennas can overcome the adverse multipath propagation typical of such environments [102]. Also in [103] the reenactments demonstrate that the execution of MIMO is superior to SISO. In [104] a timeline from Release 8 to the last Releases of MU-MIMO techniques is approached. The discussion here deals with specific aspects of MIMO implementations and related solutions in particular for MU-MIMO. To widely investigate LTE and its MIMO implementation, an eNodeB is tested in a reverberation chamber. An experimental campaign was carried out to investigate how power boosting affects eNodeBs performance in a multipath environment, (usually wireless and vehicular communications) [105]. Channel quality parameters are measured ranging from the empty chamber condition, with a very rich multipath channel, to a fully loaded condition to mitigate multipath.

Anechoic chamber testing is performed in [106]. MIMO's UEs conditions and performances are testes with the implementation of Plane-wave synthesis (PWS) and pre-fading signal synthesis (PFS) techniques.

A great influence on LTE system is owed to Frequency domain packet scheduling (FDPS)[107]. Considering how hard is to optimize the system the easiest solution could be to efficiently assign time-frequency resources to UEs using a *proportional fairness* metric. One of the first proposals to fully address LTE MIMO fair comparison of MIMO schemes is carried out in [2]. Analysis is performed with multiple spatial transmission and a unique SINR both with the effect of packet scheduling included in the post-scheduling SINR. The spectral efficiency can benefit significantly the combined use of Spatial Multiplexing and FDPS. In [108] an experimental setup a LTE eNodeB shows that the throughput at lower layers can easily be computed if the preferred CQI and number of assigned RBs are well known in advance.

Through simulation results Shidar *et al.* confirm that a Channel Quality Estimation with ICI cancellation technique reduces complexity and time of execution in MIMO networks [109]. At first the adoption of a maximum-likelihood detection interference suppression (MLD-IS) scheme is used to suppress the interfering channels then a parallel interference cancellation (PIC) method and decision statistical combining (DSC) are adopted to cancel Inter Carrier Interference (ICI) and improve data symbol detection.



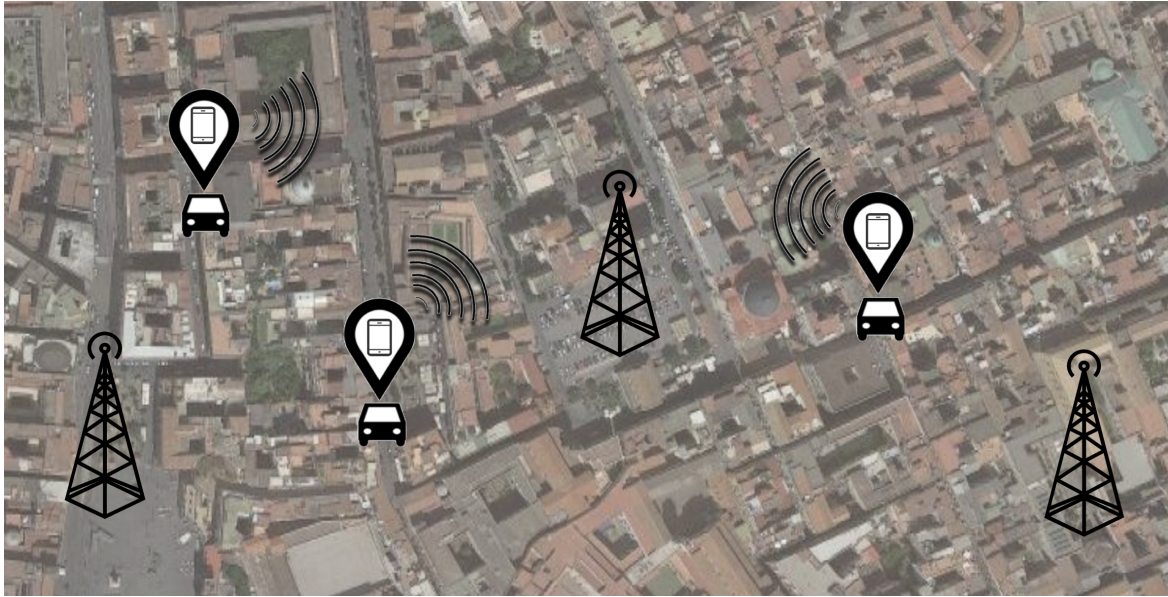


Fig. 5.1 Typical test drive configuration

The estimation process for interference arises a big criticality in LTE systems adopting MU-MIMO [110]. Its management is here approached with a framework for estimation together with a practical solution based on a suboptimal non-iterative methods. The non-ideality of MU-MIMO precoding schemas due to poor channel knowledge is also investigated and few benefits are presented with the adoption of the proposed solution. In [111] to realize spatially separated transmission links to a large number of mobile stations adopting FD-MIMO, a number of antennas is placed in a 2D antenna array configuration. The design and the implementation of the 2D antenna array, are presented in details.

A deeper analysis of LTE network performance with the usage of statistical methods reveals that standard expectations are too high with respect to an actual urban environment deployment of the system [93]. With accents on downlink channel throughput, measurements are conducted with reference to key parameters for radio optimization like SINR assessing directly on the end-user side.

Our research aims at assessing, under actual conditions, network performance when MIMO systems are fully adopted and to comparison them with those expected by the 3GPP standard.

Table 5.1 Measurement Tools

BAND	HW: SAMSUNG	NEMO HANDY-A VERS.
1	S7 Edge	2.62.337
20	S5	2.62.337
3	S5+	2.41.246
7	S5+	2.41.246

### 5.3 Experimental Setup

Measurement Campaign was conducted in a suburban area of southern city in Italy. The location cannot be disclosed due to a non-disclosure agreement signed between the Authors and the Mobile Operator. The only available information are that data were measured in a coastal city which therefore has both typical urban propagation and clutter signal due to the sea which is known to affect propagation by surface reflection and therefore possibly increase interference significantly.

Retrieved data were collected from one of the most widespread telecom operator in Italy. This operator allowed us to monitor the ongoing traffic in a urban area and to collect and to analyze the shared data for a period of 4 hours on a single day.

Multiple UE's data are collected, each at a different frequency/band:

- LTE FDD 2100 band 1 - 10 MHz
- LTE FDD 1800 band 3 - 15 MHz
- LTE FDD 2600 band 7 - 20 MHz
- LTE FDD 800 band 20 - 20 MHz

Terminals features are depicted in Table 5.1. The network we are investigating implements a 2x2 MIMO as shown in Fig. 5.2

#### 5.3.1 NEMO Handy Assessment

The measurement campaign was conducted through a *drive test* experimental activity as seen in Fig. 5.1, where the UE is placed inside a car that is driven around the investigated area to collect georeferenced measurements which are then post-processed. Such methodology has been already explored and used in [93, 112–114]. UEs have not been placed in a specific

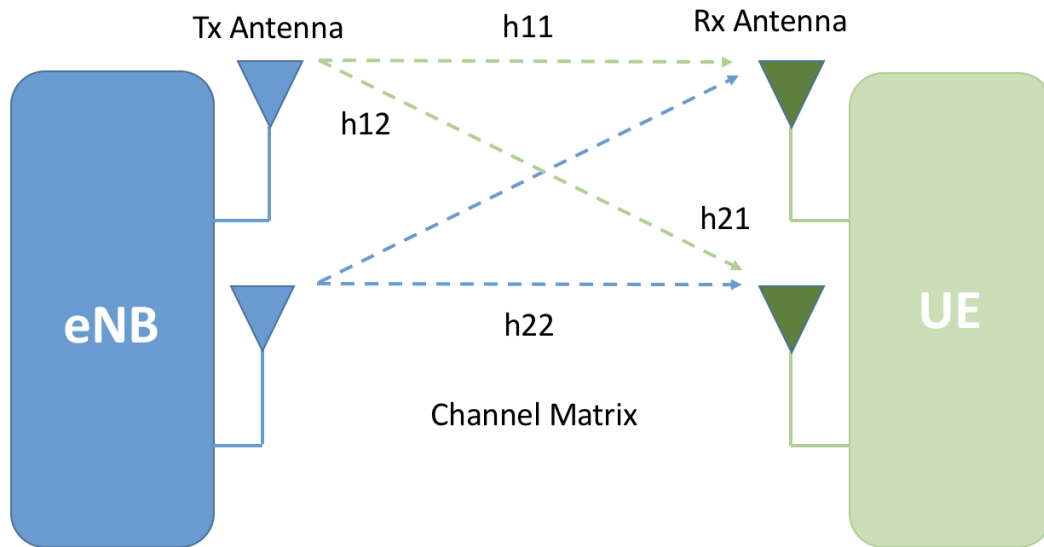


Fig. 5.2 MIMO Configuration

Table 5.2 Nemo Handy Documentation CELLMEAS

Cell Measurement (CELLMEAS)	
Event ID	CELLMEAS
Cellular System	GSM, TETRA, UMTS FDD, iDEN, UMTS TD-SCDMA, LTE FDD, LTE TDD, cdmaOne, CDMA 1x, EVDO, WLAN, GAN, WLAN, WiMAX, AMPS, DAMPS, NAMPS,
Record State	Always
Description	Recorded when parameter sample is received from the device. Note that not necessarily all received samples are recorded and currently the recording frequency is about twice per second in connected state. Separate measurement event is logged for each system.
Tool Nemo	Outdoor, Handy, Autonomous , Q

Table 5.3 Nemo Handy Documentation CQI

Channel Quality Information (CQI)	
Event ID	CQI
Cellular System	UMTS FDD,UMTS TDSCDMA,LTE FDD,LTE TDD
Record State	Packet active state
Description	Recorded every 200 milliseconds to indicate distribution of HSDPA Channel Quality Indications (CQI) transmitted to the network. The measurement event is recorded simultaneously with the PLAID measurement event. One measurement event is logged for all serving cells with HSDPA. Separate measurement event is logged for each serving cell with LTE.
Tool Nemo	Outdoor

Table 5.4 Nemo Handy Documentation CI

Carrier per interference (CI)	
Event ID	CHI
Cellular System	GSM,UMTS TDSCDMA,LTE FDD,LTE TDD,EVDO iDEN
Record State	Always
Description	Recorded when channel configuration information changes.
Tool Nemo	Outdoor, Handy

Table 5.5 Nemo Handy Documentation CHI

Channel info (CHI)	
Event ID	CHI
Cellular System	GSM,TETRA,UMTS FDD,UMTS TDSCDMA,LTE FDD,LTE TDD, cdmaOne,CDMA 1x,EVDO,GAN WLAN,WiMAX,AMPS,DAMPS, iDEN
Record State	Always
Description	Recorded when channel configuration information changes.
Tool Nemo	Outdoor, Handy

Table 5.6 RSRP Mapping - TS 36133

Value	Interval	Mapping
1	-50 dBm ... -65 dBm	very good
2	-65 dBm ... -80 dBm	good
3	-80 dBm ... -95 dBm	satisfying
4	-95 dBm ... -105 dBm	sufficient
5	-110 dBm ... -125 dBm	unsatisfying
6	-125 dBm ... -140 dBm	not sufficient

position within the car to mimic the typical position they would have during normal use, i.e. in the driver's jacket pocket, on the passenger seat or on the dashboard.

Assessment of the network performance was achieved with the *Nemo Handy* [115] tool. The software provides a complete automated data processing chain from raw measurement data to automatically generated results in workbook format. Nemo is an event-based measurement suite which acts like a Live Network Monitor. Events of our interest are reported and described in Tabs. 5.5, 5.4, 5.3 and 5.2. All the events are collected according to multiple technologies. In the Heading section the event name and event ID are displayed. In the overall measurement data section, the events are recognizable only with the event ID. Looking at an Event Info table general information about that particular event are shown such as the cellular system where this event is occurring and the Nemo tools which is now collecting informations about event. All the events collected by Nemo hardware are shown in the following table.

## 5.4 Preliminary Results

The presented analysis begins with the evaluation of channel conditions through RSRP, RSRQ, RSSI values. All the mentioned values are going to be measured for each terminal/carrier in order to evaluate performances in every band. Only after, to properly understand how the system works and if resources are efficiently employed, an analysis with respect to MIMO parameters and techniques is presented.

### 5.4.1 Reference Signal Received Power (RSRP)

RSRP, as stated in the standard, is the linear average of the downlink reference signals and provides information about signal strength but gives no indication about signal quality. It is

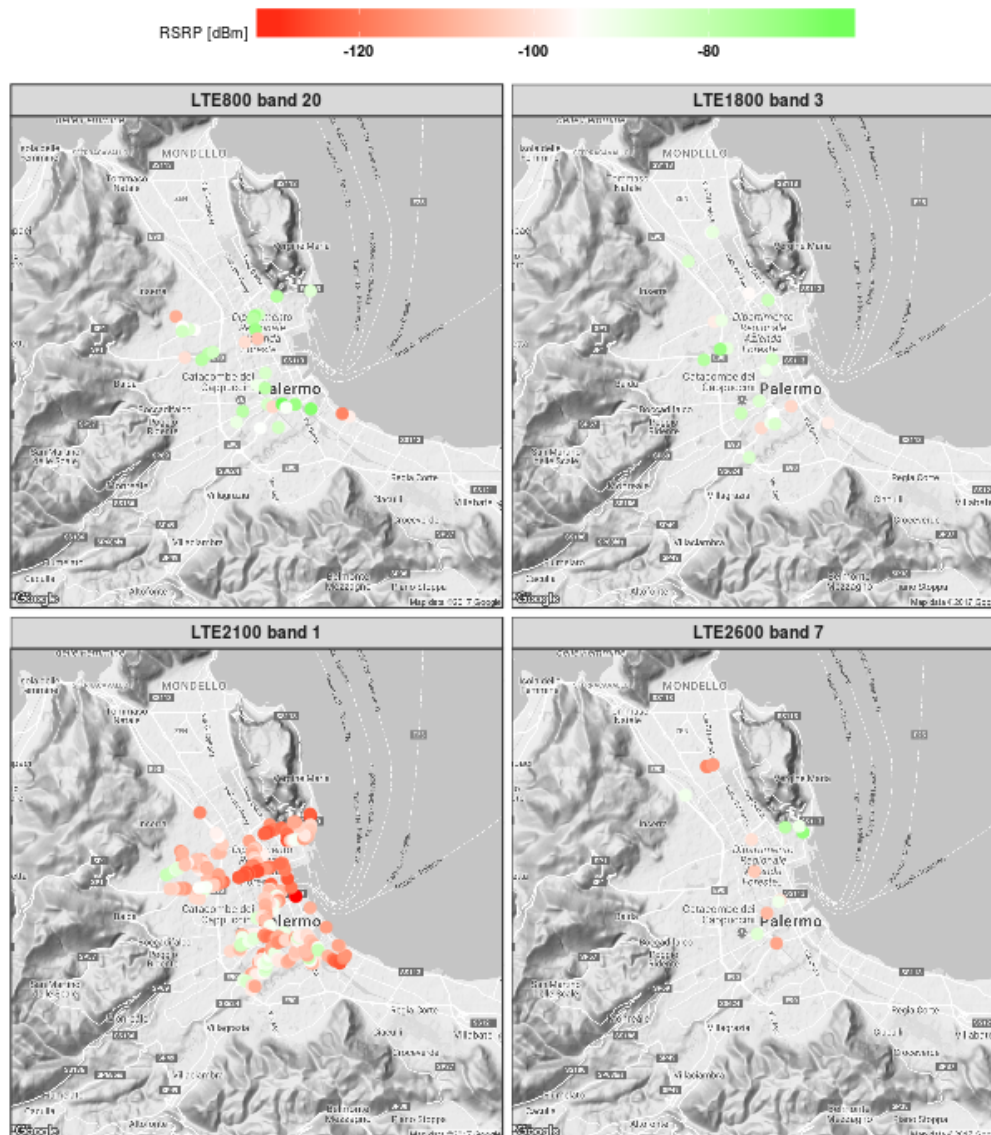


Fig. 5.3 Reference Signal Received Power - RSRP

Table 5.7 RSSI Mapping - TS 25133

Level	Interval
LEVEL 00	carrier $\leq$ -100 dBm
LEVEL 01	-100 dBm $\leq$ carrier $\leq$ -99 dBm
LEVEL 02	-99 dBm $\leq$ carrier $\leq$ -98 dBm
LEVEL ..	..
LEVEL 75	-26 dBm $\leq$ carrier $\leq$ -25 dBm
LEVEL 76	-25 dBm $\leq$ carrier

one of the most important parameters to investigate channel conditions when there is the need to evaluate quality of reception. RSRP is related to RS and because of this, its measurement would return the lowest value compared to other parameters and an idea of the strength of the signal that a UE gets from the network, but it is not a clear indicator of how good the signal quality is.

The reporting range of RSRP is defined from  $-140$  to  $-44$  dBm with 1 dB resolution. A useful 15 dB-resolution quantization of its values is reported in Table 5.6 together with a mapping of the channel quality. In Table 9.1.4-1 of [116] RSRP mapped values are reported.

Fig. 5.3 shows that the values obtained from the measurement campaign span almost over the whole range of RSRP values considered in the standard, namely from  $-60$  to  $-130$  dBm. Different carrier frequencies result in different RSRP values. For example, in Band 20 (i.e., 800 MHz), commonly used by telecom operator as the preferred carrier for cellular transmissions due to its penetration properties, RSRP spreads mostly from  $-80$  to  $-60$  dBm, which shows an efficient performance of the network in this range and supports the operator's choice of that band as the favorite one for LTE communications.

Values measured in the in Band 1 (i.e., 2100 MHz) span from a *sufficient* to *not sufficient* quality level, going from  $-80$  to  $-120$  dBm. In the 1800 MHz and 2600 MHz band, network usage is very low and values appear to be at a *sufficient* level.

#### 5.4.2 Reference Signal Strength Indicator (RSSI)

RSSI represents the whole received power including the power from the serving cell as well as all co-channel power and other sources of noise as already expressed in Eq. (1.1).

Since RSSI computation involves also interference and thermal noise, its behavior in Fig. 5.4 conforms to what expected from previous analysis. Here, in fact, RSSI ranges from LEVEL 76 to LEVEL 03 as shown in Tab. 9.1.18.5.1-1 of [116] and here reported in Tab. 5.7.



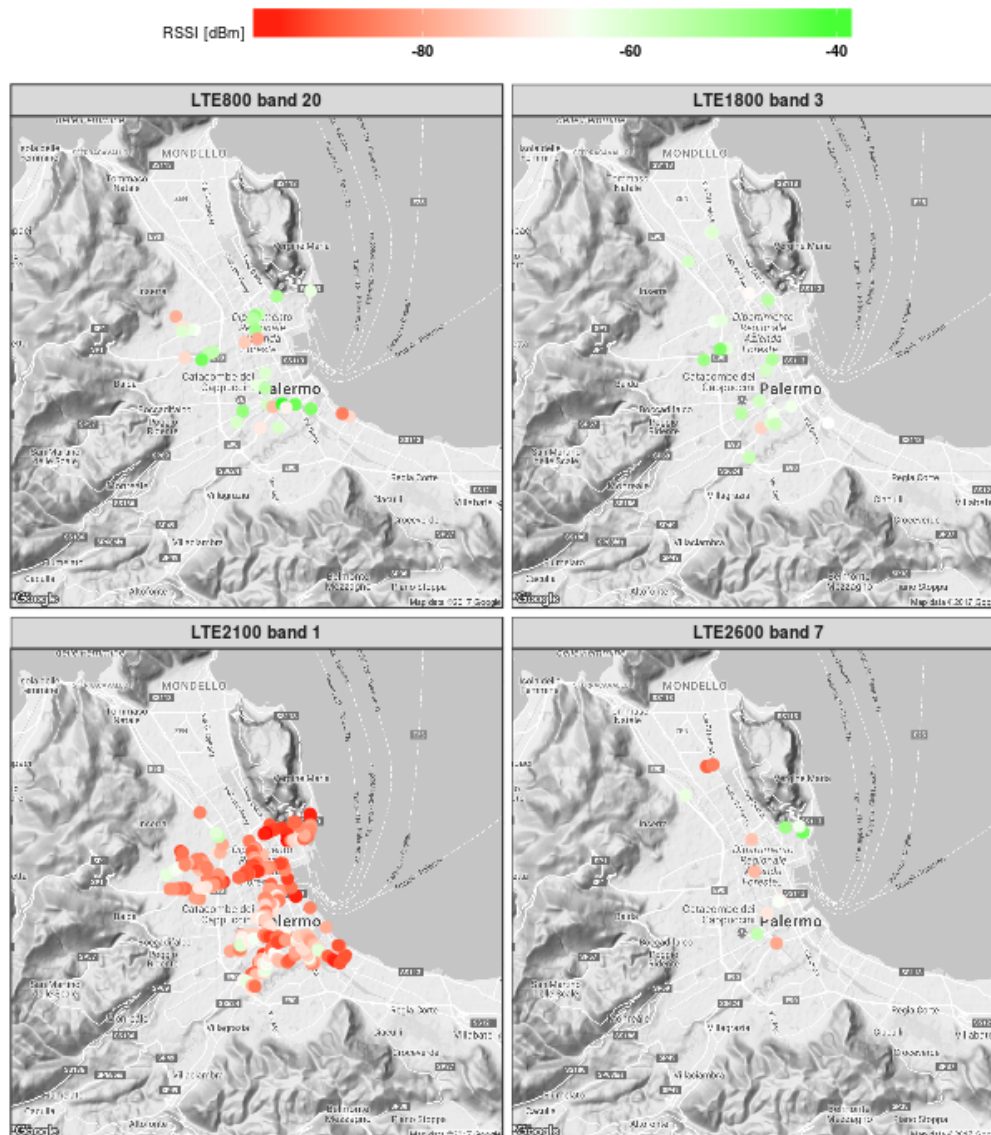


Fig. 5.4 Reference Signal Strength Indicator - RSSI



Table 5.8 RSRQ Mapping - TS 36133

Value	Interval	Mapping
1	-3 dB	very good
2	-4 dB ... -5 dB	good
3	-6 dB ... -8 dB	satisfying
4	-9 dB ... -11 dB	sufficient
5	-12 dB ... -15 dB	unsatisfying
6	-16 dB ... -20 dB	insufficient

### 5.4.3 Reference Signal Received Quantity (RSRQ)

While RSRP represents RS's only signal strength, RSSI takes into account the overall bandwidth signal power but also interference and thermal noise. Since RSRQ calculation uses both RSRP and RSSI, it indicates the *overall quality* of received reference signal.

Lower values of RSRQ show a highly interferenced scenario where the serving eNodeB's power is lower than the neighbors' one. In this scenario a handover is recommended to ensure that UEs experiences better performances.

RSRQ values here, span from -3 dB to -20 dB as shown in Table 9.1.7-1 of [116] and here reported in Tab. 5.8. In Band 1 even if RSRP is low, RSRQ is at a sufficient value. Again we can notice this behavior in Band 7. Fig. 5.5 highlights higher RSRQ values that are mostly visible in Band 20. Here, in fact, values range from -3 dB to -15 dB.

### 5.4.4 Signal to Interference Noise Ratio (SINR)

SINR is defined as the ratio of the signal power to the sum of the average interference power from other cells and the background noise. RSRP, RSRQ and RSSI measurements are defined by 3GPP, while SINR is not defined in 3GPP specifications but fully addressed in UE vendor's standards. Mapped parameters can be found in Tab. 9.1.17.1-1 of [116]. Here we can appreciate only reported values for Band 1 and 20, since too few samples were reported for other frequencies. Again we can spot the same behavior for both SINR and RSRP. RSRP, in fact, is expected to be proportional to SINR.

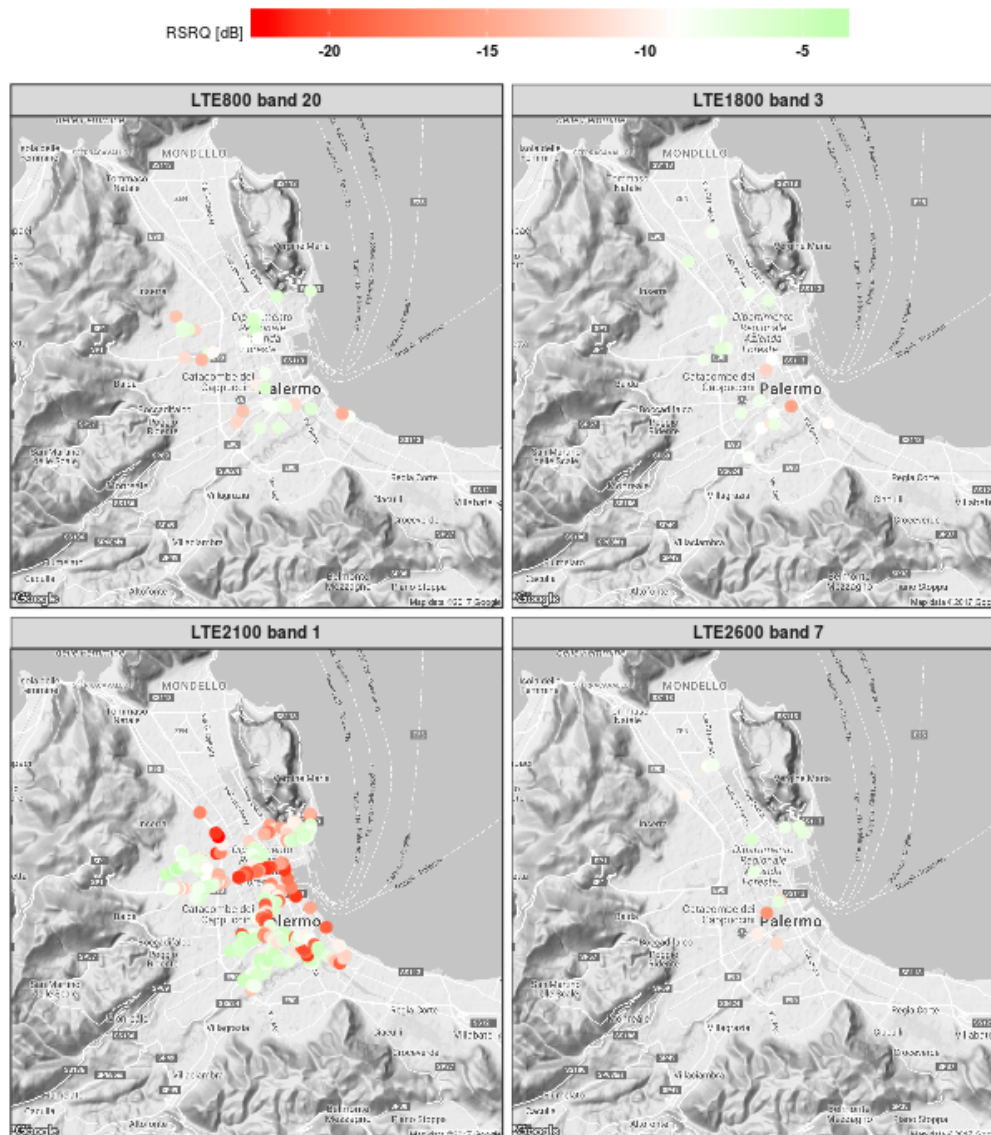


Fig. 5.5 Reference Signal Received Quality - RSRQ

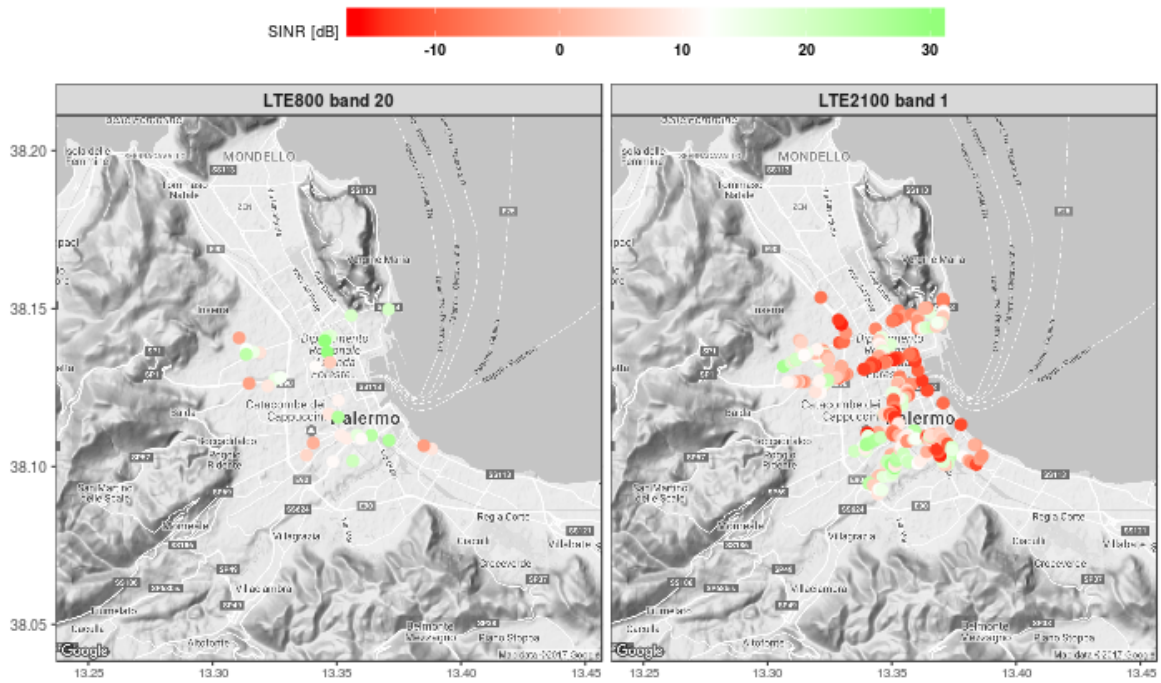


Fig. 5.6 RS Signal Reported - SINR

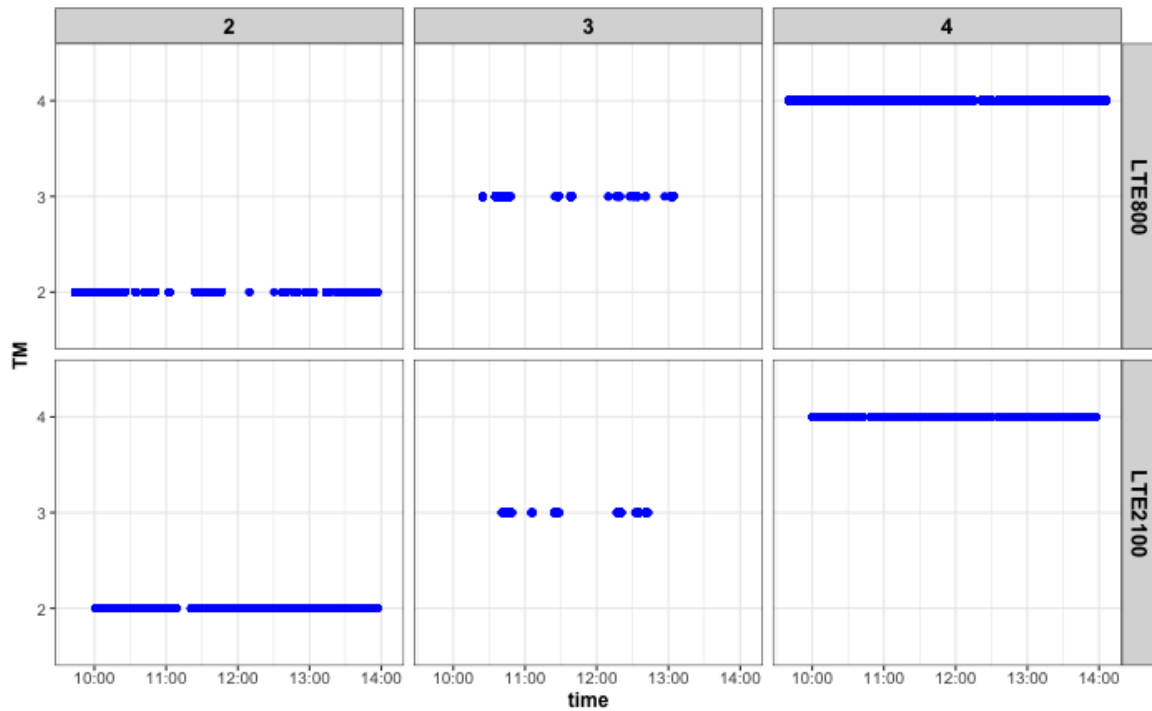


Fig. 5.7 TM Implementation with respect of frequencies

## 5.5 MIMO Analysis

In this section we present a MIMO analysis for the supervised Operator. In Fig. 5.7 TM adoption is depicted for both Band 20 and Band 1. From this point on, we will refer only to these two Bands due to a lack of samples in the other bands.

For the majority of time both systems adopt TM4 with *Closed Loop Spatial Multiplexing* and TM2 with *Transmit Diversity*. As already stated, TM4 is in use when channel condition are favourable, so we expect to have good channel condition showing from physical layer parameters. As noticeable in fact, from Fig. 5.7 for Band 20 channel condition are shown to be in a good range, while for Band 1 only with RSRQ and SINR we can appreciate higher reported values for the channel. Each vendor operates differently when to calculate CQI and 3GPP does not mandate how to computer CQI. In this experiment, however, if the eNodeB follows UE's indication withouth overriding them, CQI appears to be computed on RSRQ and SINR quantities. This indication could be truthful since, as stated, RSRQ calculation indicates the overall quality of the received reference signal and it seems to be the best parameter to calculate CQI.

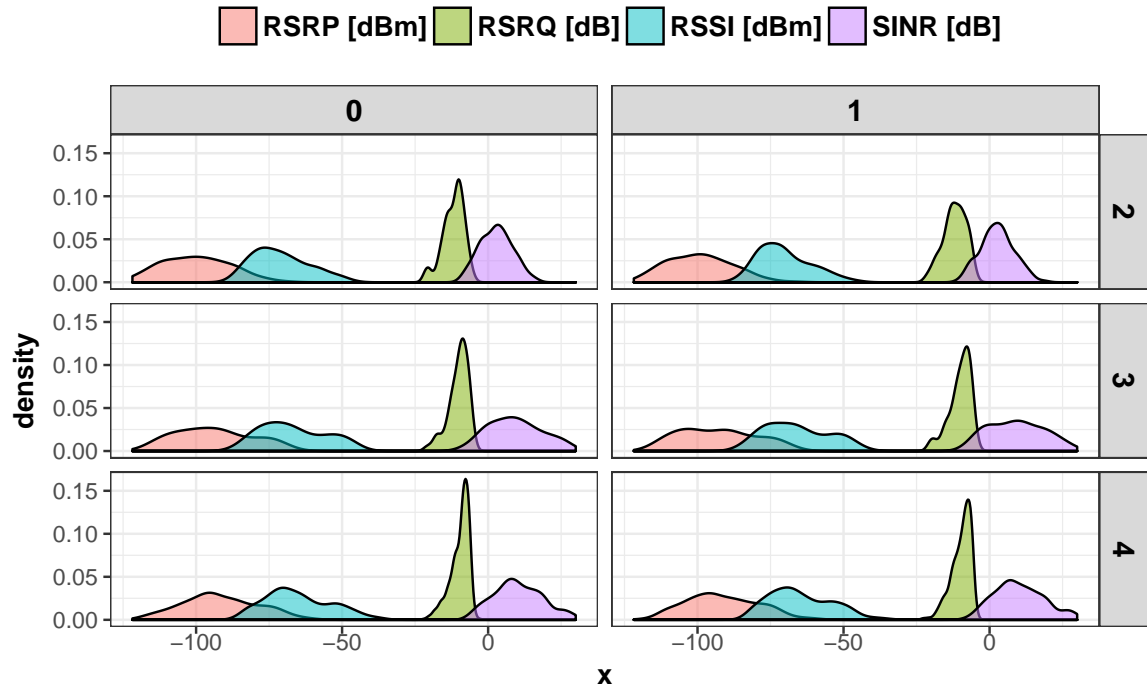


Fig. 5.8 RS-related quantities density for each Transmission Mode and CodeWord for Freq. 800 MHz

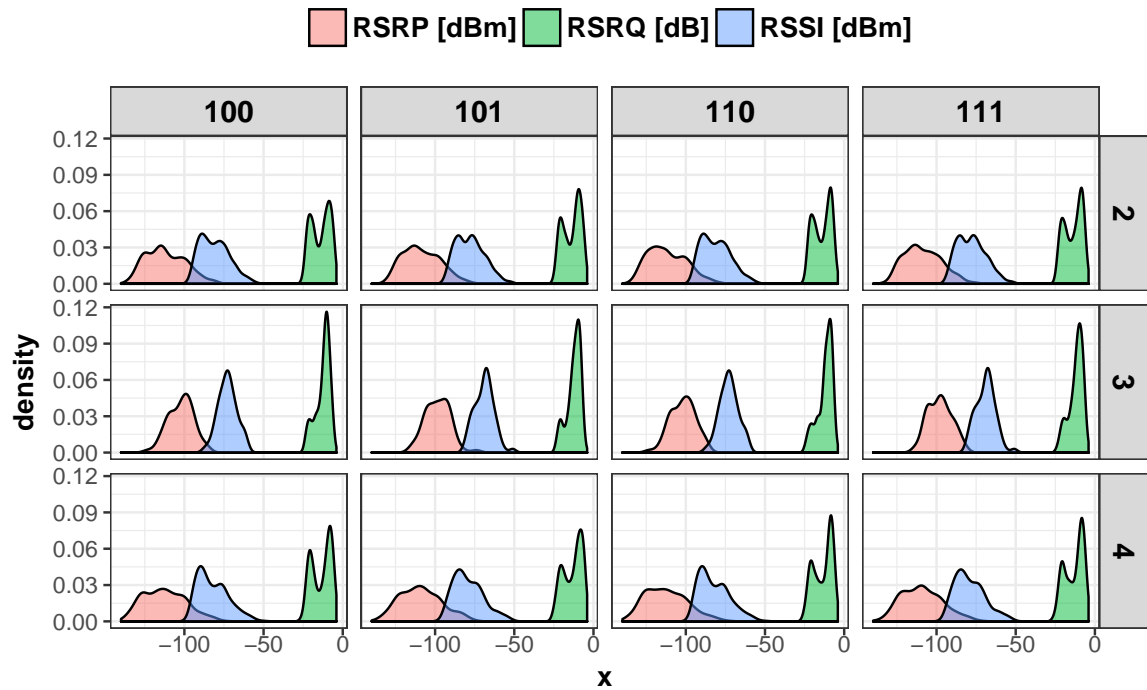


Fig. 5.9 RS-related quantities density for each Transmission Mode and CodeWord for Freq. 2100 MHz

Table 5.9 Port Mapping

	TX0	TX1	TX2	TX3
RX0	100	110	120	130
RX1	101	111	121	131
RX2	102	112	122	132
RX3	103	113	123	133

### 5.5.1 Physical Layer Quantities Statistical Analysis

The experimental probability density function (epdf) corresponding to physical layer parameters presented in the last section are presented in Fig. 5.8, 5.9 with respect to different TMs and Ports. Port Mapping for Nemo Software is shown in Tab.5.9. For Band 20 only values measured at TX (0,1) are collected while for Band 1 values are collected for both TXs and RXs.

With reference to Fig. 5.8, we cannot spot much differences between different TMs and code-words besides a slight and statistically insignificant shift to the left in SINR's density peak value position and smaller variance value for TM2, unlike the expected behavior since TM2, which is based on Transmission Diversity, is designed to enhance network performance in terms of SINR. In addition it is apparent from the picture that RSRQ, unlike the other quantities, has a smaller variance, i.e. it is pretty stable about its mean, leading to an overall *stable* quality of the RS. Furthermore, the significant difference between RSSI and RSRP, the former being about 25 dB greater than the latter, shows that the network is affected by a pretty large interfering signal. In Fig. 5.9 it is TM3 that differs from the other two modes. As a matter of facts, with that mode RSRQ presents a less prominent bimodality, while RSRP and RSSI are slightly shifted to larger values yet with a smaller variance and almost monomodal behavior (less so for RSRP).

In Figs. 5.10 and 5.11, the evolution over time of RSRP, RSSI, RSRQ and SINR are shown. For both systems, when TM3 is in use we can see fewer values reported, matching the TM's standard specifications, which, in facts, implements Open Loop Spatial multiplexing and is adopted when few retrievals by the user is required to have the system work (poor channel conditions). On the other hand we can see almost continuous reporting of values when TM4 is adopted. Again, this fully respects standard specifications since it implements Closed Loop Multiplexing.

RSRQ values are higher for Band 1 while RSRP, RSSI are similar. For Band 1 too few values of SINR are measured and therefore they are not shown in the figure.

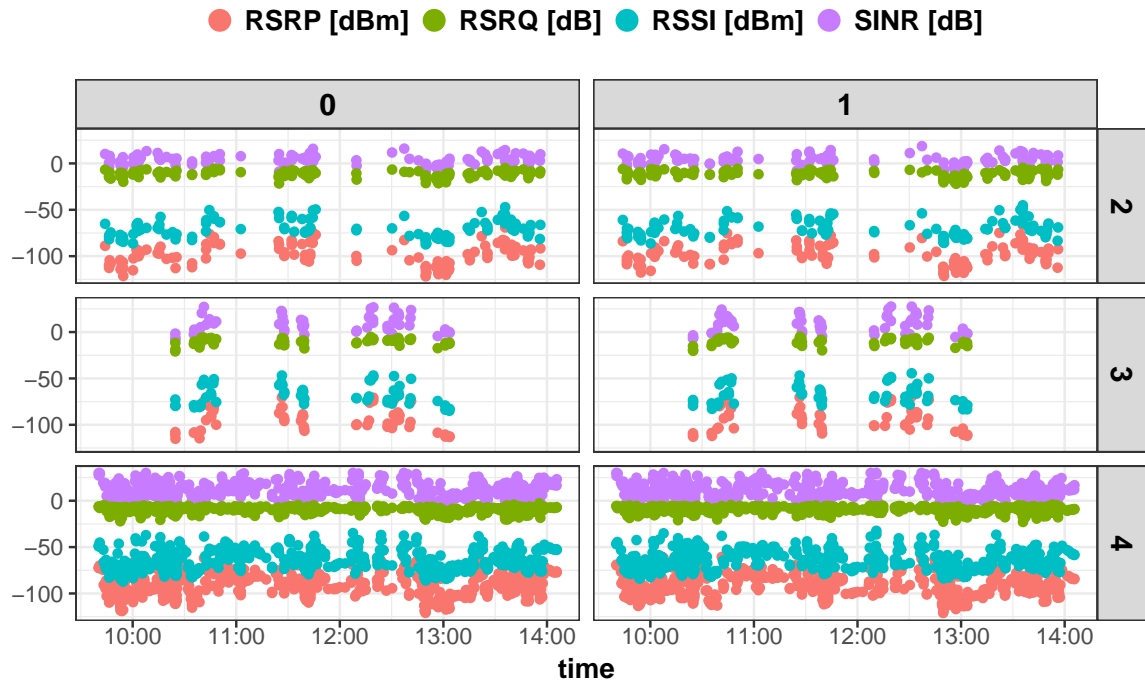


Fig. 5.10 RS related quantities for Freq. 800 MHz

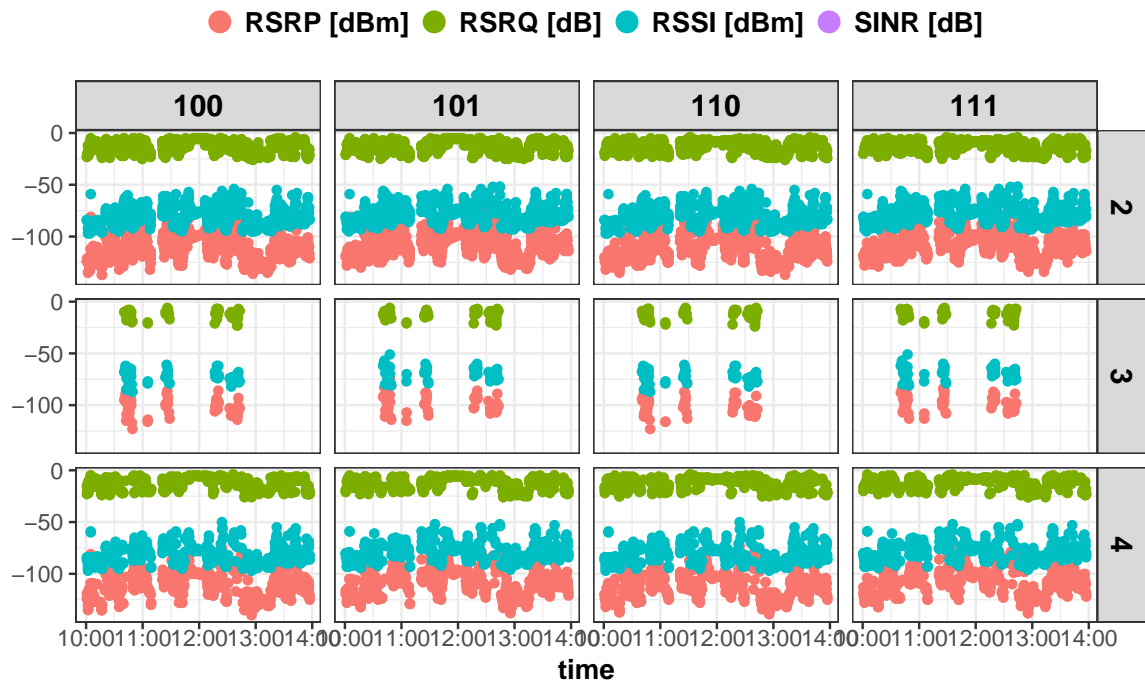


Fig. 5.11 RS related quantities for Freq. 2100 MHz

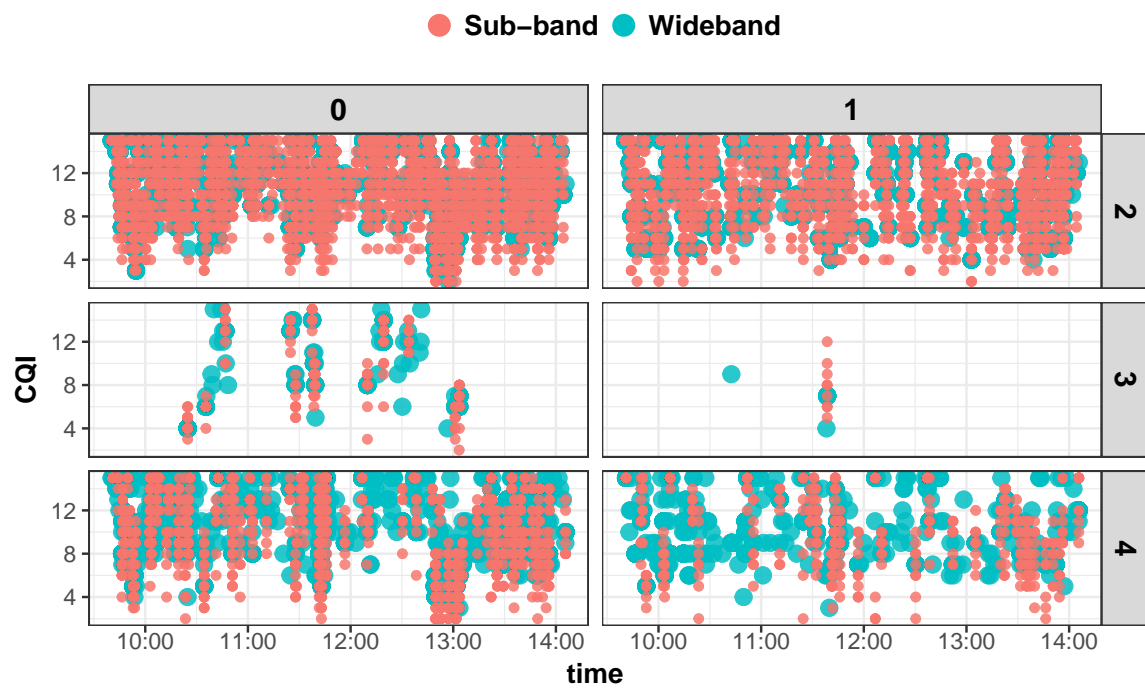


Fig. 5.12 CQI Reporting for each Transmission Mode and CodeWord for Freq. 800 MHz

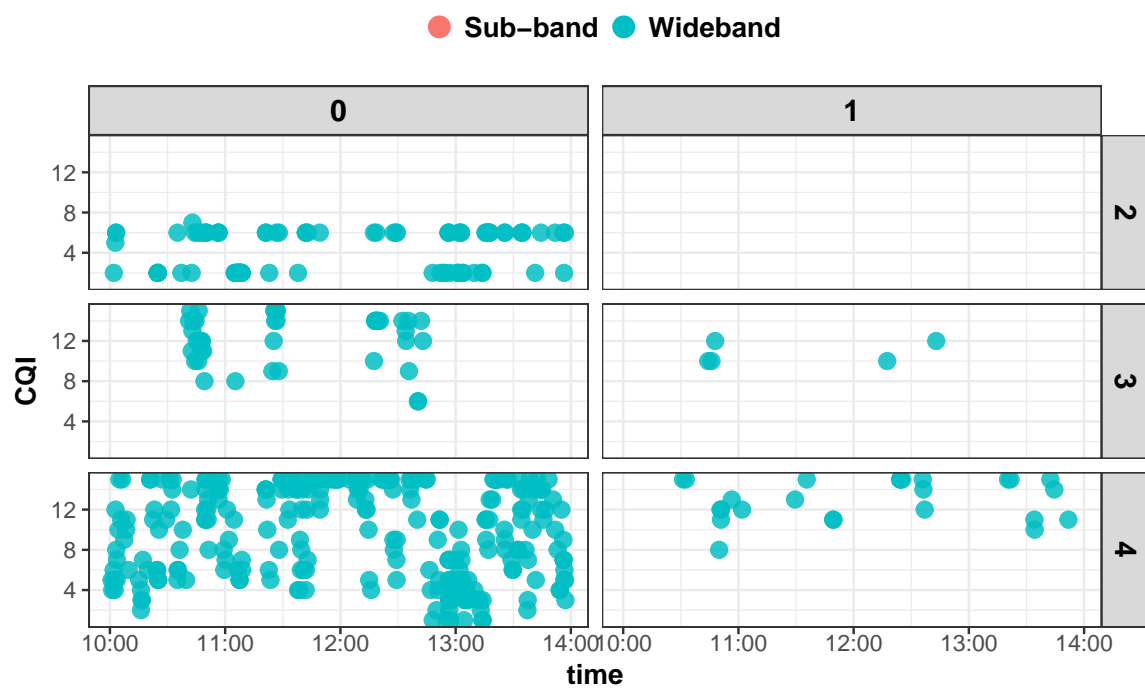


Fig. 5.13 CQI Reporting for each Transmission Mode and CodeWord for Freq. 2100 MHz



### 5.5.2 Channel State Information (CSI) Reporting Analysis

As presented in Chapter 1, UEs periodically report information on channel condition. In this subsection we present an analysis of the actual CSI feedback. At first we investigate CQI values with respect to code-words (0,1) and bands (20,1).

In Fig. 5.12, UE CQI reporting is shown for band 20. As seen in Tab. 2.3 and accordingly to Open Loop implementation with TM3, *UE selected sub-band CQI* and *wide-band CQI* are here reported. Values reported are few since UE adopts this TM rarely and are higher with code-word 0. With TM4 and TM2, also, *UE selected sub-band* and *wide-band CQI* per code-word are reported. With TM4 again, values are heavily collected, while with TM2, implementing Transmit Diversity, sub-band CQI has a predominant role. For both TM4 and TM3 we can immediately appreciate that values are quite higher and for most of the time higher order modulations are suggested to be used for UE transmissions.

In Fig. 5.13 a massive wide-band CQI report takes place while no sub-band CQI values are reported. Even if for code-word 1 we do not hold many samples, we can appreciate a different behavior with TM2. Here fewer and lower wide-band CQI are reported. On the other hand, with the adoption of same TMs we can appreciate an opposite behavior as for band 20 with TM3 and 4 with higher values for codeword 1.

Comparing physical layers parameters shown in Figs. 5.10 and 5.11 with the relatives CQI shown in Figs. 5.12 and 5.13, we can state that, as expected, with better channel condition higher modulation are suggested through CQIs and the reporting is performing as depicted in 3GPP Standard.

Together with CQI reporting also PMI and RI are collected accordingly with Tab. 2.3, for band (1,20). The LTE UE uses PMI information to indicate the preferred set of weights to be applied during the pre-coding process. UE does this in order to maximize the downlink SINR ratio. In band 1, for respectively TM2 and 3 *UE selected sub-band CQI + wide-band CQI and no PM* are required while for TM4 also PMI is mandatory. With band 20, instead, even for TM2 and 3 PMI is reported accordingly to the periodicity of wide-band CQI.

In Fig. 5.14, Requested Rank is shown, that is the portion of time when the mobile would have been able to receive data using the defined rank. Measurements show a Rank 4 reported as used for the 0% of the overall time for both band 1 and 20 and for all TMs. The behaviour is completely normal and expected since a MIMO 2x2 is adopted as shown in Fig. 2.4. Rank 2, representing MIMO in its full implementation, was mostly in use together with Rank 1 (representing Transmit Diversity implementation) as also confirmed with TM adoption (TM2, TM3, TM4). Rank 3 was never in use again in line with operator architecture. For TM3 very few values are reported while none should be collected.

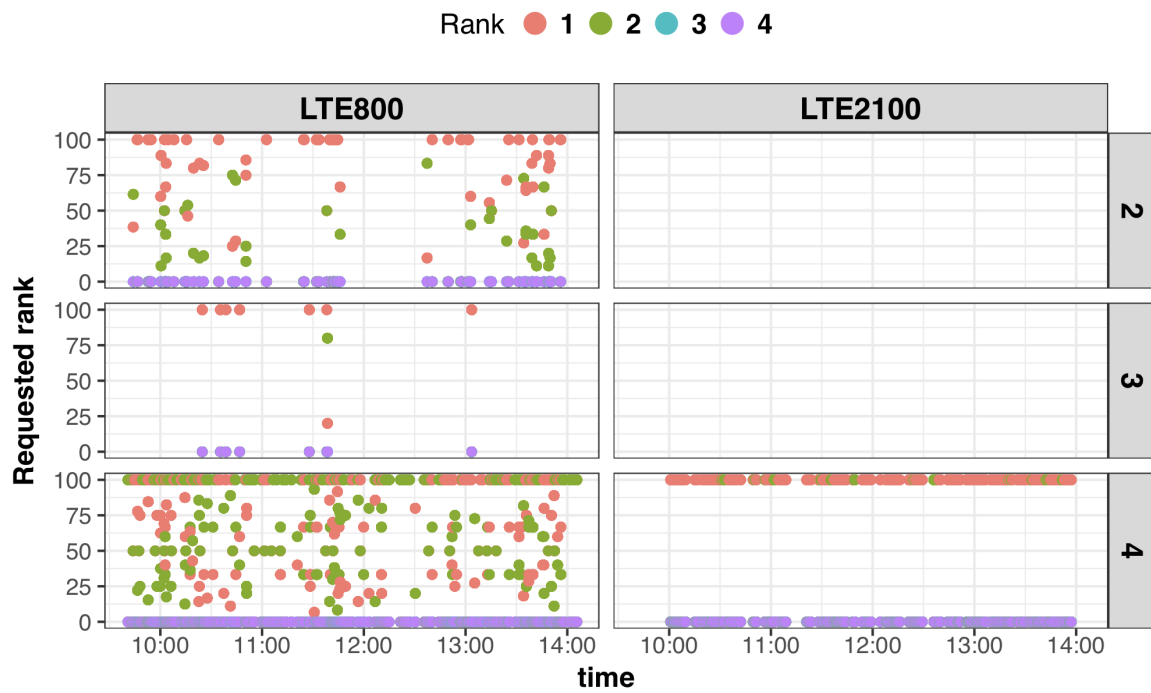


Fig. 5.14 Rank Reporting for each Transmission Mode

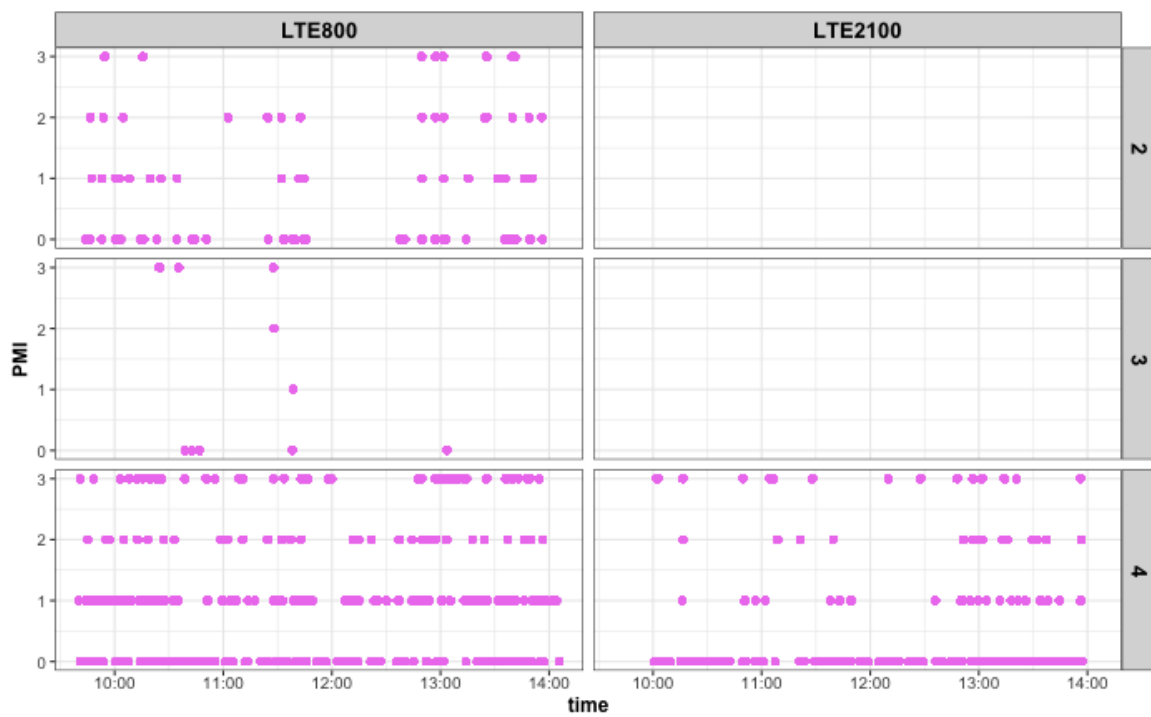


Fig. 5.15 PMI Reporting for each Transmission Mode

## 5.6 Conclusions

In this chapter we provided the results on a still ongoing smartphone-based experimental characterization of LTE network's MIMO performance. With reference to the investigated physical-layer parameters, it is shown that the LTE architecture is performing as expected by the standard, although it is necessary to investigate the relationship between them and some more strictly user-related parameters such as the network throughput.



# Chapter 6

## Conclusions

In this thesis, we investigated how to optimise LTE Radio Layer at different levels. 3GPP architecture was fully explored in its physical and radio layer procedure dealing especially with Adaptive Modulation and Coding Scheme Mechanism.

To cope with this technique, we focused our attention on how scheduling processes take place at the eNodeB and on how measurement at physical layer, to report CQI value, is conducted by the UE.

In chapter 4 we proposed an innovative approach to test performance of the LTE network from an end-user perspective. By using a smartphone-based measurement, the network was tested under actual working and operational condition without the limitations in terms of variations of parameters that a controlled environment would pose. Experimental outcomes were mainly that the 3 Gbps throughput advocated by the standard is far from being achieved. As a matter of fact, LTE network in a real test-bed scenario is quite under-performing when compared to the 3GPP previsions.

As a comparing campaign and with the purpose of validating an testing how measurement campaign are carried out, in chapter 5 we then performed an assessment with the usage of a smartphone methodology. We mostly showed that the adoption of carrier aggregation and higher modulation orders allows LTE network to achieve acceptable end-user performance in terms of channel physical layer quality indicators although not as good as the expected one. This work will be used as a baseline dataset for further MIMO analysis.

Both from chapter 4 and 5 it is clear that Adaptive modulation and coding adopted by LTE is implemented sharply following the standard as we can determine by the average CQI in use with different modulation order. In Chapter 5, our study is investigating deeply the path of MIMO being involved in LTE architecture and how the network performances are affected by its usage. LTE performance assessment when a Single User MIMO is adopted.

Then the performance issues deriving from the coexistence of Wi-Fi and LTE in the unlicensed bands were investigated in Chapter 3. This topic has lately attracting much interest, both from research community and standardization bodies. So we first described the main techniques used by the approaches proposed so far, Listen Before Talk (LBT) and Almost Blank Subframe (ABS). Then, we presented the solutions the standardization bodies are developing: LTE-U, LAA and MuLTEfire. Finally, we surveyed the proposals appeared in the literature so far.

Future works will deal with an assessment on LTE actual throughput when SU-MIMO and MU-MIMO techniques are adopted.

# References

- [1] A. Ghosh, J. Zhang, J. G. Andrews, and R. Muhamed, *Fundamentals of LTE*. Pearson Education, 2010.
- [2] N. Wei, A. Pokhariyal, T. B. Sørensen, T. E. Kolding, and P. E. Mogensen, “Performance of spatial division multiplexing mimo with frequency domain packet scheduling: From theory to practice,” *IEEE Journal on Selected Areas in Communications*, vol. 26, no. 6, pp. 890–900, August 2008.
- [3] P. Kyösti, P. Kemppainen, and T. Jämsä, “Radio channel measurements in live LTE networks for MIMO Over-the-Air emulation,” in *8th Eur. Conf. Antennas Propag. (EuCAP 2014)*. IEEE, apr 2014, pp. 3679–3683. [Online]. Available: <http://ieeexplore.ieee.org/document/6902628/>
- [4] A. Kalachikov and N. S. Shelkunov, “Channel parameters and capacity measurement of MIMO LTE wireless channel,” in *2014 12th Int. Conf. Actual Probl. Electron. Instrum. Eng.* IEEE, oct 2014, pp. 349–351. [Online]. Available: <http://ieeexplore.ieee.org/document/7040915/>
- [5] L. Angrisani, N. Pasquino, R. Schiano Lo Moriello, and M. Vadursi, “Facing synchronization problems in MIMO measurement systems,” in *2011 IEEE Int. Instrum. Meas. Technol. Conf.* IEEE, may 2011, pp. 1–6. [Online]. Available: <http://ieeexplore.ieee.org/document/5944321/>
- [6] S. Yi, Y. Zhang, Z. Sun, and M. Lei, “Channel Measurement and Channel Quality Reporting in LTE-Advanced Relaying Systems,” in *2012 IEEE Vehicular Technology Conference (VTC Fall)*, Sept 2012, pp. 1–5.
- [7] 3gpp tr 36.889 v13.0.0 (2015-06 - 3rd generation partnership project; technical specification group radio access network; study on licensed-assisted access to unlicensed spectrum; (release 13).
- [8] C. Y. Wong, R. S. Cheng, K. B. Letaief, and R. D. Murch, “Multiuser OFDM with adaptive subcarrier, bit, and power allocation,” *IEEE J. Sel. Areas Commun.*, vol. 17, no. 10, pp. 1747–1758, 1999.
- [9] (2016-01) Lte; evolved universal terrestrial radio access (e-utra); physical channels and modulation.
- [10] (2009-10) Etsi ts 136 213 v8.8.0 technical specification lte; evolved universal terrestrial radio access (e-utra); physical layer procedures (3gpp ts 36.213 version 8.8.0 release 8).

- [11] C. S. Park and S. Park, "Analysis of rsrp measurement accuracy," *IEEE Communications Letters*, vol. 20, no. 3, pp. 430–433, 2016.
- [12] (2007-12) 3gpp ts 36.101 v8.0.0 technical specification 3rd generation partnership project; technical specification group radio access network; evolved universal terrestrial radio access (e-utra); user equipment (ue) radio transmission and reception (release 8).
- [13] (2015-02) Etsi ts 136 306 v12.3.0 technical specification lte; evolved universal terrestrial radio access (e-utra); user equipment (ue) radio access capabilities (3gpp ts 36.306 version 12.3.0 release 12).
- [14] [Online]. Available: <http://www.rfwireless-world.com/calculators/LTE-code-rate-calculator.html>
- [15] R. S. W. Paper, "Introduction to mimo."
- [16] (2012-10) Lte; evolved universal terrestrial radio access (e-utra); user equipment (ue) conformance specification; radio transmission and reception; part 1: Conformance testing (3gpp ts 36.521-1 version 10.3.0 release 10).
- [17] [Online]. Available: <https://www.qualcomm.com/invention/technologies/lte/unlicensed/>
- [18] M. D. Foegelle, "Coexistence of LTE-U and LAA in a Wi-Fi world," in *European Conference on Antennas and Propagation (EuCAP)*, April 2016, pp. 1–5.
- [19] S. Dimatteo, P. Hui, B. Han, and V. O. Li, "Cellular traffic offloading through wifi networks," in *2011 IEEE Eighth International Conference on Mobile Ad-Hoc and Sensor Systems*. IEEE, 2011, pp. 192–201.
- [20] Qualcomm Incorporated, "Extending LTE Advanced to unlicensed spectrum," <https://www.qualcomm.com/media/documents/files/white-paper-extending-lte-advanced-to-unlicensed-spectrum.pdf>, December 2013, accessed May 2017.
- [21] "<http://www.lteuforum.org/>."
- [22] Qualcomm Incorporated, "Introducing MulteFire: LTE-like performance with Wi-Fi-like simplicity," <https://www.qualcomm.com/news/onq/2015/06/11/introducing-multefire-lte-performance-wi-fi-simplicity>, June 2015, accessed May 2017.
- [23] Ericsson, "LTE License Assisted Access," [https://www.ericsson.com/res/thecompany/docs/press/media\\_kits/ericsson-license-assisted-access-laa-january-2015.pdf](https://www.ericsson.com/res/thecompany/docs/press/media_kits/ericsson-license-assisted-access-laa-january-2015.pdf), January 2015, accessed May 2017.
- [24] HUAWEI, "U-LTE: Unlicensed Spectrum Utilization of LTE," [www.huawei.com/ilink/en/download/HW\\_327803](http://www.huawei.com/ilink/en/download/HW_327803), February 2014, accessed May 2017.
- [25] N. Rupasinghe and I. Guvenc, "Licensed-assisted access for WiFi-LTE coexistence in the unlicensed spectrum," in *Globecom Workshops*. IEEE, 2014, pp. 894–899.



- [26] S. Sagari, I. Seskar, and D. Raychaudhuri, "Modeling the coexistence of LTE and WiFi heterogeneous networks in dense deployment scenarios," in *International Conference on Communication (ICC) Workshop on LTE in Unlicensed Bands: Potentials and Challenges*. IEEE, 2015, pp. 2301–2306.
- [27] Y. Jian, C.-F. Shih, B. Krishnaswamy, and R. Sivakumar, "Coexistence of Wi-Fi and LAA-LTE: Experimental evaluation, analysis and insights," in *International Conference on Communication (ICC) Workshop on LTE in Unlicensed Bands: Potentials and Challenges*. IEEE, 2015, pp. 2325–2331.
- [28] T. Nihtila, V. Tykhomyrov, O. Alanen, M. A. Uusitalo, A. Sorri, M. Moisio, S. Iraj, R. Ratasuk, and N. Mangalvedhe, "System performance of LTE and IEEE 802.11 coexisting on a shared frequency band," in *IEEE Wireless Communications and Networking Conference (WCNC)*, 2013.
- [29] S. Sagari, S. Baysting, D. Saha, I. Seskar, W. Trappe, and D. Raychaudhuri, "Coordinated dynamic spectrum management of LTE-U and Wi-Fi networks," in *IEEE International Symposium on Dynamic Spectrum Access Networks (DySPAN)*. IEEE, 2015, pp. 209–220.
- [30] D. Raychaudhuri, I. Seskar, M. Ott, S. Ganu, K. Ramachandran, H. Kremo, R. Siracusa, H. Liu, and M. Singh, "Overview of the ORBIT radio grid testbed for evaluation of next-generation wireless network protocols," in *Wireless Communications and Networking Conference (WCNC)*, vol. 3. IEEE, 2005, pp. 1664–1669.
- [31] R. Ratasuk, M. A. Uusitalo, N. Mangalvedhe, A. Sorri, S. Iraj, C. Wijting, and A. Ghosh, "License-exempt LTE deployment in heterogeneous network," in *International Symposium on Wireless Communication Systems (ISWCS)*. IEEE, 2012, pp. 246–250.
- [32] A. K. Sadek, T. Kadous, K. Tang, H. Lee, and M. Fan, "Extending LTE to unlicensed band-Merit and coexistence," in *International Conference on Communication (ICC) Workshop on LTE in Unlicensed Bands: Potentials and Challenges*. IEEE, 2015, pp. 2344–2349.
- [33] MADWIFI project, "Minstrel rate control algorithm for mac80211," [https://sourceforge.net/p/madwifi/svn/HEAD/tree/madwifi/trunk/ath\\_rate/minstrel/minstrel.txt](https://sourceforge.net/p/madwifi/svn/HEAD/tree/madwifi/trunk/ath_rate/minstrel/minstrel.txt), 2005, accessed May 2017.
- [34] A. M. Cavalcante, E. Almeida, R. D. Vieira, F. Chaves, R. C. Paiva, F. Abinader, S. Choudhury, E. Tuomaala, and K. Doppler, "Performance evaluation of LTE and Wi-Fi coexistence in unlicensed bands," in *77th Vehicular Technology Conference (VTC Spring)*. IEEE, 2013, pp. 1–6.
- [35] Qualcomm Incorporated, "Reply comments of qualcomm incorporated," <http://apps.fcc.gov/ecfs/document/view?id=60001104452>, June 2015, accessed May 2017.
- [36] J. Jeon, Q. C. Li, H. Niu, A. Papathanassiou, and G. Wu, "LTE in the unlicensed spectrum: A novel coexistence analysis with WLAN systems," in *Global Communications Conference (GLOBECOM)*. IEEE, 2014, pp. 3459–3464.

- [37] A. M. Voicu, L. Simic, and M. Petrova, "Coexistence of pico-and femto-cellular LTE-unlicensed with legacy indoor Wi-Fi deployments," in *IEEE International Conference on Communication (ICC) Workshop on LTE in Unlicensed Bands: Potentials and Challenges*. IEEE, 2015, pp. 2294–2300.
- [38] Y. Gao, X. Chu, and J. Zhang, "Performance Analysis of LAA and WiFi Coexistence in Unlicensed Spectrum Based on Markov Chain," in *Global Communications Conference (GLOBECOM)*. IEEE, December 2016, pp. 1–6.
- [39] H. Zhang, Y. Xiao, L. X. Cai, D. Niyato, L. Song, and Z. Han, "A Multi-Leader Multi-Follower Stackelberg Game for Resource Management in LTE Unlicensed," *IEEE Transactions on Wireless Communications*, vol. 16, no. 1, pp. 348–361, January 2017.
- [40] K. Hamidouche, W. Saad, and M. Debbah, "A Multi-Game Framework for Harmonized LTE-U and WiFi Coexistence over Unlicensed Bands," *IEEE Wireless Communications*, vol. 23, no. 6, pp. 62–69, December 2016.
- [41] A. M. Voicu, L. Simić, and M. Petrova, "Inter-Technology Coexistence in a Spectrum Commons: A Case Study of Wi-Fi and LTE in the 5-GHz Unlicensed Band," *IEEE Journal on Selected Areas in Communications*, vol. 34, no. 11, pp. 3062–3077, November 2016.
- [42] X. Wang, T. Q. S. Quek, M. Sheng, and J. Li, "Throughput and Fairness Analysis of Wi-Fi and LTE-U in Unlicensed Band," *IEEE Journal on Selected Areas in Communications*, vol. 35, no. 1, pp. 63–78, January 2017.
- [43] O. Sandoval, G. D. González, J. Hämmäläinen, and S. Yoo, "Indoor planning and optimization of LTE-U radio access over WiFi," in *27th Annual International Symposium on Personal, Indoor, and Mobile Radio Communications (PIMRC)*. IEEE, September 2016, pp. 1–7.
- [44] Z. Ali, B. Bojovic, L. Giupponi, and J. M. Bafalluy, "On Fairness Evaluation: LTE-U vs. LAA," in *Proceedings of the 14th ACM International Symposium on Mobility Management and Wireless Access*, ser. MobiWac '16. ACM, 2016, pp. 163–168.
- [45] B. Jia and M. Tao, "A channel sensing based design for LTE in unlicensed bands," in *International Conference on Communication (ICC) Workshop on LTE in Unlicensed Bands: Potentials and Challenges*. IEEE, 2015, pp. 2332–2337.
- [46] S. Dama, A. Kumar, and K. Kuchi, "Performance Evaluation of LAA-LBT Based LTE and WLAN's Co-Existence in Unlicensed Spectrum," in *Globecom Workshops (GC Wkshps)*. IEEE, 2015, pp. 1–6.
- [47] C. Chen, R. Ratasuk, and A. Ghosh, "Downlink Performance Analysis of LTE and WiFi Coexistence in Unlicensed Bands with a Simple Listen-Before-Talk Scheme," in *81st Vehicular Technology Conference (VTC Spring)*. IEEE, 2015, pp. 1–5.
- [48] E. Almeida, A. M. Cavalcante, R. C. Paiva, F. S. Chaves, F. M. Abinader, R. D. Vieira, S. Choudhury, E. Tuomaala, and K. Doppler, "Enabling LTE/WiFi coexistence by LTE blank subframe allocation," in *International Conference on Communications (ICC)*. IEEE, 2013, pp. 5083–5088.

- [49] A. Mukherjee, J. F. Cheng, S. Falahati, L. Falconetti, A. Furuskär, B. Godana, D. H. Kang, H. Koorapaty, D. Larsson, and Y. Yang, "System Architecture and Coexistence Evaluation of Licensed-Assisted Access LTE with IEEE 802.11," *International Conference on Communication (ICC) Workshop on LTE in Unlicensed Bands: Potentials and Challenges*, pp. 2350–2355, June 2015.
- [50] J. Perez-Romero, O. Sallent, R. Ferrus, and R. Agustí, "A Robustness Analysis of Learning-based Coexistence Mechanisms for LTE-U Operation in Non-Stationary Conditions," in *82nd Vehicular Technology Conference (VTC Fall)*. IEEE, 2015, pp. 1–5.
- [51] J. Jeon, H. Niu, Q. Li, A. Papathanassiou, and G. Wu, "LTE with listen-before-talk in unlicensed spectrum," in *International Conference on Communication (ICC) Workshop on on LTE in Unlicensed Bands: Potentials and Challenges*. IEEE, 2015, pp. 2320–2324.
- [52] J. Jeon, H. Niu, Q. C. Li, A. Papathanassiou, and G. Wu, "LTE in the unlicensed spectrum: Evaluating coexistence mechanisms," in *Globecom Workshops (GC Wkshps)*. IEEE, 2014, pp. 740–745.
- [53] O. Sallent, J. Perez-Romero, R. Ferrus, and R. Agusti, "Learning-based coexistence for LTE operation in unlicensed bands," in *International Conference on Communication (ICC) Workshop on LTE in Unlicensed Bands: Potentials and Challenges*. IEEE, 2015, pp. 2307–2313.
- [54] Y. Li, J. Zheng, and Q. Li, "Enhanced listen-before-talk scheme for frequency reuse of licensed-assisted access using LTE," in *26th Annual International Symposium on Personal, Indoor, and Mobile Radio Communications (PIMRC)*. IEEE, 2015, pp. 1918–1923.
- [55] T. Tao, F. Han, and Y. Liu, "Enhanced LBT algorithm for LTE-LAA in unlicensed band," in *26th Annual International Symposium on Personal, Indoor, and Mobile Radio Communications (PIMRC)*. IEEE, 2015, pp. 1907–1911.
- [56] R. Kwan, R. Pazhyannur, J. Seymour, V. Chandrasekhar, S. Saunders, D. Bevan, H. Osman, J. Bradford, J. Robson, and K. Konstantinou, "Fair co-existence of Licensed Assisted Access LTE (LAA-LTE) and Wi-Fi in unlicensed spectrum," in *Computer Science and Electronic Engineering Conference (CEEC), 2015 7th*. IEEE, 2015, pp. 13–18.
- [57] A. Bhorkar, C. Ibars, and P. Zong, "Performance analysis of LTE and Wi-Fi in unlicensed band using stochastic geometry," in *25th Annual International Symposium on Personal, Indoor, and Mobile Radio Communication (PIMRC)*. IEEE, 2014, pp. 1310–1314.
- [58] H. Ko, J. Lee, and S. Pack, "A Fair Listen-Before-Talk Algorithm for Coexistence of LTE-U and WLAN," *IEEE Transactions on Vehicular Technology*, vol. 65, no. 12, pp. 10 116–10 120, Dec 2016.
- [59] C. K. Kim, C. S. Yang, and C. G. Kang, "Adaptive Listen-Before-Talk (LBT) scheme for LTE and Wi-Fi systems coexisting in unlicensed band," in *13th Annual Consumer Communications & Networking Conference (CCNC)*. IEEE, 2016, pp. 589–594.

- [60] Z. Guan and T. Melodia, "CU-LTE: Spectrally-Efficient and Fair Coexistence Between LTE and Wi-Fi in Unlicensed Bands," in *35th Annual IEEE International Conference on Computer Communications (INFOCOM)*, April 2016, pp. 1–9.
- [61] A. M. Baswade and B. R. Tamma, "Channel sensing based dynamic adjustment of contention window in LAA-LTE networks," in *8th International Conference on Communication Systems and Networks (COMSNETS)*. IEEE, 2016, pp. 1–2.
- [62] Y. Li, F. Baccelli, J. G. Andrews, T. D. Novlan, and J. Zhang, "Modeling and analyzing the coexistence of licensed-assisted access LTE and Wi-Fi," in *Globecom Workshops (GC Wkshps)*. IEEE, 2015, pp. 1–6.
- [63] S. Y. Lien, J. Lee, and Y. C. Liang, "Random Access or Scheduling: Optimum LTE Licensed-Assisted Access to Unlicensed Spectrum," *IEEE Communications Letters*, vol. 20, no. 3, pp. 590–593, March 2016.
- [64] V. Janardhanan, N. Muhammed, V. Gonuguntla, and N. Akhtar, "LTE-Wi-Fi coexistence in 5 GHz band," in *International Conference on Advanced Networks and Telecommunications Systems (ANTS)*. IEEE, 2015, pp. 1–6.
- [65] T. Novlan, B. L. Ng, H. Si, and J. C. Zhang, "Overview and evaluation of licensed assisted access for LTE-advanced," in *49th Asilomar Conference on Signals, Systems and Computers*. IEEE, 2015, pp. 1031–1035.
- [66] M. Xing, Y. Peng, T. Xia, H. Long, and K. Zheng, "Adaptive Spectrum Sharing of LTE Co-existing with WLAN in Unlicensed Frequency Bands," in *81st Vehicular Technology Conference (VTC Spring)*. IEEE, May 2015, pp. 1–5.
- [67] A. Babaei, J. Andreoli-Fang, Y. Pang, and B. Hamzeh, "On the impact of LTE-U on Wi-Fi performance," *International Journal of Wireless Information Networks*, vol. 22, no. 4, pp. 336–344, 2015.
- [68] N. Rupasinghe and I. Guvenc, "Reinforcement learning for licensed-assisted access of LTE in the unlicensed spectrum," in *Wireless Communications and Networking Conference (WCNC)*. IEEE, 2015, pp. 1279–1284.
- [69] C. Cano and D. J. Leith, "Coexistence of WiFi and LTE in unlicensed bands: A proportional fair allocation scheme," in *International Conference on Communication (ICC) Workshop on LTE in Unlicensed Bands: Potentials and Challenges*. IEEE, 2015, pp. 2288–2293.
- [70] M. Khawer, J. Tang, and F. Han, "usICIC—A Proactive Small Cell Interference Mitigation Strategy for Improving Spectral Efficiency of LTE Networks in the Unlicensed Spectrum," *IEEE Transactions on Wireless Communications*, vol. 15, no. 3, pp. 2303–2311, March 2016.
- [71] S. Choi and S. Park, "Co-existence analysis of duty cycle method with Wi-Fi in unlicensed bands," in *International Conference on Information and Communication Technology Convergence (ICTC)*. IEEE, 2015, pp. 894–897.
- [72] Y. Pang, A. Babaei, J. Andreoli-Fang, and B. Hamzeh, "Wi-Fi Coexistence with Duty Cycled LTE-U," *Wireless Communications and Mobile Computing*, vol. 2017, 2017.

- [73] V. Valls, A. Garcia-Saavedra, X. Costa, and D. J. Leith, "Maximizing LTE Capacity in Unlicensed Bands (LTE-U/LAA) While Fairly Coexisting With 802.11 WLANs," *IEEE Communications Letters*, vol. 20, no. 6, pp. 1219–1222, June 2016.
- [74] "ETSI EN 301 893, Broadband Radio Access Networks (BRAN); 5 GHz high performance RLAN; Harmonized EN covering the essential requirements of article 3.2 of the R&TTE Directive."
- [75] R. Yin, G. Yu, A. Maaref, and G. Y. Li, "LBT-Based Adaptive Channel Access for LTE-U Systems," *IEEE Transactions on Wireless Communications*, vol. 15, no. 10, pp. 6585–6597, October 2016.
- [76] H. Zhang, X. Chu, W. Guo, and S. Wang, "Coexistence of Wi-Fi and heterogeneous small cell networks sharing unlicensed spectrum," *IEEE Communications Magazine*, vol. 53, no. 3, pp. 158–164, 2015.
- [77] J. H. Jang and H. J. Choi, "A fast automatic gain control scheme for 3GPP LTE TDD system," in *72nd Vehicular Technology Conference Fall (VTC 2010-Fall)*. IEEE, 2010, pp. 1–5.
- [78] M. Labib, J. H. Reed, A. F. Martone, and A. I. Zaghloul, "Coexistence between radar and LTE-U systems: Survey on the 5 GHz band," in *United States National Committee of URSI National Radio Science Meeting (USNC-URSI NRSM)*, 2016, pp. 1–2.
- [79] S. Aghaeinezhadfirouzja, H. Liu, B. Xia, and M. Tao, "Implementation and measurement of single user MIMO testbed for TD-LTE-A downlink channels," in *2016 8th IEEE Int. Conf. Commun. Softw. Networks*. IEEE, jun 2016, pp. 211–215. [Online]. Available: <http://ieeexplore.ieee.org/document/7586651/>
- [80] A. Miura, T. Orikasa, H. Tsuji, and M. Toyoshima, "Measurement experiment of LTE terminal transmit power for interference estimation in Satellite/Terrestrial Integrated mobile Communications System," in *2014 Int. Symp. Antennas Propag. Conf. Proc.* IEEE, dec 2014, pp. 555–556. [Online]. Available: <http://ieeexplore.ieee.org/document/7026772/>
- [81] D. Colombi, B. Thors, N. Wirén, L.-E. Larsson, and C. Törnevik, "Measurements of downlink power level distributions in LTE networks," in *2013 Int. Conf. Electromagn. Adv. Appl.* IEEE, sep 2013, pp. 98–101. [Online]. Available: <http://ieeexplore.ieee.org/document/6632196/>
- [82] J. Jiang, M. Peng, Y. Li, and Y. Wei, "Measurement-based optimizing algorithm for modulation and coding scheme selection in downlink LTE self-organizing networks," in *2012 IEEE Int. Conf. Wirel. Inf. Technol. Syst.* IEEE, nov 2012, pp. 1–4. [Online]. Available: <http://ieeexplore.ieee.org/document/6417722/>
- [83] F. Qian, Z. Wang, A. Gerber, Z. Mao, S. Sen, and O. Spatscheck, "Profiling Resource Usage for Mobile Applications: A Cross-layer Approach," in *Proceedings of the 9th International Conference on Mobile Systems, Applications, and Services*, ser. MobiSys '11. New York, NY, USA: ACM, 2011, pp. 321–334. [Online]. Available: <http://doi.acm.org/10.1145/1999995.2000026>

- [84] C. Shepard, A. Rahmati, C. Tossell, L. Zhong, and P. Kortum, "Livellab: Measuring wireless networks and smartphone users in the field," *SIGMETRICS Perform. Eval. Rev.*, vol. 38, no. 3, pp. 15–20, Jan. 2011. [Online]. Available: <http://doi.acm.org/10.1145/1925019.1925023>
- [85] J. Huang, Q. Xu, B. Tiwana, Z. M. Mao, M. Zhang, and P. Bahl, "Anatomizing Application Performance Differences on Smartphones," in *Proceedings of the 8th International Conference on Mobile Systems, Applications, and Services*, ser. MobiSys '10. New York, NY, USA: ACM, 2010, pp. 165–178. [Online]. Available: <http://doi.acm.org/10.1145/1814433.1814452>
- [86] M. B. Albaladejo, D. J. Leith, and P. Manzoni, "Measurement-based modelling of lte performance in dublin city," in *2016 IEEE 27th Annual International Symposium on Personal, Indoor, and Mobile Radio Communications (PIMRC)*, Sept 2016, pp. 1–6.
- [87] J. Huang, F. Qian, A. Gerber, Z. M. Mao, S. Sen, and O. Spatscheck, "A close examination of performance and power characteristics of 4g lte networks," in *Proceedings of the 10th international conference on Mobile systems, applications, and services*. ACM, 2012, pp. 225–238.
- [88] LTE-Advanced - Author: Jeanette Wannstrom, for 3GPP. [Online]. Available: <http://www.3gpp.org/technologies/keywords-acronyms/97-lte-advanced>
- [89] V. Buenestado, J. M. Ruiz-Avilés, M. Toril, S. Luna-Ramírez, and A. Mendo, "Analysis of throughput performance statistics for benchmarking lte networks," *IEEE Communications Letters*, vol. 18, no. 9, pp. 1607–1610, Sept 2014.
- [90] K. Pedersen, T. Kolding, I. Kovacs, G. Monghal, F. Frederiksen, and P. Mogensen, "Performance analysis of simple channel feedback schemes for a practical ofdma system," *IEEE Transactions on Vehicular Technology*, vol. 58, no. 9, pp. 5309–5314, Nov 2009.
- [91] J. Jiang, M. Peng, Y. Li, and Y. Wei, "Measurement-based optimizing algorithm for modulation and coding scheme selection in downlink lte self-organizing networks," in *2012 IEEE International Conference on Wireless Information Technology and Systems (ICWITS)*, Nov 2012, pp. 1–4.
- [92] L. Angrisani, N. Pasquino, R. Schiano Lo Moriello, and M. Vadursi, "Facing synchronization problems in MIMO measurement systems," in *2011 IEEE Int. Instrum. Meas. Technol. Conf.* Binjiang, Hangzhou; China: IEEE, may 2011, pp. 1050–1055. [Online]. Available: <http://ieeexplore.ieee.org/document/5944321/>
- [93] S. Avallone, N. Pasquino, S. Zinno, and D. Casillo, "Smartphone-based measurements of LTE network performance," in *2017 IEEE Int. Instrum. Meas. Technol. Conf.* IEEE, may 2017, pp. 1–6.
- [94] R. Subramanian, K. Sandrasegaran, and X. Kong, "Benchmarking of real-time lte network in dynamic environment," in *Communications (APCC), 2016 22nd Asia-Pacific Conference on.* IEEE, 2016, pp. 20–25.

- [95] J. Medbo, I. Siomina, A. Kangas, and J. Furuskog, "Propagation channel impact on lte positioning accuracy: A study based on real measurements of observed time difference of arrival," in *2009 IEEE 20th International Symposium on Personal, Indoor and Mobile Radio Communications*. IEEE, 2009, pp. 2213–2217.
- [96] W. Li, R. K. Mok, D. Wu, and R. K. Chang, "On the accuracy of smartphone-based mobile network measurement," in *2015 IEEE Conference on Computer Communications (INFOCOM)*. IEEE, 2015, pp. 370–378.
- [97] Freewill FX Company Limited, "Azenqos," <http://www.azenqos.com/>.
- [98] "Cell mapper." [Online]. Available: <https://www.cellmapper.net>
- [99] D. Kahle and H. Wickham, "ggmap: Spatial Visualization with ggplot2," *The R Journal*, vol. 5, no. 1, pp. 144–161, 2013. [Online]. Available: <http://journal.r-project.org/archive/2013-1/kahle-wickham.pdf>
- [100] S. Sesia, M. M. P. J. Baker, and I. Toufik, *LTE - The UMTS Long Term Evolution: From Theory to Practice*. Wiley, 2009.
- [101] A. Benjebbour, A. Li, K. Takeda, Y. Kishiyama, T. Nakamura, Y. Inoue, Y. Kishiyama, and T. Nakamura, "Advanced Multiple-access and MIMO Techniques," in *Toward 5G Appl. Requir. Candidate Technol.*, Rath Vannithamby and Shilpa Talwar, Ed. Chichester, UK: John Wiley & Sons, Ltd, nov 2016, ch. 11, pp. 222–249.
- [102] D. Nguyen-Thanh, T. Le-Tien, C. Bui-Thu, and T. Le-Thanh, "LTE indoor MIMO performances field measurements," in *2014 Int. Conf. Adv. Technol. Commun. (ATC 2014)*. IEEE, oct 2014, pp. 84–89.
- [103] T. PadmaPriya and V. Saminadan, "Performance improvement in long term evolution-advanced network using multiple input multiple output technique," *J. Adv. Res. Dyn. Control Syst.*, vol. 9, no. Special Issue 6, pp. 990–1010, 2017.
- [104] C. Lim, T. Yoo, B. Clerckx, B. Lee, and B. Shim, "Recent trend of multiuser mimo in lte-advanced," *IEEE Communications Magazine*, vol. 51, no. 3, pp. 127–135, March 2013.
- [105] D. Micheli, M. Barazzetta, F. Moglie, and V. M. Primiani, "Power boosting and compensation during ota testing of a real 4g lte base station in reverberation chamber," *IEEE Transactions on Electromagnetic Compatibility*, vol. 57, no. 4, pp. 623–634, Aug 2015.
- [106] M. S. Miah, D. Anin, A. Khatun, K. Haneda, L. Hentila, and E. T. Salonen, "On the Field Emulation Techniques in Over-the-Air Testing: Experimental Throughput Comparison," *IEEE Antennas Wirel. Propag. Lett.*, vol. 16, pp. 2224–2227, 2017.
- [107] Q. ul Ain, S. R. ul Hassnain, M. Shah, and S. A. Mahmud, "An evaluation of scheduling algorithms in lte based 4g networks," in *2015 International Conference on Emerging Technologies (ICET)*, Dec 2015, pp. 1–6.

- [108] M. Slanina, L. Klozar, and S. Hanus, "Practical measurement of data throughput in LTE network depending on physical layer parameters," in *2014 24th Int. Conf. Radioelektronika, RADIOELEKTRONIKA 2014 - Proc.* IEEE, apr 2014, pp. 1–4.
- [109] P. Sridhar and M. R. Sumalatha, "Interference cancellation and channel estimation for mimo-lte-a networks," in *2016 International Conference on Wireless Communications, Signal Processing and Networking (WiSPNET)*, March 2016, pp. 2098–2103.
- [110] R. A. Abdelaal, A. S. Behbahani, and A. M. Eltawil, "Practical framework for downlink mu-mimo for lte systems," *IEEE Wireless Communications Letters*, vol. 6, no. 3, pp. 314–317, June 2017.
- [111] Y. Kim, H. Ji, J. Lee, Y. H. Nam, B. L. Ng, I. Tzanidis, Y. Li, and J. Zhang, "Full dimension mimo (fd-mimo): The next evolution of mimo in lte systems," *IEEE Wireless Communications*, vol. 21, no. 3, pp. 92–100, June 2014.
- [112] F. Afroz, R. Subramanian, R. Heidary, K. Sandrasegaran, and S. Ahmed, "SINR, RSRP, RSSI and RSRQ Measurements in Long Term Evolution Networks," *Int. J. Wirel. Mob. Networks*, vol. 7, no. 4, pp. 113–123, aug 2015.
- [113] M. B. Albaladejo, D. J. Leith, and P. Manzoni, "Measurement-based modelling of lte performance in dublin city," in *2016 IEEE 27th Annual International Symposium on Personal, Indoor, and Mobile Radio Communications (PIMRC)*, Sept 2016, pp. 1–6.
- [114] S. Avallone, N. Pasquino, S. Zinno, and D. Casillo, "Experimental characterization of lte adaptive modulation and coding scheme under actual operating conditions," in *2017 IEEE International Workshop on Measurement and Networking (M N)*, Sept 2017, pp. 1–6.
- [115] "Nemo handy." [Online]. Available: <https://www.keysight.com/en/pd-2767485-pn-NTH00000A/nemo-handy?cc=IT&lc=ita>
- [116] "Etsi ts 136 133 v14.3.0 (2017-04), lte; evolved universal terrestrial radio access (e-utra); requirements for support of radio resource management."